DIFFUSIONLESS TRANSFORMATIONS IN IRON ALLOYS

E.A. Wilson

A thesis submitted in partial fulfilment of the requirements for the degree of Ph.D. in the University of Liverpool.

October 1965.

SYNOPSIS

The gamma to alpha transformation has been studied in pure iron, iron-nickel and iron-chromium alloys. A rapid response thermal-arrest technique was used to determine the variation of transformation temperature with cooling rate. The product of the transformation was examined by optical microscopy and thin film electron-microscopy. Three types of transformation were found depending on composition and cooling rate:-

(a) Massive ferrite.

(b) Massive martensite.

(c) Acicular martensite.

All the transformations were diffusionless in the sense that the product of the transformation had the same composition as the parent.

The massive ferrite transformation was found in Fe-Cr alloys and Fe-Ni alloys containing less than 10% Ni. This transformation occurred up to cooling rates as high as 5,000°C sec^{-1}. The product of the transformation consisted of large irregular grains which crossed the parent austenite grain boundaries. Thin film electron-microscopy showed a high dislocation density and high angle boundaries. The transformation is thought to occur by nucleation at the austenite grain boundaries and rapid growth by short range diffusion.

At higher cooling rates the transformation to massive martensite was obtained. The transformation was also observed at normal cooling rates in Fe-Ni alloys containing 15 to 29% Ni. This transformation

gave rise to parallel surface tilts on a pre-polished surface. Thin film electron-microscopy showed parallel plates containing a high dislocation density. However the individual plates were not revealed by the standard optical metallographic techniques and the structure appeared to consist of irregular grains bounded by straight edges.

The term massive has been used to describe both the massive ferrite and massive martensite transformations since the polished microstructures resemble the microstructures of the massive transformation found in β brasses. But in this study a clear distinction has been made between those microstructures consisting of large irregular grains, massive ferrite, and those with straight edges, massive martensite. The effect of austenitising temperature on the transformation to massive ferrite and massive martensite was also studied.

In iron-nickel alloys containing more than 30% Ni cooled below room temperature acicular martensite was obtained. This is also a martensitic transformation and the structure consisted of large lenticular plates formed at an obtuse angle to each other. Previous work has shown the habit plane to be $\{259\}_{\gamma}$ [9] and thin film electron-microscopy[11,12] showed that the plates were internally twinned on a fine scale.

CONTENTS

1. INTRODUCTION

Since iron forms the basis of steels it is important both from an academic and a practical viewpoint to understand the physical metallurgy of the metal and its alloys. Of particular interest is the manner in which the high temperature phase austenite, changes to the low temperature equilibrium phases. The nature of this phase transformation depends on a wide variety of variables, such as temperature of transformation, cooling rate and alloying additions and is used to impart different properties to steels. The mechanism of the decomposition of austenite has been studied extensively in high carbon steels, and although the general nature of the reactions which occur in steels are well known, the exact details are not very well understood. In contrast to this, comparatively little study has been made of the transformations in pure iron and binary alloys and it is of some interest to see whether the different reactions encountered in carbon steels can also occur in the pure parent metal and its alloys. Further, results obtained on steels are difficult to analyse theoretically and calculations of such parameters as the thermodynamic driving force for the reaction are complicated. In pure binary alloys these calculations are to some extent simpler and the results obtained on pure alloys more ameniable to theoretical analysis. Thus an examination of the transformations which can occur in pure iron and binary alloys may lead to a deeper understanding of the reactions which occur in steels. It was for these reasons that an

investigation of the effect of cooling rate on the $\gamma \rightarrow \alpha$. transformations in pure iron and its binary alloys was made by Gilbert under Professor W.S. Owen. This thesis describes the continuation of those studies.

2. REVIEW OF LITERATURE

2.1. Introduction

To attempt to review the various mechanisms reported for the decomposition of austenite in steels would be an impossible task for the purpose of this thesis. However it appears from the present work, that in the absence of carbon, the decomposition of austenite is generally simpler and two types of transformation can be recognised

(a) Martensitic transformations

(b) Massive transformations.

The review has therefore been confined to these two types of transformations, together with a more particular review of the individual alloy systems studied in this investigation.

2.2. Martensitic Transformations

2.2.1. Definition

Originally reserved for the quenched product found in steel, the term martensite has assumed a more general meaning to describe the product of a phase change which occurs by shearing of the lattice. The most recent definition is that due to Bilby and Christian[1]:- "A structural transformation is classed as martensitic if the atoms on a primitive lattice defined by a selected unit cell of the parent structure moved to positions on a primitive lattice defined by some unit cell of the product structure in such a way that the displacements constitute a homogeneous deformation. This deformation may be different in adjacent small regions."

In practice this means that a shape change is produced in a pre-polished surface[2] as shown in Figures 1 and 2.

The diffusionless nature of the transformation is illustrated by the fact that if the parent phase is ordered then the martensitic product retains the order after transformation and is itself ordered. Thus atoms can only move a fraction of an atomic spacing during transformation. This has been observed in the martensitic transformation in certain brasses[3].

2.2.2. Crystallography

The shear nature of the transformation results in a distinct habit and orientation relationship between the parent and the martensite. In steels and iron alloys various habits and orientation

relationships have been found depending on the composition of the alloy. These are summarised in Table 1. The most frequently reported habit plane in steels are the $\{225\}_\gamma$ and $\{259\}_\gamma$. Mehl and Van-Winkle[18] showed that both the $\{225\}_\gamma$ and $\{259\}_\gamma$ habit occur together in some quenched steels, but the proportion of martensite plates with a $\{259\}_\gamma$ habit increases with carbon content. Recently Entwistle and Brook[23] have shown that the $\{259\}_\gamma$ habit is associated with martensite which is produced in bursts.

The fact that transformation occurs by a shearing of the lattice to give plates of known habit and orientation has resulted in geometrical theories describing the movement of atoms that take place during the transformation. Bain[24] was the first to attempt to explain the atom movements which occurred in the austenite to martensite reaction in steels. He pointed out that the interstitial solid solution of austenite referred to different axis, could be regarded as a body-centred-tetragonal structure. Bain proposed that during transformation a simple compression of the "c" axis and expansion of the "a" axis occurred resulting in the tetragonal martensite structure. It is now known that these simple movements do not adequately explain all the observed features of the transformation. Nevertheless the 'Bain strain' has remained an essential element of theories describing the crystallography of the transformation. The theory was developed in turn by Kurdjumov and Sachs[16], Nishiyama[8] and Greninger and Troiano[17]. These latter workers, who investigated the $\{259\}_\gamma$ habit (more accurately

TABLE I. CRYSTALLOGRAPHY OF MARTENSITE TRANSFORMATIONS IN STEELS

Material	Structural Change	Habit Plane	Orientation Relationship	Remarks and References	Electronmicroscopy Observations
Pure Iron	f.c.c. → b.c.c.	$\{111\}_\gamma$	Possibly K/S	Found by (4) (5) (4) reports some evidence that orientation relationship is K/S.	None.
Fe - Ni 27% Ni to 34% Ni	f.c.c. → b.c.c.	$\{111\}_\gamma$	$(111)_\gamma // (110)_\alpha$ $[110]_\gamma // [111]_\alpha$ (Kardjumov-Sachs relation)	(6) (7) (8) & (9) Considerable scatter in the observed habits and orientation relation. However, in general it would appear from (9) that $\{111\}_\gamma$ habit and K/S relation is observed in alloys transformed above room temperature and $\{259\}_\gamma$ and N. relation in those transformed below room temperature.	Present work and that of (10) shows parallel plates with high dislocation density. (11) & (12) showed martensite obtained on cooling below room temperature is internally twinned with $\{259\}_\gamma$ habit.
		~ $\{259\}_\gamma$	$(111)_\gamma // (110)_\alpha$ $[211]_\gamma // [110]_\alpha$ (Nishiyama relation)		
Fe - C 0-0.4% C.	f.c.c. → b.c.t.(?)	$\{111\}_\gamma$	Presumably K/S	(6) (3) Laths with long direction $<110>_\gamma$ Bowles thought laths represented degeneration of $\{225\}_\gamma$ plates into needles	(14) Observed parallel plates with high dislocation density.
0.5-1. C	f.c.c. → b.c.t.	$\{225\}_\gamma$	K/S relation	(6) (13) (15) (16) (7). With decreasing carbon plates degenerate into laths with axis $<110>_\gamma$	(14) found plates internally twinned in this carbon range.
1.5-1.8% C	f.c.c. → b.c.t.	$\{259\}_\gamma$	Unknown	(6)	
Fe-22% Ni - 0.8% C.	f.c.c. → b.c.t.	Between $(3,10,15)_\gamma$ and $(9,22,33)_\gamma$	$(111)_\gamma$ ~ 1° from $(101)_\alpha$ $[1\bar{2}1]_\gamma$ ~ 2° from $[10\bar{1}]_\alpha$	(17) Precision determination Known as Greninger and Trocano (G/T) relation. Note some workers maintain that N. and G/T relation are essentially the same.	
Fe - 1.2% C - 1.5% Ni	f.c.c. → b.c.t.	~ $\{259\}_\gamma$		(6)	
Fe - C Fe-Ni-C Various high C contents	f.c.c. → b.c.t.	~ $\{225\}_\gamma$ and ~ $\{259\}_\gamma$ occours together	?	(18) Relative amounts of the two habits varied with C content, but also thought to depend on Ms.	(14) Fe-20% Ni - 0.8% C. Predominately $\{225\}_\gamma$ at -95°C and majority $\{259\}_\gamma$ at -195°C Both were internally twinned $\{225\}_\gamma$ obeyed K/S relation $\{259\}_\gamma$ obeyed G/T relation
Fe - 18% Cr - 8% Ni	f.c.c. → b.c.c.	~ $\{225\}_\gamma$ and $\{111\}_\gamma$	K/S	A c. ph. phase ε is also produced in these steels during cooling and deformation. X-ray and metallographic investigation by (20) showed plates were long and narrow bounded by $\{111\}_\gamma$ planes. In the case of the $\{225\}_\gamma$ habit the long direction was $<110>_\gamma$	Electronmicroscopy investigation by (19) showed ε formed from stacking faults. Also intersecting ε plates nucleates martensite (α). Inhomogenous shear markings were observed in plates with $\{225\}_\gamma$ habit.
Fe - 16% Cr - 12% Ni	f.c.c. → b.c.c.	~ $\{225\}_\gamma$	K/S	X-ray investigation by (21) Similar observations to (20)	
(a) Fe-18% Cr -7.5% Ni (b) Fe-16% Cr. - 8% Ni	f.c.c. → b.c.c.	~ $\{225\}_\gamma$ ~ $\{259\}_\gamma$	Possibly K/S	X-ray and electronmicroscopy investigation by (22) Similar observations to (19) and (20) with plates bounded by $\{111\}_\gamma$ planes. Steel (a) had $\{225\}_\gamma$ habit with long direction $<110>_\alpha$ Inhomogenous shear markings were observed on two $\{110\}_\alpha$ planes at 60° to each other. Steel (b) had a $\{259\}_\gamma$ habit. Inhomogenous shear markings on $\{112\}_\alpha$ planes.	

$\{3, 10, 15\}_\gamma$) in an Fe-22% Wi - 0.8% C steel, showed that a second shear by twinning within the martensite plate was necessary to produce the correct relationship. In the last decade these phenomological theories of martensite formation have received considerable attention and developed independently by Wechsler, Liebermann and Read[25] (W-L-R) and by Bowles and Mackenzie[26] (B-M). The essential feature of these theories is that the habit plane remains plane and unrotated during transformation. Hence the shape strain S, which gives rise to the change of shape on a pre-polished surface, is an invariant plane strain. The shape strain S is accompanied by an inhomogeneous strain or complementary strain C, which produces no further volume or shape change. This is achieved by slip or twinning on a fine scale. The total strain T is then given by,

$$T = S \times C$$

In the theory of Bowles and Mackenzie a small dilatation λ is allowed at the interface during the shape strain. Both the theory of B-M and W-L-R successfully predicted the habit plane and orientation relationship found by Greninger and Troiano[17] for the Fe-22% Ni - 0.8% C steel. However the W-L-R theory could not predict the $\{225\}_\gamma$ habit and the theory of B-M required rather a large dilatation, $\sim$1.5% to predict the $\{225\}_\gamma$ habit. For this reason there has been some reluctance to accept the theory of B-M. However, recent direct measurement of the dilatation in martensite with a $\{225\}_\gamma$ habit indicate that the

dilatation does in fact exist and is of this order[27].

Kelly and Nutting confirmed the presence of twinning in high carbon martensites[14] by thin film electron-microscopy. They found two types of martensite:

(1) Large lenticular plates, which were internally twinned on a fine scale,

(2) Laths or needles which contained a high dislocation density and lay in parallel sheets. Single surface analysis indicated that the large axis of the needle was $\langle 111 \rangle_{\alpha}$.

Type 1. martensite was observed in an Fe-20% Ni - 0.8% C steel and in plane carbon steels in the range 0.8% to 1.4% C. In the former case, due to the presence of retained austenite, it was possible to identify the $\{225\}_{\gamma}$ and the $\{259\}_{\gamma}$ habits. Both were twinned and the $\{225\}_{\gamma}$ obeyed K/S relationship, and the $\{259\}_{\gamma}$ the G/T orientation relationship.

Type 2. martensite was observed in a 18/8 stainless steel quenched below room temperature and in plain carbon steels in the range 0.14 to 0.8% C. In the latter case some twinned plates were observed and the proportion of these increased with carbon content. The orientation between needles in a sheet were substantially the same, but in certain cases twin-related needles were found.

2.2.3. Nucleation of Martensite

Various theories have been suggested for the nucleation

of martensite. At one time martensite was thought to be nucleated by pre-existing embryos of ferrite in the austenite[28]. Cohen[29] argued that from statistical considerations there would be local variations of carbon content in the austenite and regions low in carbon may act as nucleating sites. Dislocation arrays and interactions in the austenite are now thought to be the most likely nucleating centres for martensite, at least in stainless steels. Venables[19] has produced some evidence that stacking faults nucleate martensite in stainless steel. This was obtained from thin film electron-microscopy studies on an 18/8 stainless steel. He showed that stacking faults expand to produce the c.ph. phase ϵ and that intersection of these lamellae may act as nucleating sites for martensite (α)

i.e. s.f. in $\gamma \longrightarrow \epsilon \longrightarrow \alpha$.

However more recently Goldman[30] et al have suggested that the formation of the c.ph. phase ϵ in stainless steel may be a result of the large shear strain $\sim 10^0$ associated with the direct $\gamma \rightarrow \alpha$ martensite transformation rather than an intermediate structure in martensite transformations.

2.2.4. Kinetic Behaviour

Considerable undercooling is usually required to start the martensite reaction, at least in steels and iron alloys. In general for a given austenitising temperature, the start temperature M_s for a particular steel is constant for a wide range of cooling rates and cannot be suppressed[31,32]. There are important exceptions to this, which

will be discussed later. The M_s of a steel increases slightly with grain size[33] but is mainly dependent on composition. Figure 3 from the work of Greninger[32] shows the variation of M_s with carbon content in Fe-C alloys. Steven and Haynes[34] determined an empirical formula for the variation of M_s with composition for steels,

$$M_s{}^{\circ}C = 561 - 474\ {}^{w}/_{o}\ C - 33\ {}^{w}/_{o}\ Mn - 17\ {}^{w}/_{o}\ Ni - 17\ {}^{w}/_{o}\ Cr - 21\ {}^{w}/_{o}\ Mo.$$

In the majority of steels martensite forms athermally, that is, martensite only continues to form as the temperature falls. If the temperature is held constant for a while, on continuing the cooling the transformation does not start immediately but at some lower temperature [35,36]. This phenomena is known as stabilisation and is both time and temperature dependent[36]. Philibert[37] found an activation energy of 11,000 cals $mole^{-1}$ for the process and showed that stabilisation depends on carbon (or nitrogen) content and is absent in decarburised specimens.

At one time athermal kinetics was thought to be an essential feature of martensite transformation. However isothermal formation of martensite has now been observed in a number of steels[38-45] and athermal kinetics is no longer thought of as a general feature. Kurdjumov and Maksimova[38] first observed isothermal martensite in a steel containing 0.6% C, 6.0% Mn and 2% Cu. In this alloy it was possible to completely suppress the martensite reaction by rapidly quenching to -196°C. Thus the property of insuppressibility mentioned earlier is not always a

pre-requisite for martensite formation. Fletcher, Averbach and Cohen[49] also observed the slow isothermal formation of martensite in high carbon tool steels at room temperature. Isothermal martensite has been observed in the absence[42] and the presence[90,91] of athermal martensite. In the latter case it has been observed to form above and below the athermal M_s[41]. In general isothermal martensite obeys a "c" curve relationship[41,42] and occurs by nucleation of new plates[39,40] rather than by growth of pre-existing plates. Isothermal martensite has been observed in other systems such as Uranium-chromium[46], however in this case martensite forms by slow growth and thickening of existing plates as well as nucleation of new ones.

Since the martensite reaction occurs by shear it is to be expected that the reaction will be effected by applied stress. It is well known for example that deformation raises the M_s in stainless steels[47]. The results of more quantiative work considering both elastic and plastic stresses and the amount of deformation are to some extent conflicting[48,49]. However in general it would appear that both plastic and elastic stresses can raise M_s to a limiting value, M_d[49,50,51]. At large amounts of deformation, slip occurs rather than martensite formation[51] and this retards the formation of martensite.

The martensite transformation is completely reversible. This cannot be observed in most steels since it is not possible to heat them fast enough to prevent the decomposition of martensite by other processes. However the phenomena has been observed in certain alloys where the M_s

temperature is below room temperature and the reverse transformation can be observed by rapid heating and subsequent cooling to room temperature. G. Khandros and Y.M. Golovchiner[52] have observed the reverse martensite transformation in pre-polished specimens of Cu-24.6% Sn and Fe-29.0% Ni respectively. They found that the individual martensite plates reverse to the parent phase producing surface relief in the opposite sense. Moreover the martensite plates which form first in cooling are the first to reverse in heating. Thus the reverse transformation is itself martensitic and starts at a particular temperature. In iron alloys the transformation usually occurs with considerable hysterisis, the reverse transformation temperature A_s, being generally a few hundred degrees higher than M_s[51].

The speed of formation of individual martensite plates is usually extremely rapid. This was originally measured by Scheil and Forster[53] in an Fe-2.9% Ni alloy transformed below room temperature. They estimated the time of propagation of an individual plate to be less than 7×10^{-5} seconds and called the reaction "Umklappvorgangen" or "Click-over reactions" as they had demonstrated earlier[54] that an accoustical click accompanies the reaction. Bunshah and Mehl[55] have since repeated the experiments on the same alloy and found the time of formation to be 3×10^{-7} seconds and the rate of propagation 3,300 ft/sec, which is the order of speed of sound for this material. However it is not true to say that martensite always grows at this speed. In their original paper[53] Scheil and Forster also measured the speed of a

reaction which they called "Schiesbungumwandlungen" or "Slip reactions". This was observed in Fe-Ni alloys containing less than 25% Ni reacted above room temperature. The reaction had a different morphology to the "Umklapp" reaction and proceeded in a slow continuous manner, whereas the growth of the "Umklapp" reaction was rapid and discontinuous. The reaction does however seem to possess some of the characteristic of the martensite reaction. Slow isothermal growth of martensite has also been observed in uranium-chromium alloys[56].

2.2.5. Kinetic Theories

The fact that the martensite reaction is reversible means that the transformation can be treated by classical thermodynamics. This lead to the concept of a temperature T_o at which the difference in chemical free energy between austenite and martensite, $\Delta G^{\alpha \rightarrow \gamma}$ is zero[56,57]. Above this temperature transformation to martensite cannot occur since this would lend to an increase in free energy. Below T_o transformation to martensite is possible as this results in a lowering of free energy.

Early workers envisaged small embryos or nuclei of martensite in the austenite[28,29]. On cooling below T_o these were assumed to be thermodynamically stable but not able to grow due to surrounding constraint. However at M_s it was thought the driving force $\Delta G^{\alpha \rightarrow \gamma}$ exceeded the energy arising from these constraints and the plate was "triggered" or released to its full size[29]. The athermal nature of the transformation was explained by the martensite plates partitioning the austenite, thus

restricting the size of succeeding plates. These then required a greater driving force for propagation which was achieved by a fall in temperature.

The discovery of isothermal martensite resulted in the transformation being treated as a classical nucleation and growth process. Since the growth of individual plates is often extremely rapid it was thought that the activation energy for growth is essentially zero and the critical event is nucleation. The occurrence of athermal transformation was explained by assuming that the nucleation rate (N) was strongly temperature dependent. In Fe-Ni alloys Fisher[58] assumed that M_s is the temperature at which $\dot{N}$ is one nucleus/cc/sec. Thus, on this assumption, at temperatures close to M_s martensite can be thermally activated. At higher temperatures $\dot{N}$ is so small that isothermal transformation is not observed in reasonable times while at lower temperatures $\dot{N}$ is so large that nucleation is not usually suppressed by rapid cooling. However this theory predicted a lower temperature limit to martensitic formation and it was destroyed by Kaufman and Cohen's[59] observation of an M_s temperature of 50°K in an Fe-33 a/o Ni alloy.

In the next development of the theory the transformation was treated as being hetrogeneous, rather than homogeneous. By assuming that nucleation occurs at preferred sites, the amount of energy required for nucleation was considerably reduced[60]. However even this was insufficient to account for the extremely low value (6,500 - 14,000 cals $mole^{-1}$) of the activation energy which was observed experimentally over the complete

temperature range of transformation[61].

Finally Kaufmann and Cohen[60] did a detailed analysis of the energy required to expand the dislocations at the interface of the martensite nucleus. In essence, they calculated an activation energy for growth as a function of nucleus size. It was assumed that the starting nucleus already possessed a size which was critical on the old homogeneous theory. However they found that further energy was required to expand this nucleus and the energy required for each growth step (i.e. expansion of the dislocation loop by one Burger's vector) increased with size of the nucleus to a maximum value (ΔW_*^1) and then decreased to zero. Thus once the size of the nucleus exceeds that corresponding to ΔW_*^1 catastropic growth occurs and the plate grows to full size. On continuous cooling M_s can be identified with this event and on isothermal holding the observed activation energy is ΔW_*^1. An interesting point about this theory, was that the problem of nucleation was avoided, by considering only the initial growth of existing nuclei, rather than the production of a nucleus of critical size or the statistical number of these nuclei in existence. That is the theory did not predict the length of the incubation period, but only the initial rate of reaction after this period. This is in fact what is measured experimentally. However the theory requires the existence of rather large embryos (about 200°A diameter) in the austenite at temperatures near M_s. Richman et al claimed to have seen embryos of this size by transmission electron-microscopy in Fe-30% Ni. However Gaggero and Hull[12] showed

that these were fine twins associated with a martensitic phase produced spontaneously during thinning. In fact their work showed that martensite was produced above M_s by thinning due to the removal of the surrounding constraints. As stated earlier recent experiments[19] suggest that the nucleation of martensite occurs by dislocation interactions rather than the existence of large embryos in the austenite. Nevertheless the basic concept behind Kaufman and Cohen's theory is probably correct and could be applied to these more sophisticated dislocation movements.

2.3. Massive Transformations

This type of reaction was first observed in alloys of β brass. Since the alloys studied in this investigation were found under certain circumstances to transform by a similar mechanism, this type of transformation is reviewed briefly. For the sake of clarity the review has been divided into work on individual alloy systems rather than describing the literature in strict chronological order. Studies on the martensite transformations observed in these alloy systems are also included.

2.3.1. Copper-Zinc alloys

The massive reaction was first encountered by Philips[63] in studying the decomposition of β brass. The Cu-Zn system is shown in Figure 3, the temperatures at 453°C and 470°C are the ordering temperatures for f.c.c. β brass. In low zinc alloys slow cooling from the β region resulted in decomposition into equilibrium ($\alpha + \beta$). However on rapid quenching an alloy containing 38% Zn transformed into large units of α without any change in composition. This was the massive α structure although this description was actually not applied until a later date. Philips also found that at zinc contents higher than 38% the β phase could be retained by rapid quenching. Subsequent work[64,65] showed that on cooling below room temperature the α phase transforms martensitically into a lattice of low and uncertain symmetry. More recently Jolley[66] has examined the martensitic structure by electron-microscopy and found the structure to be orthorhombic. He also observed that the plates are heavily faulted. These were thought to be microtwins.

The work of Hull[67,68] showed that for an alloy containing 39% Zn, the $\beta \rightarrow \alpha_2$ reaction., that is the massive transformation, could be supressed by judicious choice of quenching mechanism. The massive α_2 nucleates at the β grain boundaries or on equilibrium α needles growing into the β matrix. Typical microstructures taken from this work are shown in Figures 4 and 5. The massive α areas on the photomicrographs are enclosed by jagged boundaries made up of straight sections. Single surface trace analysis indicated that these were parallel to planes of low index.

2.3.2. Copper-Aluminium

The name 'massive' was actually first applied by Greninger (1939)[69] to an analogous transformation in a Cu-7.3% Al alloy. Greninger's microstructure is reproduced in Figure 6 together with the Cu-Al diagram. Similarly to β brass alloys it was found that at higher aluminium concentrations the massive α reaction could be suppressed and a martensitic product obtained. In this case the M_s temperature is above room temperature ~~boundary~~. In Figure 7 the variation of M_s with composition[70] has been superimposed on the phase diagram. Analysis of the crystal structure of the martensite proved difficult, Recently however, Swann and Warlimont[71] have shown that three different crystal structures are obtained depending on composition as shown in Figure 7

β^1 is f.c.c.

β_1^1 is ordered tetragonal being derived from ordered β

γ^1 is also orthorhombic also being derived from ordered β.

The martensites were also examined by electron-microscopy and their work showed that the β^1 and β_1' martensites were internally faulted and the γ^1 internally twinned.

2.3.3. Copper-Gallium

Early workers[72,73] found a massive transformation in copper-gallium alloys at compositions near the eutectoid. The relevant portions of the phase diagram are shown in Figure 9. In this case the β phase (b.c.c.) transforms to a massive ζ_s (h.c.p.) structure on quenching. Figure 10 is taken from the work of Spencer and Mack[74]. Similarly to β brass and the copper aluminium alloys, on rapid quenching into iced brine a martensite reaction is produced together with massive ζ_s. The structure of the martensite appears to be unknown and has received little attention.

By quenching to temperatures below the euctectoid horizontal, holding for short periods and subsequently quenching to room temperature Spencer and Mack were able to show that ζ_s formed isothermally and the reaction sequence

$$\beta \rightarrow \zeta_s \rightarrow \underbrace{\zeta + \gamma}_{\text{equilibrium phases}}$$

occurred.

Examination of a hyper-eutectoid alloy quenched from the two phase field ($\beta + \gamma$) indicated that ζ_s nucleates at the β grain boundaries. Massalski[75] examined a number of binary and ternary alloys of Cu-Ga in his study of the massive reaction and distinguished two extremes of

microstructure.

(1) Large ζ_s grains with incoherent boundaries. By observing the precipitation of γ rossettes in the β prior to transformation he was able to show that the massive ζ_s structure crossed prior β grain boundaries and consumed a number of β grains. These observations also indicated that there was no orientation relation between the original β and the ζ_s structure. Occasionally two adjacent ζ_s grains would be separated by a straight interface and in this case the grains were found to be twin related, but more usually the microstructure appeared as large grains separated by uniform boundaries with no straight edges, apart from long internal twins. An example of this type of microstructure is shown in Figure 11.

(2) Small ζ_s grains with straight edges and coherent boundaries. This was usually observed in alloys of low gallium content. Figure 12, taken from Massalski's paper is an example of this structure.

Massalski concluded that the massive transformation occurred by nucleation and rapid growth of an incoherent boundary. However for certain compositions and quenching rates some ζ grains may nucleate coherently and grow by a mixture of shear and short range diffusion.

Massalski finally summarised the observed features of the massive transformation as follows:-

"(1) The massive type of transformation occurs in many alloy systems and is intermediate in structural relationship, metallographic features and the amount of diffusion required between the normal nucleation and

growth and martensite transformations.

(2) The structure obtained by massive transformations studied so far corresponds with the structure of an equilibrium phase already present in the phase diagram and supersaturated to compositions which lie outside its normal homogeneity limits.

(3) In the extreme and the most striking form the massive transformation involves no crystallographic relationship with respect to the parent phase and in such cases it is extremely difficult to nucleate but once it is nucleated it proceeds by a very rapid growth of incoherent boundaries. In certain cases, however, to overcome the nucleation difficulty, partially coherent nucleation resembling martensitic nucleation can take place, and be followed by incoherent growth.

(4) If the massive transformation is suppressed by a rapid quench, a typically martensite phase is obtained upon further cooling."

2.3.4. Other Systems

Massive transformations have been reported in other eutectoid alloys. These include Cu-9.0% Si[76] and Ag-Cd[77]. In the latter alloys it is interesting to note that isothermal holding results in the precipitation of equilibrium α in parallel striations within the massive γ_s grains.

2.3.5. Summary

Massalski's summary of the massive transformation was a fairly clear statement of our knowledge concerning this reaction at that time. It would appear that the main criterion for the description massive

being applied to a reaction is its diffusionless nature giving a supersaturated solid solution. A second criterion is the 'massive' appearance of the microstructure. However it is evident that some quite different microstructures have been included in the term massive. These range from microstructures consisting of large grains with irregular boundaries to those with blocky areas bounded by straight edges. The crystallographic nature of this latter structure suggests that it may be formed at least in part, if not completely by shear. Most authors however discount the possibility of the massive transformation occurring martensitically, to some extent without experimental justification. In this respect there does not seem to have been any serious attempts to see if surface tilts are produced by the transformation.

A common feature of the massive transformations reviewed here is that at certain concentrations and quenching rates the massive reaction can be suppressed and a martensitic structure obtained at lower temperatures. The martensite plates are large and lenticular with an irrational habit and those studied so far by electron-microscopy have proved to be faulted.

2.4. Transformations in Iron Alloys

2.4.1. Pure Iron

Under normal cooling conditions the austenite to ferrite transformation occurs by nucleation and growth to give an equi-axed structure. However in 1929 Sauveur and Chou[78] showed that very rapid cooling from the austenite resulted in a martensitic structure. On a pre-polished specimen these appeared as sheets of parallel plates (or needles). Mehl and Smith[4] later showed that the habit plane of these was $\{111\}_\gamma$ and also reported some evidence that orientation relationship was Kurdjumov-Sachs. More recently Entwistle[5] has observed martensite in iron containing 0.007% (C + N) and Wayman and Altstetter[79] in zone refined iron[16]. Both report a $\{111\}_\gamma$ habit plane.

No determinations of the martensite start temperature in iron were made prior to the work of Duwez[80], although a value of 550°C is to be expected from an extrapolation of Greninger's M_s data for Fe-C alloys[32], Figure 13. Duwez studied the variation of the start temperature for the $\gamma \rightarrow \alpha$ reaction in iron containing 0.001% C with cooling rate. He employed a gas quenching and thermal arrest technique similar to that of Greninger. Duwez obtained a broad band of transformation temperatures varying from 900°C to 750°C. The lowest transformation temperature obtained was 750°C at cooling rate of $\sim$ 12,000°C sec^{-1}. Gilbert[81] whose work is described later in greater detail, obtained a value of 545°C at 5,500°C sec^{-1} in iron containing 0.010% C. Srivastara and Parr[82] obtained a value of 517 $\pm$ 5°C at 8,000°C sec^{-1} in iron

containing 0.005% C.

2.4.2. Iron-Nickel.

The iron rich end of the Fe-Ni diagram is shown in Figure 14. On cooling from the austenite a supersaturated b.c.c. structure, designated α_2, is obtained at all concentrations. This is due to the extreme sluggishness of the $\gamma \rightarrow (\alpha + \gamma)$ reaction and led to considerable inaccuracies in early determinations of the diagram. However annealing of supersaturated alpha in the two phase region results in decomposition into equilibrium ferrite and austenite. By this means Owen and co-workers[83,84,85] were able to establish the diagram above 300°C fairly accurately. The lower regions of the diagram have been predicted by thermodynamic calculation[86,87] and at higher temperatures the observed phase boundaries are in good agreement with the theoretical calculations.

Early workers found that transformation of high nickel alloys in the range 25 to 32% Ni below room temperature resulted in a martensitic transformation. Nishiyama[8] determined the orientation relationship and found it to be

$(111)_\gamma$ // $(110)_\alpha$)
$[211]_\gamma$ // $(110)_\alpha$) This is generally known as the Nishiyama relationship

and the habit plane $\{259\}_\gamma$.

Mehl and Derge[9] observed a different relationship in alloys transformed above room temperature, that of Kurdjumov-Sachs. The microstructure was also different and thought to be the same as the

Widmanstatten structure observed in meteorites with a $\{111\}_\gamma$ habit.

As mentioned earlier Scheil[53] also noted that alloys containing less than 25% nickel transformed by a different reaction to those containing more than 25% nickel and which transformed below room temperature.

The martensite reaction obtained on cooling high Fe-Ni alloys below room temperature has also been studied by thin film electron-microscopy[11,12]. It was found that the martensite plates are internally twinned on a fine scale. Shimizu[11] also confirmed that the orientation relationship is that found by Nishiyama[8] and the habit plane is $\{259\}_\gamma$.

Numerous determinations of the temperature of the $\gamma \rightarrow \alpha_2$ transformation and the reverse transformation $\alpha_2 \rightarrow \gamma$ on continuous heating and cooling have been made. All are agreed that the reaction is diffusionless and transformation temperature is independent of cooling rate. Kaufman and Cohen[87] redetermined these temperatures which they termed M_s and A_s, since they thought the transformations studied were martensitic. Moreover they carried out a rigorous thermodynamic analysis of the results using a regular solution model. They showed that $T_o = \frac{1}{2}(M_s + A_s)$, and the driving force for the martensite reaction at M_s and A_s were equal (but of opposite sign). From the experimental data, it was deduced that this driving force increases with nickel content from a low value of 20 cals mole^{-1} in low nickel alloys to 300 cals mole^{-1} in alloys reacted below room temperature. In high

Fe-Ni alloys T_o was more accurately defined by determining M_d and A_d. Haynes[88] later criticised the description of martensitic being applied to dilute Fe-Ni alloys on the grounds that the measured transformation temperatures were too high and did not conform to his empirical equation for M_s in steels.

2.4.3. Gilbert's work

Gilbert[81] studied the $\gamma \rightarrow \alpha$ transformation in a series of binary alloys of Fe-Ni (up to 15% Ni), Fe-Cr and Fe-Si. He used a gas quenching and thermal arrest technique similar to that of Greninger[32] and Duwez[80]. The highest cooling rate obtainable, using Helium was 5,500°C sec^{-1}. He found that for the iron-chromium series the transformation temperature was depressed with increasing cooling rate to a constant value as shown in Figure 15. Similar results to those in Figure 15 were obtained for the Fe-Ni and Fe-Si alloys, except in iron where at high cooling rates a much lower transformation temperature of 545°C was obtained. The chemical driving force $\Delta G^{\alpha \rightarrow \gamma}$ at the plateau temperature was computed from a regular solution model similar to Kaufman's[87] analysis. The driving force increases linearly with atomic percent solute from ~20 cals $mole^{-1}$ to ~80 cals $mole^{-1}$ at 10 atomic percent solute. This was small compared with the driving force ~300 cals $mole^{-1}$ for the martensite reaction. At the time it was not clear what type of reaction had been measured. Although x-ray work showed it was diffusionless it was not thought to be martensitic due to the low driving force and small degree of undercooling, but probably

similar to the massive transformation observed in β brasses.

2.4.4. Iron-Chromium.

The iron rich end of the iron-chromium diagram consists of a gamma loop with a minimum at 8.5% Cr. There appears to have been little work on the $\gamma \rightarrow \alpha$ transformation in iron-chromium alloys prior to Gilbert's studies. The only other studies are that of Kogan and Entin's[89] on an alloy containing 8.5% Cr and 0.05% C. By using a magnetic method they managed to obtain a TTT diagram for the $\gamma \rightarrow \alpha$ transformation in this alloy. This diagram is reproduced in Figure 16. In Figure 17 the plateau temperatures obtained by Gilbert for his iron-chromium alloys are plotted as a function of chromium content. Also included on the same diagram is the temperature at the nose of Entin's "C" curve. It will be seen that this falls near the same straight line joining Gilbert's results and thus the reaction measured by Kogan and Entin is the same as that studied by Gilbert. It is now apparent that the plateau temperatures determined by Gilbert under athermal conditions correspond to the maximum rate of transformation determined under isothermal conditions.

3. EXPERIMENTAL PROCEDURE

3.1. Specimen Material and Preparation

3.1.1. Iron

The iron used in this investigation was vacuum melted iron ARL8, obtained from B.I.S.R.A. This was supplied in the form of ½" rod and the analysis is given in Table 1.

The surface scale on the iron was first removed and the material machined to 0.040" diameter. Short lengths of the material were then annealed for approximately 3 hours at 800°C under a dynamic vacuum of 10^{-5} mms Hg. Subsequently the rod was reduced by swaging and drawing to 0.010" diameter wire. During wire drawing the ends of the wire have to be reduced to enable them to pass through the drawing dies. It was found that this was most easily achieved by thinning the ends of the wires in a solution of 45% nitric acid, 5% hydrochloric acid and 5% water.

3.1.2. Fe-Ni alloys

Alloys of the composition shown in Table 2 were available in the form of 0.040" diameter wire from Gilbert's work. These were originally prepared by Mond Nickel by powder metallurgy and are thought to be of high purity. A small amount of Fe-Ni alloys of higher composition from the work of Kaufman, was kindly supplied by M.I.T. The compositions and sizes of these are shown in Table 3.

Before drawing down to wire the Fe-Ni alloys were homogenised at

1,000°C for 3 days under a dynamic vacuum of 10^{-5}mms of Hg. To ensure correct homogenisation the specimens were heated and cooled fairly rapidly through the two phase region to prevent the reaction, $\alpha_2 \rightarrow (\alpha + \gamma)$ occurring[90]. This was achieved by allowing the annealing furnace to reach the required temperature before rolling it into position around the silica tube containing the specimen. At the end of the annealing period, the furnace was rolled clear of the silica tube and the specimen allowed to cool under vacuum.

After this treatment the material was drawn down to 0.010" diameter wire as described previously. Some of the specimens were required in the form of strip for thin film electron-microscopy or examination of pre-polished surfaces. For this purpose the wire was first drawn to a constant diameter and then rolled to the required thickness in jewellers rolls. With care the resulting strip had a uniform width and thickness and could then be heated uniformly by an A.C. current in the apparatus.

3.1.3. Fe-Cr alloys

Some of the Fe-Cr alloys from Gilbert's work were still available. These had kindly been prepared by Manlabs and were in the form of 0.0100" diameter wire and required no further treatment. Compositions and purity are shown in Table 4.

TABLE 1

Analysis of B.I.S.R.A. Iron ARL8

C	Si	Mn	S	P	Ni	Cr	Mo W V Ti Co Cu Al	O_2
0.011	0.02	0.01	0.008	0.002	0.01	0.01		0.009

TABLE 2

Dilute Fe-Ni Alloys. (Mond Nickel)

Nominal Composition	Actual Composition		
	Weight %	Atomic %	C
1%	1.00	0.96	0.010
2%	2.00	1.9	0.010
4%	3.95	3.74	0.010
6%	5.95	5.72	0.010
8%	8.10	7.65	0.01
10%	9.95	9.57	0.010
15%	15.05	10.43	0.010

TABLE 3

High Fe-Ni Alloys. (M.I.T.)

Composition		Size
w/o	a/o	
19.80	19.0	Small pieces of 0.062" diameter rod about 2 to 4" long
24.65	23.75	
31.25	30.20	
32.85	31.75	

TABLE 4

Fe-Cr Alloys. (Manlabs)

Nominal Cr Content	Actual Composition		
	Wt.% Cr	At.% Cr	C w/o
2.5	2.4	2.57	0.006
5.0	4.3	4.60	0.008
7.5	6.3	6.73	0.008
10.0	9.4	10.02	0.006

3.2. Quenching Apparatus

The quenching apparatus was essentially the same as that used by Gilbert, although it has been modified considerably to increase the maximum attainable cooling rate and ease of operation. In brief the apparatus enabled a wire or strip specimen to be austenitised by A.C. self resistance heating under vacuum and subsequently to be cooled very rapidly by gas quenching. Temperature was measured by a thermocouple spot welded to the specimen surface and the cooling curve recorded by means of an oscilloscope and camera. The apparatus is most conveniently described in two parts, that is,

(a) The vacuum system and quenching arrangement,

(b) The heating circuit and the associated equipment for temperature measurement.

3.2.1. Vacuum system

The vacuum system was constructed as far as possible of glass. A schematic diagram of the apparatus is shown in Figure 18. The vacuum chamber was evacuated by a three stage mercury diffusion pump backed by a rotary pump. A cold trap surrounded by liquid N_2 was placed between the vacuum chamber and the diffusion pump to condense any mercury carried over from the diffusion pump. Provision was also made for roughing pump the vacuum chamber and two glass taps were included in the vacuum circuit for this purpose. The vacuum was usually checked by a Pirani gauge which fitted a B14 cone. From time to time the Pirani was replaced by an ionisation gauge to obtain an absolute reading of the

vacuum. One of the major modifications to Gilbert's apparatus was the introduction of a magnetic valve for gas quenching. This enabled a good vacuum to be maintained in the system during austenitising and the heating current to be switched off at the same time as the magnetic valve was opened. A mercury manometer was also included and during quenching this allowed the excess gas to bubble off to the atmosphere.

The specimen holder is shown in Figure 19. This consisted of 6 tungsten 1½ mm rods sealed into a B34 glass cone. Two of these rods carried the heating current to the specimen, another two carried the thermocouple e.m.f., while the other two leads (which are not shown) were used for carrying the e.m.f. from potential probes during resistance experiments (see Section 3.3.). The specimen in the form of wire or strip, usually about 3 or 4" long, was clamped between two terminals. Temperature was measured by 0.002" diameter chrome-alumel thermocouples spot welded to the centre of the specimen, and was so arranged as to lie under the centre of the gas quenching nozzle. The thermocouple wires were in turn spot welded to two tungsten rods and were carried to these from the specimen by fine silica tubes.

3.2.2. Heating and temperature measuring circuits

The heating circuit for the specimen is shown in Figure 20. This consisted of a variac controlling the input to a low voltage transformer and enabled the temperature of the specimen to be controlled to $\pm 10^{\circ}C$ or better, during austenitising. It should be noted that it was necessary for the secondary of the transformer to be fully insulated

from the primary since the thermocouple T_1 was earthed to minimise A.C. pick up. A D.P.D.T. switch was also included in the circuit so the heating current could be replaced by a constant D.C. current for resistance measurements (see Section 3.3.).

During heat treatment the temperature of the specimen was observed with a Pye potentiometer, and manually controlled using the variac in the heating circuit. The usual austenitising period was about 5 minutes. If the heating current was switched off the specimen cooled by radiation at a cooling rate $\sim 100^{\circ}C\ sec^{-1}$. Under these conditions the cooling curve could be recorded on a 50 mV f.s.d. Honeywell-Brown recorder (response time, one second). It was also found that, if the variac in the heating circuit was left at the same setting used for austenitising the specimen, on re-switching the heating current on again the heating curve could be followed on the recorder. By this means the temperature of reversal of ferrite to austenite could be noted from the thermal arrest. This was usually called γ_s.

For higher cooling rates gas quenching was used, in this case the magnetic valve was opened at the same time as the heating current was switched off and the cooling gas allowed to pass through the diffusion pump. For cooling rates $\sim 2,000$ to $3,000^{\circ}C\ sec^{-1}$ argon was used, while for higher cooling rates helium was normally used, although towards the end of the experimental work it was found that equal cooling rates could be obtained, with comparative safety, using hydrogen.

During gas quenching the cooling curve was recorded using an

oscilloscope and ciné camera. In this case the same equipment as developed by Gilbert[81] was used. The thermocouple e.m.f. was fed to a D.C. amplifier and the output displayed on the oscilloscope. To reduce A.C. pick up the leads carrying the thermocouple e.m.f. from the apparatus consisted of co-axial cable. The outer screen cable was earthed and was connected to thermocouple T_1. During cooling a ciné camera attached to the front of the oscilloscope recorded the movement of the spot and hence obtained a record of the cooling curve. Since the D.C. amplifier developed by Gilbert drifted slowly with time, the thermocouple was shorted immediately after quenching to provide a zero line on the film. The deflection of the spot was then calibrated by recording a series of constant potentials supplied from the potentiometer, spaced at 5mV intervals. After development and drying the film was measured using a travelling microscope and the temperature of the arrest found by interpolation. Since the maximum deflection on the 35 mm. film was $\sim$50mV ($\simeq$1230°C) this meant that the temperature could be easily measured to $\pm$10°C. The cooling rate was measured at the thermal arrest usually over a time interval of 0.04 seconds. It should be noted that since the cooling curve is not generally linear but slightly curved, the cooling rates were usually much greater at higher temperatures than those given in the text.

3.3. Resistance Measurements

The thermal arrest technique enables the start temperature of a reaction to be measured but only gives some slight indication of the subsequent form of the transformation. It was therefore thought desirable to try and supplement the cooling curves with the measurement of some other property which would give some indication of the progress of the transformation.

Continuous recording of resistance of the specimen is a convenient way of achieving this, since the resistance of the two phases austenite and ferrite differ at a given temperature (except of course for one particular temperature). Thus during transformation the resistance changed in a manner which can be related to the percentage of ferrite formed at that temperature. Care has to be taken in the experimental procedure so that spurious effects due to temperature gradients and potential pick up do not occur. These effects are difficult to eliminate at high cooling rates and also one is limited by the response time of the recording instruments. However it was found possible to obtain simultaneous measurements of resistance and temperature at the slower cooling rates obtained by radiation cooling. The technique adopted was similar to that used by McReynolds[48] in his study of martensite in high carbon steels. In the present experiments a 0.106" diameter wire specimen, approximately 8" long was used. A thermocouple was spot welded to the centre of the specimen and two potential probes of thermocouple wire T_1 were spot welded either side of the thermocouple with a separation

of approximately 0.40" (1 cm). By use of the D.P.D.T. switch in the heating circuit, the A.C. heating current could be replaced by a constant D.C. current. Since the resistance of the specimen is small compared with the variable resistance in the D.C. circuit, the measuring current, which was ~50mA, remained constant during cooling. Thus the potential difference from the probes was directly proportional to the resistance of the specimen. The output of the potential probes was fed to a Honeywell-Brown recorder with an f.s.d. of 20mV while that of the thermocouple to another recorder with an f.s.d. of 50 mV. Both instruments had a response time of one second. The switches of the chart motors on both recorders were short circuited by a D.P.D.T. switch so that the two charts could be run simultaneously. After one cooling cycle the run was repeated with the D.C. current reversed. This was to eliminate any thermal effects due to temperature gradients and any possible potential pick up by the thermocouple, which may have arisen from a slight separation of the thermocouple leads. From the two charts, showing the variation of temperature and potential (i.e. resistance) with time it was then possible to construct a composite graph of resistance against temperature. Examples of these are shown in Figures 21 to 25. Included on the right hand side of each graph is the time scale during cooling. This gives some indication of the speed at which the reactions occurred.

3.4. Metallography

3.4.1. Optical metallography

Metallographic examination of these alloys proved difficult and specimens showed scratches even after polishing on a diamond wheel. Electropolishing was found to be the most satisfactory method for obtaining good micrographs. For this purpose a D.C. polishing set was built. This consisted of a 125 ohm variable resistance in series with a milliammeter and the polishing cell. A variable D.C. voltage 0-110 volts was available from a laboratory supply.

Before electropolishing specimens were usually mounted and polished, finishing with polishing on a 3μ diamond wheel. They were then electropolished in a chromic/acetic solution of the following composition(91)

Glacial acetic acid	133 ccs
Chromium trioxide CrO_3	25 grams
Water	7 ccs

This solution was contained in a stainless steel beaker which also served as the cathode, and a needle was used to make electrical contact with the specimen. A current density of approximately 100 to 150mA/sq cm was used with a closed circuit voltage of 25-30 volts. After electropolishing specimens were rinsed in glacial acetic acid, followed by water and alcohol. Since electropolishing tended to etch the specimen slightly it was only necessary to finally etch the specimen in ½% nital. Micrographs were taken in a Reichert projection microscope. It was difficult, however, to apply this electropolishing procedure to wire

specimens, due to their small size. In this case it was found that reasonable microstructures could be obtained by finally polishing with B.C.I.R.A. cream or fine alumina. With this procedure 5% nital was usually required to etch the specimens.

3.4.2. Thin-film electron-microscopy

In order to examine the structure by electron-microscopy, specimens in the form of thin foil ~0.002" thick by ≏ 3/8" wide were heat treated in the apparatus. As described in Section 3.1., uniform foil could be obtained from wire by careful rolling. These specimens could then be heated in the apparatus and the transformation temperature noted from the cooling curve. After heat treatment the specimens were cut in half and the central portion of the specimen near the thermocouple electrolytically thinned for examination in the microscope. The exact procedure used was as follows:-

The end of the specimens were first reduced to a long thin point, like a spear-head, by polishing in perchloric/acetic solution. This consisted of 10 parts of glacial acetic acid to 1 part perchloric and was used with a close circuit voltage of 35-40 volts and a current density of approximately 0.05-0.10 A/sq cm. With this solution polishing and thinning occurs fairly rapidly and the correct polishing conditions are obtained when a brown viscous layer appears on the specimen. A similar washing procedure to that used with the chromic/acetic solution was adopted. The specimen was then finally thinned in a chromic/acetic solution using the polishing conditions described previously. In this case

polishing occurs fairly slowly and it is possible to obtain closer control over the final thinning of the specimen. Thin portions of the material were then cut off from the end of the foil and examined in an EM6 electron-microscope.

4. EXPERIMENTAL RESULTS

4.1. Metallography

As discussed in Section 2.4., earlier work indicated that a number of different microstructures could be obtained in Fe-Ni alloys depending on such variables as composition and heat treatment. As a preliminary survey Fe-Ni alloys ranging from 0 to 32% Ni were transformed at approximately the same cooling rate and examined by optical and transmission electron-microscopy. Basically three types of microstructures were distinguished:

(1) 'Massive ferrite'

(2) 'Massive martensite'

(3) 'Acicular martensite'

4.1.1. Massive ferrite. (Equi-axed massive α).

This structure was obtained on transforming Fe-Ni alloys containing up to 10% Ni. Specimens were cooled $\sim 100^{\circ}C\ sec^{-1}$ and the transformation temperature was noted from the cooling curve. The observed transformation temperatures were in good agreement with those of Gilbert[81]. A typical microstructure of the product is shown in Figure 26. The term 'equi-axed massive alpha' has also been used to describe the appearance of this structure and to distinguish it from massive martensite (see Section 4.1.2.). However in a strict sense this is not a true description of the structure since the ferrite grains tend to be large and irregular rather than characteristic of annealed material. It appeared that there is some substructure within the large grains. Although

repeated etching tended to reveal this, the main grain boundaries became stepped and the structure difficult to photograph. Examination by thin film electron-microscopy showed high angle boundaries and quite a high dislocation density. Occasionally large areas were observed fairly free of dislocations, however there was a tendency for dislocations to be seen near grain boundaries. Tangles of dislocations were frequently observed. Figures 27 and 28 show electron-micrographs taken from an Fe-6% Ni alloy cooled $\sim 300^{\circ}C\ sec^{-1}$ which transformed at 630°C.

Examination of transformed pre-polished specimens showed only the prior austenite grain boundaries which had been revealed by thermal grooving. By etching the specimen in nital it was possible to reveal the ferrite grain boundaries. These were observed to cross the parent austenite grain boundaries in a random fashion (Figures 27-32).

4.1.2. Massive martensite

This type of structure was observed in alloys ranging from 15 to ~ 25% Ni. Transformed pre-polished specimens showed surface shear markings. These were confined to the original austenite grains and there was a distinct tendency for plates to lie in sheets. A typical microstructure is shown in Figure 33. Transmission electron-microscopy revealed a similar structure. Parallel plates were observed with a heavy dislocation density - see Figures 34 and 35. It was also noticed that the boundaries of the plates were not entirely straight, but slightly wavy. This is in contrast to the martensite plates which are internally twinned, in this case the boundaries are perfectly plane. This aspect

is considered further in the Discussion. Selected area electron-diffraction showed the same pattern from sheets of parallel plates and twin spots were not observed, indicating that there was only a small orientation difference between plates. However the possibility of the plates being twin related was not completely eliminated. This is because, even when twins are present, for a number of orientations of the foil and twinning plane, the spots from the two twin related parts of the lattice coincide. The width of the plates seen in the electron-microscope varied between 0.2 and 1.0 μ although an average width of 0.25 μ was more usually observed. This was in reasonable agreement with the width of the surface shears observed on the pre-polished specimens ($\sim$1.0 μ).

A large number of foils were examined and only plates were observed, never the cross-section of a needle. Thus, it is concluded that plates were in fact seen rather than longitudinal section of a needle. The plates are probably thin laths $\sim$ 1.0 μ wide and 0.25 μ thick.

On polishing and etching the individual plates were not revealed and large grains were seen with straight edges. This is illustrated in Figures 36 and 37. Figure 38 shows a pre-polished specimen which has been partly electro-polished and etched. It will be noticed that in this case the straight edges of the ferrite grains change direction at the austenite grain boundaries. This of course confirms the previous observation on pre-polished specimens that the plates are confined to the original austenite grains.

Although no attempt was made to determine the orientation of the ferrite plates it was noticed that a polished specimen showed never more than three orientations. This indicated that the habit plane was of low index.

4.1.3. Mixed structures

Although a clear distinction has been made between the massive ferrite structures and those obtained by the massive-martensite reaction, this distinction could only be made at slow cooling rates $\sim 100^{\circ}C\ sec^{-1}$ and in practice mixed structures were observed in the Fe-Ni alloys at higher cooling rates. Pre-polished samples for example often showed isolated surface tilts. In fact mixed structures were frequently observed in alloys in the range 8-10% Ni cooled faster than $100^{\circ}C\ sec^{-1}$. Figure 39 shows a mixed structure of massive ferrite and massive martensite observed in 'pure' iron at a cooling rate $\sim 300^{\circ}C\ sec^{-1}$.

4.1.4. Acicular martensite

On quenching to room temperature alloys containing greater than about 29% Ni were fully austenitic, but on cooling below room temperature a martensitic transformation occurs in alloys containing up to 33% Ni[59]. As indicated in the review of the literature, this transformation has received considerable attention. To compare this reaction with the massive-martensite reaction two alloys containing 30.2 a/o and 31.75 a/o Ni were examined. Specimens were austenitised at 1,000°C, quenched to room temperature and subsequently cooled in liquid nitrogen. Surface tilts were observed in a pre-polished specimen.

In this case the plates were not parallel but formed at an obtuse angle to each other with retained austenite between the plates. On polishing and etching a similar structure was obtained. The plates were large and lenticular in shape. The specimens contained about 5% by volume of retained austenite. Specimens were not examined by thin film electron-microscopy since this aspect of the structure has been amply covered by previous investigators[11,12]. Their work showed that the martensite plates are internally twinned on a fine scale and that the habit plane is irrational, i.e. $\{259\}_\gamma$.

4.2. Quenching Results

The variation of transformation temperature with cooling rate was studied by the thermal arrest technique described in Chapter 3, Section 3.2. Transformation temperatures were measured in pure iron and in a series of Fe-Cr and of Fe-Ni alloys. Specimens were subsequently mounted and examined by metallography.

4.2.1. Pure iron

In the pure iron obtained from B.I.S.R.A., at high cooling rates, transformation occurred with a marked degree of undercooling. Considerable scatter was encountered in the results and transformation temperatures varying from 870°C to 550°C were observed. In general, increasing cooling rate, resulted in a lowering of the transformation temperature, but for a given cooling rate the observed transformation temperatures were scattered over a wide range of temperatures. For example at 10,000°C sec^{-1} the transformation temperature varied between 760°C and 550°C, while at higher cooling rates $\sim$14,000°C sec^{-1} the transformation temperatures varied between 690°C and 550°C. The reasons for this scatter were not immediately apparent and are discussed in more detail in Chapter 5, Section 5.4. In general, metallographic examination of specimens showed mixed structures and usually specimens which had transformed at low temperatures showed a considerable proportion of massive martensite. Figure 41 shows a plot of the observed transformation temperature against cooling rate. The lowest transformation temperature obtained was 550 $\pm$ 10°C, an average of four determinations.

This is in agreement with the value of 545°C (2 determinations) obtained by Gilbert for iron containing 0.01% C, and the expected value for the martensite start temperature in iron, extrapolated from Greninger's M_s data for Fe-C alloys. Thus this temperature is thought to represent the start temperature for the martensite transformation in this material. It was also noticed that higher temperatures could possibly be grouped round two values, namely 760°C and 690°C. This indicated by two dotted lines in Figure 41. These points and the scatter at temperatures above 550°C are discussed more fully in Chapter 5, Section 5.4.

4.2.2. Fe-Ni alloys

Figures 42-45 show the variation of transformation temperature with cooling rate obtained for Fe-Ni alloys containing 6, 8, 10 and 15 w/o nickel. Included in the same diagram are the results obtained by Gilbert for cooling rates in the range 100 to 5,000°C sec^{-1}.

In the 15% Ni alloy the transformation temperature was lowered from 390°C to a constant value of 350°C by increasing the cooling rate from 100°C sec^{-1} to approximately 2,000°C sec^{-1} (Figure 42). Metallographic examination showed that with these austenitising conditions (5 minutes at 1,100°C) the structure of the transformed specimen was massive martensite at all cooling rates. About five determinations were made of the plateau temperature and this is thought to be accurate to ±5°C. This value is in good agreement with the value of 357°C obtained by Gilbert.

Alloys of lower nickel content transformed to 'massive ferrite'

at the relative slow rates used by Gilbert (less than 5,000°C sec^{-1}). However at higher cooling rates transformation occurred at a temperature considerably lower than those reported by Gilbert. Metallographic examination revealed a 'massive martensite' structure similar to that obtained in the 15% Ni alloy. Figures 46 and 47 show 'massive martensite' obtained on rapidly quenching Fe-10% Ni and Fe-6% Ni respectively. The massive martensite reaction was most easily obtained in the 10% Ni alloy, in fact at cooling rates as low as 1,000°C sec^{-1}. Hence in this alloy the 'plateau' temperature for the 'massive martensite' reaction was fairly accurately established at 426 ± 5°C. As the nickel content decreased it became increasingly difficult to suppress the massive ferrite reaction. Consequently the accuracy with which this plateau temperature could be measured also decreased. In the 8% Ni alloy the 'plateau' temperature of 460°C is thought to be correct to ±10°C, while the value of 520°C for the 6% Ni alloy is thought to be correct to ±15°C. In these two alloys, 8 and 6% Ni, two arrests were frequently observed on the same cooling curve. These are included in Figures 44 and 45 and are indicated by open circles. It will be seen that the first arrest corresponds to the start temperature for the massive ferrite reaction while the second arrests correspond to the massive martensite reaction.

It is clear that at these cooling rates the massive ferrite has not transformed completely and that the remainder of the austenite has transformed to massive martensite at the lower temperature, resulting in a 'mixed structure' of massive ferrite and massive martensite.

For alloys containing less than 6% Ni it proved extremely difficult to suppress the 'massive ferrite' transformation with the cooling rates available and accurate values for the start temperature of the 'massive martensite' reaction could not be obtained in these alloys.

In Figure 48(a), the upper and lower plateau temperatures are plotted as a function of nickel content. It will be seen that the start temperature for the massive martensite reaction lies in a smooth curve. The curve is dotted between pure iron and Fe-6% Ni since experimental points could not be established precisely in this region. For the start temperature of the austenite to ferrite transformation, Gilbert drew a smooth curve through his data, with an inflexion between 10 and 15% Ni. However it is now clear that this portion of the curve should be dotted as shown in Figure 48(a). When the data for the two types of transformation are separated as in Figure 48(a) this inflexion disappears. Figure 48(b) compares the results obtained by previous workers and the present investigation for all nickel contents.

4.2.3. Fe-Cr alloys

Specimens which were allowed to cool by radiation transformed at temperatures in good agreement with the results of Gilbert. Metallographic examination showed a typical massive ferrite structure and it seems fairly clear that the transformation temperatures determined by Gilbert refer to this reaction. Since only a small amount of each of the iron chromium alloys were available it was decided to quench most of the material at high cooling rates to try to obtain the 'massive

martensite' reaction in these alloys. This was successful in the alloys containing 4.3%, 6.3% and 9.4% Cr. Typical results from these experiments are shown in Figures 49 and 50, also included are the values obtained by Gilbert at lower cooling rates. Two arrests were often recorded on the cooling curve. These are also included in the figures and indicated by open circles.

The upper arrest was a little lower than the arrest temperatures obtained by Gilbert at slower cooling rates. It is probable that the upper arrest represents an undercooled value of the 'massive ferrite' transformation but this was not proved. Metallographic examination of quenched specimens showed a typical 'massive martensite' structure as shown in Figure 51. The variation of the start temperatures for the 'massive martensite' reaction with chromium content is shown in Figure 18. Included in the same diagram are the plateau temperatures obtained by Gilbert at slower cooling rates.

4.3. X-Ray Studies

Debye-Scherrer patterns were taken of transformed specimens of Fe-Ni and Fe-Cr using a 9.0 cm camera and Co $K\alpha$ radiation with an iron filter. In all cases only lines arising from a b.c.c. (alpha) lattice were obtained and no f.c.c. (gamma) lines were detected. This means that within the limits of detection ~5% neither retained austenite or equilibrium austenite were present in the specimens. This indicated that transformation had occurred without any change in composition. Measurement of the lattice parameter of the structure also supported this view, since these were the values expected on the basis of total nickel content. This confirms the previous observations of Gilbert[81] and of Massalski[75], that in the massive reaction, transformation occurs without change in composition. However Gilbert and Massalski report that the x-ray lines of the massive product are broadened. The present results differ in that it was noticed there was a difference in line broadening between the two types of massive reactions, that is massive ferrite and massive martensite. Specimens which had transformed to massive ferrite gave quite sharp lines. In fact, the α_1 and α_2 doublet could be clearly resolved in many cases as low as the $(211)_\alpha$ line. A typical film is shown in Figure 52. By comparing the x-ray films obtained from annealed iron, and those from the same iron which had been transformed to massive ferrite during quenching, it was seen that the lines arising from the latter structure, although sharp, were slightly broadened compared with annealed material. In contrast to this,

specimens which had transformed by the 'massive-martensite' reaction showed considerable line broadening. The films obtained from an Fe-10% Ni alloy transformed by the different reactions are compared in Figure 53. Thus it appears that the previous reports of line broadening in the massive reaction are partly in error. Only a small degree of line broadening is observed in the massive ferrite reaction, but the massive-martensite reaction shows considerable line broadening. The distinction between massive ferrite and massive martensite had not been made prior to this investigation and it seems likely that the previous reports of line broadening could be explained by the fact that quenched specimens would consist entirely of massive-martensite or else of a mixture of massive ferrite and massive martensite. In either case some line broadening would then be observed.

4.4. Determination of T_o

This is the temperature at which the α and γ phases are in metastable equilibrium, i.e.

$$\Delta G^{\alpha \rightarrow \gamma}\Big|_{T_o} = 0 \qquad (1)$$

Kaufman and Cohen determined the start temperatures for the $\gamma \rightarrow \alpha$ and $\alpha \rightarrow \gamma$ reactions in a series of Fe-Ni alloys containing 9.5 a/o, 14.5 a/o, 19.0 a/o Ni and alloys of higher nickel content. Kaufman showed that to a first approximation

$$T_o = \tfrac{1}{2}(M_s + A_s) \qquad (2a)$$

and

$$\Delta G^{\alpha \rightarrow \gamma}\Big|_{A_s} = \Delta G^{\gamma \rightarrow \alpha}\Big|_{M_s} = -\Delta G^{\alpha \rightarrow \gamma}\Big|_{M_s} \qquad (2b)$$

The heating and cooling rates used by Kaufman and Cohen were $4^{\circ}C\ min^{-1}$ and at that time it was thought the transformation temperatures measured in all the Fe-Ni alloys were martensitic. Theoretically, Equation (2b) will only strictly apply to a transformation which occurs athermally, that is one in which there is no thermally activation of the nucleation process. However it is now apparent that in alloys containing less than 10% Ni, transformation at low cooling rates occurs by a process which is almost certainly thermally activated (see Discussion, Section 5.1.). It was therefore thought desirable to repeat Kaufman's measurements on the dilute Fe-Ni alloys to provide sufficient experimental data to re-examine Kaufman's method.

Specimens in the form of 0.106" wire were thermally cycled in a vacuum of 10^{-4} mms Hg and the temperature was followed continuously during heating and cooling with a Honeywell-Brown 1 second recorder. The heating and cooling rates employed were $\sim 100^{\circ}C\ sec^{-1}$ and the average value of the transformation temperatures were noted from the thermal arrests.

The terms M_s and A_s are usually used for the martensitic start temperature and the temperature of reversal. Since the transformation temperature measured under these conditions were not martensitic, (except perhaps for the Fe-15% Ni alloy) the following terminology was adopted:

α_s = start temperature of the $\gamma \rightarrow \alpha_2$ reaction,

γ_s = start temperature of the reverse transformation $\alpha_2 \rightarrow \gamma$

A similar notation has been used to describe the $\beta \rightarrow \alpha$ transformation in titanium and zirconium[92]. The observed values of α_s and γ_s are plotted in Figure 54. These are the average values taken from at least three specimens of each alloy. In this Figure the mean value $\frac{1}{2}(\alpha_s + \gamma_s)$ is also compared with the theoretical value of T_o defined by Equation (1). The free energy expression $\Delta G^{\alpha \rightarrow \gamma}$ used for these calculations of T_o was the modified form of the Kaufman and Cohen expression used by Gilbert and Owen for the temperature range 800 to 1,100°K.

$$\Delta G^{\alpha \rightarrow \gamma} = (1-x)\ \Delta G^{\alpha \rightarrow \gamma}_{Fe} + x\,\Delta G^{\alpha \rightarrow \gamma}_{Ni} + \Delta G^{\alpha \rightarrow \gamma}_{M}$$

$$= (1-x)\ \left\{1474 - 3.4 \times 10^{-3} T^2 + 2 \times 10^{-6} T^3\right\}$$

$$+ x\ \left\{-3,700 + 7.09 \times 10^{-4} T^2 + 3.91 \times 10^{-7} T^3\right\}$$

$$+ x(1-x)\ \left\{3,600 + 0.58\, T\,(1 - T \ln T)\right\}\ cals\ mole^{-1}$$

It will be seen that there is reasonable agreement between the experimental and theoretical values of T_o. Thus although this experimental method of determining T_o is not strictly theoretically correct it provides a reasonably accurate and rapid method of determining T_o in alloys where transformation occurs by the massive ferrite reaction. However the method has to be used with caution. For example in the Fe-Cr alloys, γ_s was found to occur just above the gamma loop[81] and the average value of α_s and γ_s bore no resemblance to T_o. In this case agreement between the theoretically and experimental values of T_o is only obtained at very slow heating and cooling rates. T_o must however lie within the two phase fields of the gamma loop. Since this is very narrow T_o can be fairly accurately established from the phase diagram.

4.5. Kinetic Studies

This section describes attempts to obtain further details of the kinetics of the massive ferrite and massive martensite reactions by means of continuous cooling and of isothermal experiments.

4.5.1. 'Massive ferrite'

Since in the alloys studied in this investigation this reaction was extremely rapid, it was difficult to obtain any quantitative measurements of the speed of the transformation. However, by measuring the resistance of the specimens during continuous cooling it was possible to obtain some details of the transformation under athermal conditions. The experimental procedure adopted for these experiments has been described in the previous Chapter. These observations were by necessity confined to Fe-Ni alloys, since there was insufficient material for parallel experiments on Fe-Cr alloys. The resistance curves obtained during continuous cooling of dilute Fe-Ni alloys are shown in Figures 21-25. For comparison purposes the resistance values have been normalised to unity at 200°C. The time in seconds during cooling is also included on the right hand side of the diagrams. Thus from these figures the time required for complete transformation can be easily estimated. Although this time will depend to some extent on cooling rate it will also depend on the speed of the reaction, particularly where the heat of reaction is such that the temperature remains ostensibly constant during transformation. It will be seen that in most cases transformation is completed in less than 20 seconds. In the Fe-4% Ni

alloy this time is as small as 3 seconds and approximately 60% transformation occurs in less than one second while the temperature falls only 10°C. In general, it appears that the time taken for transformation increases with nickel content.

4.5.2. Massive martensite

It was not clear from the quenching experiments whether this transformation occurred isothermally or athermally. Although the depression of α_s from 380°C to a constant value of 350°C in the 15% Ni alloy suggests that the transformation is thermally activated. Some recent work by Yeo[93] on an Fe-24% Ni and an Fe-28.8% Ni alloy also suggested that this transformation could occur isothermally. Similar experiments to those described in the previous Section were performed on an alloy containing 23.75% Ni and also in the Fe-15% Ni alloy. The transformation curves obtained for these alloys are shown in Figures 25 and 24. It will be seen that the start of the transformation is not very abrupt but once it has commenced considerable transformation occurs in an extremely narrow temperature range. In the Fe-23.75% Ni alloy varying the cooling rate between 13°C sec^{-1} and 0.013°C sec^{-1} did not alter appreciably the form of the curve on the start temperature. This was achieved by cooling the specimen successively in air and then in an oil bath. In another series of experiments the quench was stopped at a temperature below the start temperature α_s but higher than the temperature for completion of the transformation. The specimen was then held isothermally for various times. In all the experiments the

transformation stopped as soon as the quench was interrupted and it did not resume until the temperature was allowed to decrease further. No evidence of isothermal transformation was obtained from these direct experiments. Attempts were also made to see if transformation could be made to occur by isbthermal holding at temperatures above α_s. This was done by austenitising the specimen in air and then immersing it in an oil bath held at temperatures above α_s. No transformation was observed for holding times as long as 12 hours. This statement requires some qualification. The experimental arrangement was such that resistance measurements could only be taken approximately 40 seconds after immersion in the oil bath. Thus these experiments did not preclude the possibility of a small amount of isothermal martensite forming fairly rapidly during this period. This part of the work is discussed further in Section 5.2.

4.6. Effect of Austenitising Temperature

In the cooling experiments reported previously a constant austenitising temperature of 1,100°C was used throughout. There is no particular reason why the results obtained for this temperature should apply to all austenitising conditions, and indeed such variables as austenite grain size, which depend on austenitising temperatures, are likely to alter the kinetics of a particular reaction. It was therefore decided to try and study the effect of austenitising temperature on the different reactions encountered in Fe-Ni alloys. For these experiments specimens were heated and cooled in the quenching apparatus from various temperatures. The temperature of the specimen was followed continuously during heating and cooling on a Honeywell-Brown recorder and the transformation temperature noted from the thermal arrest.

4.6.1. Massive ferrite reaction

The effect of austenitising temperature on the Fe-10% Ni and Fe-6% Ni alloy are shown in Figures 56 and 57. Specimens were austenitised for 5 minutes and allowed to cool by radiation ($\sim$50°C sec^{-1}). Several specimens were used some of which were cycled to various austenitising temperatures and others used for individual determinations. In the Fe-6% Ni alloy the austenitising temperature was varied from $\sim$ 800°C to $\sim$ 1,200°C. It appeared that austenitising temperature had no appreciable effect on the transformation temperature. An average transformation temperature of 640°C was noted with a scatter of $\pm$5°C. Since the reversal temperature, γ_s occurs at a lower temperature in the 10% Ni

alloy it was possible to vary the austenitising temperature over a wider range (~700°C to 1,200°C) in this alloy. Nevertheless even with this range of temperatures, the transformation temperature was observed to be approximately constant at 530°C with a maximum scatter of ±10°C. Thus it appears that within the experimental error (~ ±10°C) austenitising temperature has no appreciable effect on the transformation temperature of massive ferrite.

4.6.2. Transition from massive ferrite to massive martensite

Although austenitising temperature did not appear to effect the start temperature of the massive ferrite reaction, it was thought that increasing austenitising temperature may effect the speed of the reaction. Kurdjumov[99], for example reports that martensite can be most easily obtained in pure iron by quenching from a high austenitising temperature. This indicates that the speed of the massive ferrite reaction decreases with austenitising temperature and suggests that for a sufficiently fast cooling rate it should be possible to change from the massive ferrite transformation to massive martensite by increasing the austenitising temperature. Since the speed of the massive ferrite reaction decreases with increasing nickel content (see Sections 4.2.2. and 4.6.1.) it was thought that this could be most easily studied in the 10% Ni and 15% Ni alloys where the transition from massive ferrite to massive martensite occurred.

The effect of austenitising temperature on the transformation temperature in the Fe-15% Ni alloy at a cooling rate 50°C sec^{-1} is

shown in Figure 58(a). The lower Figure 58(b) shows schematically the results of the successive thermal cycles given to the specimen. The reversal temperature γ_s remains reasonably constant. However the transformation temperature α_s varies markedly with heat treatment. Specimens austenitised between 700°C and 900°C transformed at about 425°C but those austenitised between 900°C and 1,200°C transformed at a significantly lower temperature (393°C). This effect was found to be reproducible with different specimens of the same alloy. It was also noticed that during thermal cycling, that the effect was independent of previous heating cycles. For example after austenitising at 1,200°C and cooling to room temperature transformation occurs at 393°C. On re-austenitising at 743°C transformation occurs at 425°C. To determine if the phenomena was due to austenitising temperature per se or austenitic grain size some specimens were austenitised in two stages. All the specimens in the series were austenitised for 5 minutes at 1,200°C to establish the grain size and substructure characteristic of that temperature and then the temperature of the specimen was reduced by means of the variac to a lower austenitising temperature and held for 5 minutes. At the end of this period the heating current was switched off and the specimen allowed to cool by radiation. In all cases transformation occurred at a lower temperature even though an intermediate anneal at approximately 800°C had been given to the specimen before allowing it to cool. It was also noticed that the form of the thermal arrest varied with the transformation temperature. The transformation

temperature of 425°C lies on a smooth curve without an inflexion, joining the massive ferrite transformation in alloys of lower Ni content (see Figure 43(a)). It was therefore thought that 425°C was the start temperature for the massive ferrite reaction in the 15% Ni alloy. However optical examination of specimens transformed at the two temperatures did not appear to show any real difference in microstructure, although specimens which had transformed at 425°C could possibly be described as 'mixed'. This is not entirely surprising since specimens were cooled continuously and since the two transformation temperatures are very close together highly mixed structures would be expected if the temperature of 425°C is in fact, the start temperature for the massive ferrite reaction in the 15% Ni alloy.

Confirmation of this hypothesis was obtained in the 10% Ni alloy. Although austenitising temperature had had no effect on transformation temperature in the 10% Ni alloy at cooling rates $\sim 50^{\circ}C\ sec^{-1}$, it was thought that a similar effect to that obtained in the 15% Ni alloy may be obtained at higher cooling rates. Some difficulty was experienced at first in selecting a suitable cooling rate, but eventually it was found that the effect could be produced by heating and cooling the specimen in air when a cooling rate $\sim 300^{\circ}C\ sec^{-1}$ was obtained. To avoid excessive oxidation the austenitising time was restricted to approximately 1 minute. Heating in air naturally resulted in some scatter in the measured transformation temperature but a definite effect was observed with a number of specimens of the same alloy. In particular

with a given specimen, if a low austenitising temperature was followed by austenitising at a high temperature, then transformation occurred at a much lower temperature. The results of several determinations are shown in Figure 59. For austenitising temperatures between 700 and 1,000°C transformation occurred at approximately 510°C while for austenitising temperatures greater than 1,000°C transformation occurred at approximately 450°C. Optical examination of specimens which had transformed at 510°C showed a massive ferrite structure, although with these short austenitising times and low temperatures the wire specimen had not completely recrystallised. Specimens which had transformed at 480°C showed a massive-martensite structure. The temperature of 510°C is in good agreement for the transformation temperature of massive ferrite in the 10% Ni alloy at these cooling rates (increasing the cooling rate from 50°C sec^{-1} to 300°C sec^{-1} has lowered the transformation temperature from 530°C to 510°C) while the temperature of 450°C is also in good agreement for the start temperature of massive martensite for these cooling rates.

4.6.3. Massive martensite

In order to study the true variation of M_s with austenitising temperature for the massive martensite reaction, alloys of higher nickel content were used. The 19.0% and 24.0% alloys were chosen since it was thought that the massive ferrite reaction did not occur in these alloys and that the alloys were martensitic at all cooling rates. Further since the temperature of reversal γ_s (or A_s) is low in these

alloys 600°C it was possible to vary the austenitising temperatures over quite a wide range of temperatures. For the experiments on Fe-19% Ni specimens in the form of foil 0.10" wide x 0.002" thick were used. This had been cold reduced from swaged rod. Some of the Fe-24% Ni was available as 0.100" wire and for experiments on this material specimens were used in this form.

The results on the 19% Ni alloy are shown in Figure 60. The M_s temperature was observed to increase rapidly with austenitising temperature in the range 700 to 800°C but for austenitising temperatures greater than this, M_s was practically constant. This form of curve was observed in several specimens of the same alloy. Similar results were also obtained on the 25% Ni alloy. In contrast to the 15% Ni alloy the thermal arrest did not alter with austenitising temperature and this curve is thought to represent the variation of M_s for the massive martensite reaction with austenitising temperature, rather than a change in transformation mechanism with temperature.

Figure 60(a) shows the sequence of heating and cooling cycles given to the specimen. It will be seen that the transformation temperature was independent of previous cycles. In particular if the specimen was austenitised at a high temperature and in the next cycle a low austenitising temperature was used the transformation temperature was always characteristic of the lower austenitising treatment. If a two stage austenitising treatment was used then the transformation temperature was again always that characteristic of the higher austenitising

temperature. For example specimen No. 370 was austenitised for 5 minutes at 1,200°C and then the specimen was reduced and held for a further 5 minutes at 800°C. On cooling to room temperature, transformation occurred at 254°C rather than 226°C. At first sight the results of these thermal cycles would suggest that this variation of M_s with austenitising temperature is due to austenitising temperature per se rather than austenite grain size. This is because at the heating rates used in these determinations the reverse transformation to austenite should occur martensitically. Thus once a high austenitising treatment has been used the austenite grain size characteristic of this treatment should be retained for all subsequent cycles. However Krauss[94] has recently shown that considerable deformation of the austenite accompanies the reverse transformation of acicular martensite in Fe-33% Ni. If this is also true for the massive martensite reaction, which is quite possible, then the preceding argument is no longer valid and a large austenite grain size is unlikely to be retained for all thermal cycles.

5. DISCUSSION

The three types of reactions revealed by this investigation are first described and discussed. The results are then compared with those obtained by Parr and his co-workers[96,97] who carried out similar studies on iron and some iron-nickel alloys. Finally the transformations found in this study are compared with those observed in non-ferrous systems.

5.1. Massive Ferrite.

5.1.1. General description.

The morphology of the product of the short range diffusional transformation to massive ferrite has been described in detail in the Experimental Results section, briefly:-

(1) Grains are large and irregular but approximately equiaxed.

(2) Ferrite grains cross the parent austenite grain boundaries without hindrance.

(3) Surface tilts are not observed on pre-polished specimens.

(4) Electron microscopy reveals high angle boundaries and a high dislocation density.

(5) The x-ray lines obtained from specimens with this structure are sharp compared with those for massive martensite and in the case of Fe-Ni alloys the product is supersaturated.

It is now fairly clear that the majority of transformation temperatures measured by Gilbert refer to this reaction, the exceptions being those obtained for Fe-15% Ni and the M_s temperature of 545 $\pm$ 5°C

obtained for pure iron. The values of the chemical driving force computed by Gilbert and Owen[81] will also apply to this reaction.

The general metallographic features of the reaction suggest that it can be classified as one of nucleation and growth. However it is unusual in that it can occur extremely rapidly and without any change in composition. The speed of the reaction is illustrated by the continuous cooling curves and the high cooling rate required to suppress the reaction. For example in the Fe-8% Ni alloy the reaction is completed in less than 20 seconds during continuous cooling, and a cooling rate $\sim 5{,}000^{\circ}C\ sec^{-1}$ is required to suppress the reaction. The fact that in the Fe-Ni alloys only lines of the b.c.c. lattice are obtained on Debye-Scherrer patterns, although the equilibrium phases are ferrite and austenite, shows that the reaction is diffusionless in the sense that there is no change in composition. However since shear plates are not evident on pre-polished specimens or in electron-micrographs it must be concluded that this is not a co-operative shear transformation. Since it is not martensitic some diffusion must occur during the growth of the ferrite, but it is probably limited to atomic movements over a few atomic spacings, that is short range diffusion. In fact the manner in which ferrite grains cross the austenite grain boundaries, suggests that nucleation of ferrite occurs at these boundaries and then grows by rapid atom transfer across the austenite/ferrite interface. The experiment on the Fe-10% Ni alloy and the Fe-15% Ni alloy in which, for a constant cooling rate, it was found to

be possible to change from massive ferrite to massive martensite by changing the austenitising temperature also suggests that the massive ferrite nucleates at the austenite grain boundaries. This is because increasing the austenitising temperature produced an appreciable increase in the size of the γ-grains and thus a decrease in the grain boundary area per unit volume. Thus, if it is assumed that massive ferrite is nucleated at the boundaries of the γ-grains, the effect of austenitising temperature may be simply to decrease the grain boundary area per unit volume to a point at which the number of nuclei formed in a measurable time is negligible.

In the case of the Fe-Cr alloys at the transformation temperature ferrite alone is the equilibrium phase and it does not necessarily follow that the transformation in these alloys is the same as in the Fe-Ni alloys. However the following features which the transformation has in common with that in the Fe-Ni alloys suggests that the transformation is essentially the same.

(1) The Fe-Cr alloys give rise to a similar morphology as in the Fe-Ni alloys.

(2) A plateau is obtained in a plot of transformation temperature versus cooling rate, similar to that obtained in Fe-Ni alloys[81].

(3) The reaction can occur at high cooling rates and requires a cooling rate $> 5{,}000^{\circ}C\ sec^{-1}$ to suppress the reaction.

(4) The chemical driving force $\Delta G^{\gamma-\alpha}$ computed by Gilbert and Owen[81] required for the reaction is similar to that for Fe-Ni alloys.

5.1.2. Kinetic features.

One of the most striking features of the reaction is the speed at which it can occur. This means that it is difficult to study the reaction under isothermal conditions and in this investigation the kinetic features of the transformation had to be inferred from continuous cooling experiments.

The fact that the transformation temperature is lowered as the cooling rate is increased until it reaches a constant value and at higher cooling rates is entirely suppressed, suggests that the reaction is thermally activated and can occur isothermally. The "C" curve obtained by Kogan and Entin[89] in an Fe-8.5% Cr alloy and its correlation with Gilbert's result (see Review of Literature section 2.4.4.) is of course direct evidence of isothermal behaviour.

As indicated in the literature review it should be possible to construct a schematic T.T.T. curve for the massive ferrite reaction as shown in Figure 61. The temperature at the nose of the "C" curve, T_a, that is, at the maximum rate of transformation, should correspond to the plateau obtained in the plot of transformation temperature versus cooling rate. The incubation period t_o, or more specifically the expression $T_o - T_a/t_o$ will be related to the critical cooling rate required to suppress the transformation. To provide the chemical driving force $\Delta G^{\gamma \rightarrow \alpha}$ clearly the transformation to massive ferrite must occur at temperatures below T_o. At temperatures close to T_o the driving force is very small and transformation will only occur after

extremely long holding times. Thus the upper portion of the "C" curve is probably asymtopic to T_o.

It is also apparent that in alloys such as Fe-Ni, isothermal holding would eventually lead to the formation of equilibrium ferrite and austenite. That is, on isothermal holding the reaction sequence,

$$\gamma \longrightarrow \alpha_2 \longrightarrow (\alpha + \gamma)$$

supersaturated ferrite Equilibrium phases

would be observed, although the second reaction would be a lot slower than the initial transformation to α_2. In this respect, Allen and Earley[98] have reported the isothermal formation of equilibrium ferrite and austenite from supersaturated ferrite at temperatures within the two phase field, but below the reversal temperature γ_s.

In alloys, such as Fe-Ni, with an extensive $(\alpha + \gamma)$ phase field, at temperatures above T_o and between the $\gamma/(\alpha + \gamma)$ phase boundary the reaction

$$\gamma \rightarrow (\alpha + \gamma)$$

is also possible. However in Fe-Ni alloys due to the sluggishness of the diffusion of nickel in austenite this is an extremely slow reaction. Nevertheless it is possible that the reaction may be observed in alloys in which diffusion is considerably faster.

At lower temperatures and higher cooling rates the transformation to massive martensite is obtained. This is represented by the horizontal line on the diagram. It is believed that the ideas expressed in this

schematic T.T.T. diagram apply to pure iron and other binary iron alloys. In certain alloys, however, such as Fe-Cr the reaction $\alpha_2 \longrightarrow (\alpha + \gamma)$ will be absent since ferrite is the equilibrium phase.

In Fe-Ni alloys the incubation period t_c at the nose of the "C" curve representing the start of the transformation to massive ferrite must be of the order of milliseconds because of the high cooling rate necessary to suppress the reaction. This incubation period t_c also increases with nickel content since with increasing nickel content it becomes easier to suppress the reaction. Similar comments apply to the effect of chromium, in fact in general alloy additions appear to increase t_c. In this respect interstitial solute elements appear to be the most effective elements. In the Fe-Cr alloy studied by Kogan and Entin it was possible to obtain a T.T.T. curve, whereas in the Fe-Cr alloys studied in this investigation a cooling rate of greater than 5,000°C sec^{-1} was required to suppress the reaction. This is thought to be due to the presence of 0.05% C in Entin's alloy compared with 0.008% C in the alloys studied in this investigation.

In the Fe-15% Ni and the 10% Ni alloy it was found that for a given cooling rate, it was possible to change from the massive ferrite reaction to the massive martensite reaction by increasing the austenitising temperature. This suggests that the incubation period t_c also increases with austenitising temperature. As stated earlier,

the effect can be explained if it is assumed that the massive ferrite nucleates at the austenite grain boundaries. Then increasing the austenitising temperature results in an increase of the γ grain size and a decrease in the number of nucleating sites per unit volume for massive ferrite.

It is not immediately apparent why t_c is altered by composition or even what is the physical significance of the incubation period. Clearly the incubation is made up of two parts.

(a) Time required for nucleation.

(b) Time required for the new phase to become physically observable.

The nucleation period (a) is sometimes described as the time required for embryos characteristic of the solution temperature, to grow to the size characteristic of the isothermal holding temperature, and it is maintained that this time is the main factor determining the incubation period. Alternatively it is often claimed that the time interval (b) is the major factor determining the duration of the incubation period. This interval is controlled by the exponential nature of the initial portion of the isothermal rate curve. It is difficult to see which of these explanations, if either, is the correct one. However since both factors involve activation and growth of an embryo of some description, it seems reasonable to assume that factors which alter nucleation and growth also effect the incubation period. In Fe-Ni alloys the increase of t_c with nickel is probably due to the

TABLE 6

Details of Kinetic Features and Composition of Alloys studied by Kogan and Entin

Composition							A_3 °C	t_o (5% transformation) Mins.
C	Si	Mn	Cr	Ni	Mo	Co		
0.05	0.06	0.39	8.5				805	1 Min.
0.04	0.35	0.12	8.36	2.46			740	20 Mins.
0.04	0.40	0.07	6.88	1.94			830	1 Min.
0.03	0.23	0.30	3.76	2.59	0.70		745	100 Mins.
0.06	0.16	0.20	8.05			5.0	800	7 Mins.

decrease of T_o with nickel content, causing the reaction to occur at lower temperatures when less thermal energy is available for activation and growth. However, this does not appear to be a general explanation of the effect of alloy additions on t_c. Entin [89] reports an incubation period of about 100 minutes in an alloy containing Fe + 3.5% Cr + 2.5% Ni + 0.7% Mo with an A_3 point as high as 745°C. Some of the results of Kogan and Entin's studies [89] on the transformation in other alloys are shown in Table 6. These measured incubation periods are the times to 5% transformation and consequently they must reflect both growth and nucleation kinetics, however it does appear that t_c can be markedly increased by alloying elements without any appreciable lowering in T_o. Although carbon also lowers T_o it seems unlikely that this would account completely for the very marked effect of this interstitial element on t_c and thus other factors which may influence the nucleation and growth of the transformation must be examined.

It seems likely that the reaction occurs by nucleation at the austenite grain boundaries and movement of a high angle boundary with short range atom transfer across the interface. Kurdjumov [99] has described this type of reaction as "disorderly growth" and compared it with recrystallisation. Indeed there are many similarities between boundary movements in recrystallisation and those in the massive ferrite reaction. For example, the driving force $\Delta G^{\gamma \rightarrow \alpha}$ at the maximum rate of transformation for the massive ferrite reaction is the same

order as that encountered in recrystallisation. In the latter case the driving force arises due to differences in dislocation density between the two sides of the boundary, whereas in the massive ferrite reaction it is due to the difference in crystal structure. Interstitials are also known to have a marked effect on the speed of recrystallisation kinetics. These are thought to be dragged along with the interface and slow down the movement of the high angle boundary. Thus the interaction of alloy elements, particularly interstitials with the movement of a high angle boundary may explain the change in the speed of the massive ferrite reaction with alloying elements.

Alternatively the effect of alloying elements on the speed of the reaction could be due to their effect on the strain energy accompanying the transformation. Strain energy will tend to oppose the transformation to ferrite and thus decrease the speed of the reaction. The magnitude of this strain energy will depend on the volume change occurring in the transformation and the relative strength of the two phases. In this respect it is well known that interstitials make a marked contribution to solid solution hardening and the strain energy accompanying the transformation may be considerable in the presence of interstitials.

Clearly the number of factors influencing the massive ferrite reaction are many and complex. Further work will be required to elucidate the exact role of alloy additions.

It is interesting to note that theoretically the massive ferrite

reaction is possible in Fe-C alloys at temperatures below T_o. Whether this reaction will occur in practice will depend on the relative speeds of the two reactions

$$\gamma \longrightarrow \alpha_2$$

and

$$\gamma \longrightarrow (\alpha + \gamma)$$

Certainly it appears that the massive ferrite reaction occurs in iron containing 0.01% C and possibly at higher concentrations. Large areas of 'blocky ferrite' and 'massive ferrite' are also encountered in the pro-eutectoid ferrite reaction[100] and some of the microstructures certainly resemble the massive ferrite microstructures found here. However it is usually thought that the various morphologies in the eutectoid reactions are obtained by long range diffusion of carbon through austenite to form equilibrium ferrite. There does not appear however to have been any verification that the ferrite formed has the equilibrium concentration of carbon. It is not suggested that all the various morphologies such as 'Widmanstattun sideplates' and 'intergramular plates' occur by the massive ferrite reaction since some of these appear to form at temperatures above T_o.

5.2. Massive Martensite.

5.2.1. General description.

In parallel with the discussion of the transformation to massive ferrite, a brief summary of the essential features of massive-martensite is first presented followed by a more particular discussion of the transformation.

(1) Surface tilts are seen on a pre-polished specimen. These are long and narrow and lie in parallel sheets.

(2) Electron-microscopy reveals a similar structure with parallel plates $\sim 0.25\mu$ in width. The plates contain a high dislocation density.

(3) However, the polished microstructure does not reveal the individual plates and large massive areas are seen bounded by straight edges.

(4) In the alloys studied in this investigation the structure of the product is b.c.c. and the x-ray lines show considerable broadening.

Yeo[93] has observed similar structures in an Fe-28.8% Ni alloy. Surface tilts were observed on a pre-polished specimen, but on polishing and etching the microstructure had a massive appearance similar to the structures observed in β brass. Thus it would appear that under normal cooling conditions this reaction occurs in Fe-Ni alloys ranging from 15% to approximately 29% Ni. This is supported by the fact that the start temperature (i.e. M_s) for these alloys lie on a smooth curve

as shown in Figure 48(b). Undoubtedly this transformation is also the same as the 'Schiesbung' reaction reported by Scheil in 1940[53]. The polished microstructure of Fe-24% Ni shown in Figure 37 is very similar to that for an Fe-23% Ni alloy published by Scheil.

The microstructure of the transformation obtained at high cooling rates in the Fe-Cr alloys is similar to that obtained in Fe-Ni alloys. Unfortunately it was not possible to examine these alloys for surface tilts or by transmission electron-microscopy since the Fe-Cr alloys were only available in the form of 0.10" diameter wire. However since the transformation occurs at low temperatures and resembles the microstructures obtained in Fe-Ni alloys it seems likely that this transformation is also martensitic and can be described as 'massive martensite'.

The appearance of surface tilts on a pre-polished specimen and parallel plates in electron-micrographs suggest that the reaction occurs predominantly, if not entirely by shear. The wavy nature of the interface of the plates seen in electron-micrographs is however rather disturbing. In acicular martensite the interface is perfectly straight and existing theories of martensite crystallography require the interface to be plane and undistorted. The waviness of the plates in the massive structure shows that in this case the interface of the plate is not completely planar and suggests that either distortion of the habit plane to accomodate successive plates occurs during transformation, or that the formation of the plate is accompanied by some

diffusion. The electron-micrographs bear a strong resemblance to those of Kelly and Nutting's low carbon martensite and suggests that it is also essentially the same reaction. In this respect it is interesting to note that T. Bell et al[101] have recently observed that the polished microstructure of a quenched iron-nitrogen alloy containing less than 0.7% nitrogen is similar to massive martensite.

5.2.2. Crystallography.

Although no crystallographic studies were carried out in this investigation it is possible to make one or two observations from the morphology of the product and by comparison with other work. First the heavy dislocation density within the martensite plates suggests that in this martensitic transformation the inhomogeneous or complementary shear occurs by slip. Second it now seems clear that the crystallographic studies by Mehl and his co-workers[4,9] on iron and iron-nickel alloys refer to this reaction. They found that the habit plane was $\{111\}_\gamma$ and the orientation was the Kurdjumov-Sachs relationship;

$$(111)_\gamma \,//\, (110)_\alpha$$
$$[110]_\gamma \,//\, [111]_\alpha$$

Entwistle[5] and Wayman and Alstetter[79] also report that the habit plane of martensite in iron is $\{111\}_\gamma$. The fact that in this investigation only three traces were seen on pre-polished specimens also suggests a $\{111\}_\gamma$ habit plane.

This $\{111\}_\gamma$ habit, however is in conflict with a recent crystallographic theory of martensite due to Kelly[102]. Kelly has attempted to reconcile the various crystallographic and electron-microscopic studies of martensite in steels. He concludes there are essentially two types of martensite:-

Name	Habit plane	Orientation relationship	Predominant inhomogeneous shear
1. Twinned martensite	$(225)_\gamma$ and $(259)_\gamma$	Greninger-Troiano	Twinning $(110)_\gamma[\bar{1}\bar{1}0]_\gamma$ i.e. $(112)_\alpha[11\bar{1}]_\alpha$
2. Lath martensite	near $(\bar{1}\bar{1}2)_\gamma$	Kurdjumov-Sachs	Slip $(111)_\gamma[1\bar{2}1]_\gamma$ i.e. $(101)_\alpha[10\bar{1}]_\alpha$

In this theory slight departures from the theoretical habit plane are possible by variations in the dilatation parameter and this accounts for the variation from $(225)_\gamma$ to $(259)_\gamma$. 'Lath martensite' is thought to be made up of thin parallel laths bounded by $\{111\}_\gamma$ planes with the long axis parallel to $<110>_\gamma$. Thus on the basis of this classification 'massive martensite' belongs to the category of Type 2 martensite, i.e. 'lath martensite' with a $\{112\}_\gamma$ habit not $\{111\}_\gamma$. Kelly suggests that since the plates lie in $\{111\}_\gamma$ sheets and are bounded by $\{111\}_\gamma$ planes this could result in an apparent $\{111\}_\gamma$ habit and that possibly the intersection of a sheet of plates with a free surface was measured rather than a distinct habit plane. It is also true that in the original studies an exact determination of the habit plane was not possible due to the absence of retained austenite. Instead the habit

plane had to be determined by two surface trace analysis with its attendant errors. However, if in fact the laths (or plates) are bounded by $\{111\}_\gamma$ planes, this suggests that in certain orientations comparatively short lengths of parallel plates would be observed on a pre-polished specimen. There did not appear to be any evidence of this in the specimens examined in this investigation. Kelly's explanation of the apparent $\{111\}_\gamma$ habit also suggests that in some cases the surface shears are perpendicular to the straight edges of the polished microstructure. In fact, both in this investigation and that of Yeo's, the shear plates were always observed parallel to the main crystallographic facets of the polished and etched microstructure.

Kelly's theory requires also that adjacent plates within each sheet are twin related. This is contrary to his earlier reported observations of 'lath martensite' in low carbon steels[14] in which 'the orientation of plates within a sheet was substantially the same'. Similar observations were found in the electron diffraction studies of 'massive-martensite' in this investigation. However as explained earlier this observation may arise due to a particular orientation between the foil and twinning plane and the possibility of the plates being twin related cannot be excluded.

Unfortunately, there are insufficient crystallographic data relating to massive martensite to decide whether or not Kelly's suggestion is correct and further observation would appear necessary.

It should be remembered that in some electron-microscopic studies more than one trace of the inhomogeneous shear has been reported within the martensite plates (see for example (22) and (103)). None of the existing phenomological theories encompass this possibility.

5.2.3. Kinetic Features.

The evidence concerning the kinetic features of the transformation is conflicting. The experiments on the Fe-24% Ni alloy indicates that transformation occurs athermally, since cooling rate within the range examined, 0.013 to 13°C sec^{-1} did not alter the resistance/temperature curves obtained on continuous cooling. Stabilisation, which is usually associated with athermal behaviour was also observed in this alloy. However although a similar curve was obtained in the Fe-15% Ni alloy, increasing the cooling rate lowered the transformation temperature from 390°C to a constant value of 350°C, indicating that the process is thermally activated. The form of the resistance/temperature curve is interesting, approximately 80% transformation being completed over a very narrow temperature range (about 20°C).

On the other hand Yeo[93] has obtained clear evidence of isothermal transformation in an Fe-22.7% Ni and an Fe-28.8% Ni alloy. As mentioned earlier the microstructures obtained are similar to 'massive martensite'. In both cases the upper portion of a "C" curve was obtained, but in the Fe-28.8% Ni alloy it was

possible to observe the isothermal formation of plates on a pre-polished specimen at room temperature. The growth rate was surprisingly slow $\sim 3 \times 10^{-4}$ ft/sec. compared with Bunshah and Mehl's observation of 3×10^{3} ft/sec. in an Fe-29.5% Ni alloy. Scheil and Forster described the 'Schiesbung' reaction (i.e. massive martensite) as slow and continuous while the 'Umklapp' reaction (i.e. acicular martensite) was rapid and discontinuous. The ciné films taken by Yeo during isothermal transformation show that the main rate controlling factor for isothermal formation is the infrequent nucleation of new plates rather than their slow growth. These measurements were by necessity restricted to temperatures above the nose of the "C" curve and the controlling process for transformation below the nose could not be ascertained. In his earlier work[93] Yeo demonstrated that isothermal formation occurred only in the absence of carbon, otherwise a very small amount of martensite formed isothermally followed by stabilisation and subsequent athermal transformation. Thus a possible explanation of athermal transformation observed in this investigation in the Fe-24% Ni alloy could be that in this alloy the carbon content is high enough to cause the alloy to exhibit athermal characteristics.

Entin[89] has also reported the formation of isothermal martensite in the Fe-8.5% Cr alloy (0.05%C). However in this case a small initial amount of martensite forms extremely rapidly without an incubation period, and then ceases. Lowering the temperature then

results in further transformation in the same manner. This would appear to be similar to the transformation studied in this investigation where appreciable transformation occurs over an extremely narrow temperature range. Indeed it is questionable if the response time of Entin's apparatus was sufficiently rapid to detect isothermal transformation within these short periods (approximately 2-3 seconds). Under these conditions the distinction between athermal and isothermal transformation is extremely difficult to make and to some extent it is one of pedantics. Clearly, further experiments are required in this direction with instruments of known rapid response.

Surprise has been expressed at the comparative slow growth of the martensite plates[93]. However if the formation of martensite plates is compared with deformation processes the slow growth of massive martensite does not appear so unusual. It is possible that the rate controlling process in the formation of individual martensite plates is the rate at which the inhomogeneous shear occurs. In acicular martensite the inhomogeneous shear occurs by twinning and both deformation twins and acicular martensite grow at the speed of sound. Also in both, the formation of acicular martensite and deformation twinning, an audible click accompanies the processes. In 'massive martensite' or the 'Schiesburg' reaction the inhomogeneous shear occurs by slip. Now it is well known that in plastic deformation slip can occur comparatively slowly, particularly when the stress level is low and movement of dislocations

is thermally activated, as for example in creep. Thus on the basis of this analogy, the slow growth of massive martensite does not seem unreasonable, particularly at these low temperatures, i.e. 20°C.

Kaufman and Cohen's treatment of the kinetics of the martensite reaction[60], results in an activation energy which is markedly temperature dependent and indicates an upper limit for isothermal martensite formation. Yeo's observation of isothermal martensite at temperatures above ambient led him to criticise the treatment of Kaufman and Cohen. However Kaufman and Cohen's treatment results in an activation energy for growth which is zero once the nucleus has exceeded a critical size and is therefore only applicable to acicular martensite where growth is very rapid. In the case of massive martensite, the growth rate is not so rapid and there will be a finite value for the activation energy for growth.

5.2.4. Chemical Driving Force $\Delta G^{\gamma\to\alpha}$

The value of the driving force $\Delta G^{\gamma\to\alpha}$ was calculated for the 'massive martensite' reaction from the start temperatures determined in this investigation.

For a binary solution Fe-A the change in free energy accompanying the austenite to ferrite transformation ($\Delta G^{\gamma\to\alpha}$) can be expressed as

$$\Delta G^{\gamma\to\alpha} = (1-x)\,\Delta G^{\gamma\to\alpha}_{Fe} + x\,\Delta G^{\gamma\to\alpha}_{A} + \Delta G^{\gamma\to\alpha}_{M} \qquad (1)$$

where $\Delta G^{\gamma\to\alpha}_{Fe}$ is the change in free energy accompanying the austenite to ferrite transformation in pure iron.

$\Delta G_A^{\gamma\to\alpha}$ is the hypothetical change in free energy accompanying the change from f.c.c. to b.c.c. in the element A.

$\Delta G_M^{\gamma\to\alpha}$ is the change in free energy of mixing accompanying the transformation.

x is the atomic percent of solute element A.

The expression $\Delta G^{\alpha\to\gamma} = 1202 - 2.63 \times 10^{-3}T^2 + 1.54 \times 10^{-6}T^3$ cals mole^{-1} was used for $\Delta G_{Fe}^{\alpha\to\gamma}$ (51). This is valid for the temperature range $200^\circ K < T < 800^\circ K$.

For Fe-Ni alloys an expression deduced from a regular solution model and due to Kaufman and Cohen(51) was used

$$\Delta G_A^{\alpha\to\gamma} = \Delta G_{Ni}^{\alpha\to\gamma} = -3,700 + 7.09 \times 10^{-4}T^2 + 3.91 \times 10^{-7}T^3$$

and $\Delta G_M^{\alpha\to\gamma} = x(1-x)\{3,600 + 0.58T(1-\ln T)\}$

Similarly, for the Fe-Cr alloys the following expressions due to Kaufman(104) were used

$$\Delta G_A^{\alpha\to\gamma} = \Delta G_{Cr}^{\alpha\to\gamma} = 460 + 1.0T$$

and $\Delta G_M^{\alpha\to\gamma} = x(1-x)\{-2,800 + 0.75T\}$

In all these calculations the 'M_s' temperature characteristic of a higher austenitising treatment has been used.

The results of these calculations are shown in Figure 62. The error band includes the errors found in the determination of M_s for the iron-nickel and iron-chromium alloys. These calculated values

are only accurate to within 20-50 cals mole^{-1}. In the Fe-Ni alloys the driving force is approximately 200 to 300 cals mole^{-1} whereas in Fe-Cr alloys it is $\sim$300 cals mole^{-1}. It is not quite clear why there is this difference in driving force. However it should be emphasised that the expressions for the change in chemical free energy depend heavily upon the theoretical thermodynamic model and there is very little experimental evidence to support the calculations. Nevertheless it is clear that the driving force for the transformation to massive-martensite is very much greater than that for the transformation to massive-ferrite. In the case of the transformation to massive-ferrite the chemical driving force is 20 to 80 cals mole^{-1}[81].

5.2.5. Effect of Austenitising Temperature.

The effect of austenitising temperature on the start temperature M_s for the transformation to massive martensite in a 19% Ni alloy is shown in Figure 60. The form of this curve is rather surprising since in alloy steels M_s usually increases steadily with austenitising temperature. However, in this case M_s increases rapidly for austenitising temperature in the range 700 to 900°C and is approximately constant for austenitising temperatures greater than 900°C. It was therefore encouraging to find that independently West and Sastri[105] had obtained similar results in an Fe-20% Ni alloy.

This variation of M_s with austenitising temperature could explain the discrepancy between the M_s values found by Kaufman and those determined in this investigation. Although Kaufman and Cohen

do not give details of their austenitising conditions it seems likely that they only heated to a temperature high enough to obtain complete reversion to austenite (i.e. a fairly low austenitising temperature). The fact that M_s is practically constant for austenitising temperatures greater than 900°C also explains why Bibby and Parr[97] observed no variation of M_s with austenitising temperature in pure iron (see Section 5.4.).

It is difficult to see why M_s varies with austenitising temperature in this manner. It is usually assumed that M_s in steels increases with austenitising temperature due to increasing grain size thus making it easier to form martensite at higher temperatures. However it seems unlikely that this explanation is possible in this case, since for temperatures greater than 900°C, M_s is practically constant. At least, if the relation between M_s and grain size d is of the form,

$$M_s \propto d^n$$

the value of the index n must be quite small, certainly less than 0.5. In the Fe-24% Ni alloy and the results of Sastri and West, M_s is constant above 900°C and this kind of variation seems even more unlikely in these alloys. It is possible that once a given grain size has been achieved, M_s could remain constant, but intuitively this seems unlikely.

The most probable explanation is the one proposed by Sastri and

West[105] who suggested that M_s depends on the strength of austenite and that above a certain austenitising temperature the strength of the austenite is effected only slightly by increasing temperature. Krauss[94] has shown that in an Fe-33% Ni alloy the reverse martensite transformation results in considerable deformation of the austenite raising its strength two or three fold. Thus for low austenitising temperatures the heavy dislocation density produced by the reverse transformation may not completely recover resulting in a low M_s. At higher temperatures complete recovery will occur and the strength of the austenite will be reasonably independent of austenitising temperature.

5.3. Acicular Martensite.

This reaction occurs in Fe-Ni alloys containing more than 30% Ni transformed below room temperature. The transformation was not studied as extensively as the other diffusionless transformations since this has been amply covered by previous work. However, since this reaction would appear to be a basic transformation occurring in iron alloys it is discussed briefly.

5.3.1. General description.

Previous work and the optical micrograph of martensite in Fe-31.75% Ni, Figure 40, shows that:

(1) The plates of martensite are lenticular in shape.

(2) The habit plane is irrational and the plates form at an obtuse angle to each other with retained austenite between the plates.

(3) Thin film electron-microscopy by Shimizu et al[11] and Hull[12] has shown that the plates are internally twinned.

In Fe-Ni alloys it seems clear this is the 'Umklapp' reaction referred to by Scheil and that each individual plate grows extremely rapidly[53,54]. This form of martensite was not observed in the Fe-Cr alloys and it seems likely that it occurs only in substitional alloys transforming at very low temperatures. That is acicular martensite would only be observed in substitional alloys which stabilise austenite to room temperature or below. In interstitial alloys the situation is different and the transformation can be

compared with the twinned martensite observed by Kelly in high Fe-C alloys[14].

5.3.2. Kinetic features.

No kinetic experiments were carried out on this transformation in this investigation, but previous work has shown that the reaction can occur athermally and isothermally[40]. When isothermal behaviour is observed a small percentage of martensite is formed fairly rapidly, but the transformation soon slows down after this initial reaction and no further isothermal martensite is formed until the specimen is cooled to a lower temperature when a similar rate curve is obtained. The percentage of martensite formed isothermally depends on the temperature and the amount of prior athermal martensite in the specimen. Usually, about 10% martensite is formed in 10 to 20 minutes. In this respect the kinetics of the transformation are similar to those observed by Kogan and Entin for the martensite reaction in Fe-8.5% Cr - 0.05% C, although in the latter case the reaction is considerably faster and is completed in about 2-3 seconds. Also in contrast to the transformation to massive-martensite the formation of acicular martensite occurs by the nucleation of new plates and their rapid growth whereas the massive martensite reaction proceeds by slow growth of old plates as well as nucleation of new ones.

5.3.3. Chemical driving force $\Delta G^{\gamma \to \alpha}$.

The calculations of Kaufman and Cohen[51] for M_s in

high Fe-Ni alloys indicate that the driving force for the transformation is approximately 300-320 cals mole^{-1}. They also calculated the driving force for the martensite reaction in Fe-C alloys using the M_s data of Greninger[32]. (This is for carbon contents varying from 0.2 to 0.6%). These calculations show that the driving force is constant at approximately 300 cals mole^{-1}. Thus, it appears that the driving force for acicular martensite is about 300 cals mole^{-1}.

5.3.4. Crystallography.

The crystallography of acicular martensite in iron-30% Ni alloys has been studied extensively previously[9]. The habit plane is $\{259\}_\gamma$ and the orientation relationship is that found by Nishiyama[8]:

$$(111)_\gamma \;//\; (110)_\alpha$$
$$[2\bar{1}1]_\gamma \;//\; [110]_\alpha$$

The irrational habit $\{259\}_\gamma$ is consistent with the metallographic observation that the plates form at an obtuse angle to each other. The habit plane would also appear to agree with the $\{259\}_\gamma$ habit observed in high carbon steels[6,17]. However the orientation relationship in plain-carbon steels is the Greninger-Troiano relation:

$$(111)_\gamma \sim 1^\circ \text{ from } (10\bar{1})$$
$$[1\bar{2}1]_\gamma \sim 2^\circ \text{ from } [10\bar{1}]_\alpha$$

Kelly[102] points out that this is not far from the Nishiyama relationship and maintains that the G/T relationship is the correct one for the $\{259\}_\gamma$ habit. On the basis of Kelly's rationalisation

of the crystallography of martensite[102], acicular martensite belongs to type 1 martensite with the predominant inhomogeneous shear as twinning $(110)_\gamma\ [1\bar{1}0]_\gamma$, i.e. $(112)_\alpha\ [11\bar{1}]_\alpha$. This agrees with the observation of twinning observed by thin film electron-microscopy.

5.4. Comparison with the Results of Parr and Other Workers.

Recently Parr and his co-workers[96,97] have carried out studies on the effect of cooling rate on the transformation temperature in pure iron and iron-nickel alloys. The cooling rates used were much higher than those used in this investigation. Since these studies are similar to those reported here, their work is reviewed below and compared with the present findings.

Bibby and Parr[97] studied the $\gamma \rightarrow \alpha$ transaformation in two batches of pure iron:

(a) 0.025% C 0.001% Si 0.005% Mn 0.003% Cu 0.001% Ni 0.001 % O & N

(b) 0.0017% non-metallic impurities and 0.0015% metallic impurities.

Cooling rates as high as 50,000°C sec^{-1} were used. The results obtained on source (a) iron are reproduced in Figure 63. The first plateau at 742°C did not give rise to surface rumpling on a pre-polished specimen, whereas surface tilts typical of martensite were observed on specimens which transformed at the second plateau temperature of 694°C. However a number of specimens from source (a) were observed to transform at the more usually observed M_s temperature of 540°C. There was appreciable scatter between 540°C and 695°C, in the transformation temperatures recorded.

The high purity iron (b), transformed martensitically at

750 ± 5°C when a cooling rate of 52,000°C sec^{-1} was used. Changing the austenitising temperature between 950°C and 1,300°C did not alter M_s. Bibby and Parr concluded that iron containing 0.005 to 0.010% C transforms at an M_s temperature of 540°C, but that as the carbon content is decreased below this value M_s rises sharply with decreasing carbon content. They thought the scatter encountered in the specimens from source (a) was due to local heterogeneity in the carbon content and that some of the specimens had carbon contents appreciably less than the bulk value of 0.025% C and consequently transformed at a higher temperature. Two possible explanations were advanced for this rapid initial decrease of M_s with carbon content.

(1) That the first few carbon atoms alter significantly the stability of the austenite lattice causing martensite to form at a lower temperature.

(2) That up to carbon contents of 0.001%, carbon fills vacancy sites in the austenite in preference to interstitial ones and enables martensite to form at a higher temperature.

In their study of Fe-Ni alloys containing 0.009% C, Swanson and Parr[96] also obtained two plateaux. A typical curve is reproduced in Figure 64. Specimens which transformed at temperatures corresponding to the first plateau did not show surface rumpling and were described as having a massive appearance. The second plateau was martensitic as shown by surface tilts. In the highest nickel alloy examined, Fe-10% Ni, the structure was martensitic at all

cooling rates.

Considerable scatter in the experimental transformation temperatures obtained for iron containing 0.011% C was also encountered in the present investigation. These results are shown in Figure 41. The lowest transformation obtained was 550°C and this is thought to be the M_s for this material. It is possible to draw a mean line through the other experimental points at 760°C and 690°C but in view of the scatter this cannot be done with any confidence. Contrary to the observations of Parr, the same specimens did not always transform at the same temperature for a given cooling rate. In some cases transformation occurred at a high temperature and in a later run at 550°C, in others, transformation at 550°C was followed by transformation at a higher temperature. These observations eliminate the possibility of the scatter being caused by a specimen becoming decarburised during successive runs and causing transformation to occur at a higher temperature. They also indicate that local hetrogeneity in carbon content of specimens could not cause the variation in transformation temperature. Both Luwes[80] and Parr[97] report considerable scatter between 750°C and approximately 900°C. It is possible that these two plateaux of 760°C and 690°C represent two transformation mechanisms above the martensitic one of 550°C. However there is no definite cooling rate at which transformation changes from one plateau to the next. It should be noted however that these two possible plateaux at 760°C and 690°C are very close

to the two plateaux of 742°C and 694°C reported by Parr for source (a) iron containing 0.025% C. The scatter in the results may also arise from the small size of the specimens. These were 0.010" diameter wire. If nucleation of the high temperature transformations is a rare event these transformations may be suppressed in some specimens simply because the volume of the specimen is too small to contain a nucleus. This can be compared with Turnbull's[108] droplet experiment where a similar scatter in the results was observed.

As with Parr's work, it is possible to interpret the present results as revealing two plateaux in alloys containing less than about 10% nickel. However the transformation temperatures obtained in this investigation differ considerably from those reported by Parr. The results are compared in Figure 65. The temperatures recorded for the transformation to massive ferrite are considerably higher than the temperatures reported by Parr and Swanson[96] and the massive-martensite temperatures are more in agreement with the temperatures obtained by Parr et al for the first plateau, which however was not reported as being martensitic. It is not clear why there is this large discrepancy between the results. It is thought that the temperatures determined in this investigation are correct within the limits stated and that any possible experimental errors are too small to account for this large discrepancy. In particular the results obtained at slow cooling rates are in good agreement with those of Gilbert[81] and of previous workers[86,51]. Unfortunately,

Swanson and Parr do not quote values for similar cooling rates and the two measuring systems cannot be directly compared. Since the exact measuring system used by Parr is not known it would be presumptuous to postulate possible errors. The discrepancy must be treated as a real one in need of explanation.

It is possible that with the cooling rates employed by Parr et al they failed to observe the transformation to massive ferrite and that their first plateau corresponds to the transformation to massive-martensite observed in this investigation. However this does not explain why Parr et al observed two plateaux at temperatures lower than the transformation to massive ferrite or why surface tilts were not reported for the microstructure of Parr's first plateau. A possible explanation is that the massive-martensite temperatures determined in this investigation for the 15, 10, 8 and 6% Ni alloys do not refer to a completely martensitic transformation, but one which occurs by shear and short range diffusion and that at higher cooling rates and lower temperatures a truly martensitic transformation is obtained. The wavy nature of the plates observed in the electron-micrographs of Fe-15% Ni, suggests that the transformation may be accompanied by short range diffusion and supports this view.

It is interesting to note that in a 9% Ni steel containing 0.1% C three reactions have been reported[107]. The TTT diagram for this steel is reproduced in Figure 66, and the temperatures at the maximum rate of reaction are superimposed on Figure 65. As pointed

out in the discussion of the massive ferrite reaction, Section 5.1., it is possible that in alloys of higher carbon content, the massive ferrite reaction becomes associated with the pro-eutectoid reaction. On this basis the bainite reaction would be associated with the 'massive-martensite' temperatures in the 8, 10 and 15% Ni alloys. It is known that the bainite reaction produces surface tilts on a pre-polished specimen, but proceeds slowly by a process of shear and diffusion. However a direct comparison between the bainite reaction and transformations in the binary Fe-Ni alloys is not really possible since in the former case the transformation is accompanied by precipitation of carbides. It is not suggested that the transformation in the lower nickel alloys produces acicular martensite. The microstructures probably closely resemble the massive-martensite structure obtained for the 24% Ni alloy.

The fact that the temperatures obtained for the 'massive-martensite' reaction in the dilute Fe-Ni alloys seems to extrapolate to a higher value than 550°C in pure iron would also support this explanation. If in fact there are other transformations between the transformation to massive-martensite and that to massive ferrite, this may explain some of the scatter in the results on pure iron above the martensite temperature of 550°C. This explanation would also account for the difference in driving force $\Delta G^{\gamma \to \alpha}$ computed for the massive martensite reaction in Fe-Ni and Fe-Cr alloys. The M_s in Fe-Cr alloys lies on a smooth curve extrapolating to 550°C in iron with a driving

force $\sim$ 300 cals mole^{-1}. Thus, it is probably a true massive martensite reaction.

5.5. Comparison with Non-Ferrous Systems.

As indicated in the review, Chapter 2, Section 2.3., the massive transformation was first encountered in non-ferrous systems. On the basis of this previous work it would appear that a suitable definition for the massive transformation is as follows:- "A Massive Transformation is a diffusionless transformation in the sense that the parent phase changes to the product without any change in composition. The crystal structure of the product is one which is already present in the phase diagram and may or may not be supersaturated depending on the form of the equilibrium diagram. On polishing and etching, the microstructure consists of large grains or massive areas without any apparent microstructure within the transformed regions". It should be noted that this definition only describes the product of the transformation and does not attempt to discuss possible mechanisms of its formation. As stated in the Review some quite different microstructures have been included in the term massive. It is now apparent that these can be divided into two categories each of which form by different mechanisms.

(1) "Massive ferrite". This presumably forms by nucleation at the parent grain boundaries and growth by movement of a high angle boundary with short range diffusion across the austenite/ferrite interface.

This transformation gives rise to a structure which consists of large irregular grains which cross the parent grain boundaries.

(2) "Massive martensite". This transformation occurs by nucleation of martensitic plates and slow growth by shear. In some cases the shear may be accompanied by short range diffusion. Parallel surface tilts are evident on a pre-polished surface but the polished microstructure consists of large grains bounded by straight edges. In this case the ferrite grains are confined to the parent grains. Thus the microstructure, reproduced in Figure 6, to which Greninger[69] originally applied the description of massive α, resembles the massive martensite structures studied here and probably occurs by shear. In contrast to this, Figure 11, of massive ζ in Cu-Ga alloys (after Massalski[75]) resembles 'massive ferrite'. In particular it will be noticed that the massive ζ_s grains in Massalski's structure also cross the parent grain boundaries and should be compared with Figures 29 to 32 of massive ferrite in Fe-4% Ni. However, it appears that it is also possible to form 'massive martensite' at certain compositions in the Cu-Ga system as for example in Figure 12, also taken from Massalski's work. In fact Figure 10 from the work of Spencer and Mack[74] would appear to be a mixed structure of 'massive ζ_s' and 'massive martensite' in Cu-Ga. This should be compared with Figure 39 showing a mixed structure of 'massive ferrite' and 'massive martensite' in 'pure' iron. It is not clear to what category the microstructures of massive α in Cu-Zn found by Hull belong. These massive areas in the microstructure are bounded by straight edges so it is possible that these belong to the category of 'massive martensite'.

Clearly in the light of the present findings the massive structures in non-ferrous alloys need to be re-examined more closely. In particular pre-polished specimens need to be examined for surface tilts and the microstructures examined by thin film electron-microscopy

6. CONCLUSIONS

(1) At low degrees of undercooling and comparatively slow cooling rates, transformation of austenite to ferrite in Fe-Ni alloys containing less than 10% Ni, and Fe-Cr alloys, occurs by a transformation to give a structure which has been termed massive-ferrite.

(a) The transformation is diffusionless in the sense that the product has the same composition as the parent.

(b) However the transformation does not occur by shear since surface tilts are not evident on pre-polished specimens. The transformation presumably occurs by nucleation at the austenite grain boundaries and rapid growth by short range diffusion.

(c) The polished microstructure shows large irregular grains.

(d) Electron-microscopy shows high angle boundaries and a heavy dislocation density.

(e) The ferrite grains cross the parent austenite grain boundaries without hinderance.

(2) At large degrees of undercooling and higher cooling rates transformation of austenite to ferrite in Fe-Ni and Fe-Cr alloys occurs by a shear transformation. This transformation has been termed massive-martensite. The transformation is observed at normal cooling rates in Fe-Ni alloys containing 15 to 30% Ni. The product of the transformation has the following characteristics:-

(a) Parallel surface tilts are observed on a pre-polished specimen.

(b) Electron-microscopy shows parallel plates with a high dislocation density.

(c) The polished microstructure, however, does not reveal the individual plates and large massive areas are observed bounded by straight edges.

(d) The ferrite grains are confined to the original austenite grains.

(3) For a constant cooling rate it is possible to change from transformation to the massive-ferrite reaction to transformation to the massive-martensite reaction by changing the austenitising temperature.

(4) The M_s temperature for the transformation to massive-martensite increases by 30°C on increasing the austenitising temperature from 750°C to 900°C. However for austenitising temperatures greater than 900°C, M_s is approximately constant.

(5) In Fe-Ni alloys containing more than 30% Ni cooled below room temperature, transformation occurs martensitically. However the morphology of the product is different from that of massive martensite and it has been termed acicular martensite.

(a) Plates are large and lenticular in shape.

(b) The plates are internally twinned[11,12].

(c) The habit plane is $\{259\}_\gamma$ and the orientation relationship that of Nishiyama[9].

7. SUGGESTIONS FOR FURTHER WORK.

(1) It is difficult to study the kinetics of the massive ferrite transformation in binary substitional alloys because the transformation occurs so rapidly. However the work of Entin[89] on an Fe-8.5% Cr - 0.05% C alloy and an Fe-8.5% Cr - 2.5% Ni showed that the transformation is much slower in these alloys and it is possible to obtain a TTT curve for the reaction. It is suggested that Entin's work should be repeated on these alloys or alloys of similar composition and a detailed analysis made of the kinetics of the reaction. Isothermal examination of the transformation on a hot stage microscope would also be of interest.

(2) It would be profitable to study the variation of transformation temperature with cooling rate and composition for the massive transformation in a non-ferrous system. This could most easily be done for the massive transformation in the Cu-Al system.

(3) A particularly pertinent experiment would be to examine the massive structures in non-ferrous alloys for surface tilts on a pre-polished specimen.

(4) A thorough crystallographic study of the massive-martensite transformation would also appear necessary. This could most easily be done in iron-nickel alloys in the range 15 to 30% Ni where the massive-martensite reaction is obtained on comparatively slow cooling.

REFERENCES

1. B.A. Bilby & J.W. Christian, "The Mechanism of Phase Transformations in Metals, p.121, 1956, London (Inst. Metals).

2. D. Hull, Bull. Inst. Metals, 1954, 2, (11), p.134.

3. G. Kurdjumov, V. Miretskii & T. Stelletskaya, J. Tech. Physics U.S.S.R., 1938, 8, p.1959.
   See also Henry Brutcher Translation No. 2,300.

4. R.F. Mehl & D.W. Smith, Trans. A.I.M.E., 1934, 113, p.203.

5. A.R. Entwistle, "The Mechanism of Phase Transformations in Metals, p.315, 1956, London (Inst. Metals).

6. A.B. Greninger & A.R. Troiano, Trans. A.I.M.E., 1940, 140, p.307.

7. G. Wasserman, Mitt. Kaiser-Wilhelm Inst. Eisenforsch, Dusseldorf, 1935, 17, p.149.

8. Z. Nishiyama, Sci. Repts. Tokohu. Imp. Univ., 1934, 23 (4), p.637.

9. R.F. Mehl & G. Derge, Trans. A.I.M.E., 1937, 125, p.482.

10. G.R. Speich, Trans. A.I.M.E., 1963, 227, p.1426.

11. Z. Nishiyama, K. Shimizu & K. Sugino, Acta Met., 1961, 9, p.620,680.

12. J. Caggero & D. Hull, Acta Met., 1962, 10, p.995.

13. R.F. Mehl, C.S. Barrett & D.W. Smith, Trans. A.I.M.E., 1933, 105, p.215.

14. P.M. Kelly & J. Nutting, J.I.S.I., 1961, 197, p.199.

15. G.V. Smith & R.F. Mehl, Trans. A.I.M.E., 1942, 150, p.211.

16. G. Kurdjumov & G. Sachs, Z. Physik, 1930, 64, p.325.

17. A.B. Greninger & A.R. Troiano, Trans. A.I.M.E., 1941, 145, p.291,
   also ibid 1949, 185, p.590.

18. R.F. Mehl & D.M. Van Winkle, Rev Met, 1953, 50, p.465.

19. J.A. Venables, Phil. Mag., 1962, 7 (73), p.35.

20. P.R. Reed, Acta Met., 1962, 10, p.865.

21. J.F. Breedis & W.D. Robertson, Acta Met., 1962, 10, p.1077.

22. R. Lagneborg, Acta Met., 1964, 12, p.823.

23. R. Brook & A.R. Entwistle, Private communication.

24. E.C. Bain, Trans. A.I.M.E., 1924, 70, p.25.

25. M.S. Wechsler, D.S. Liebermann & T.A. Read, J. of Metals, 1953, 5, p.1503.

26. J.S. Bowles & J.K. Mackenzie, Acta Met., 1954, 2, p.129, 224.

27. J.S. Bowles & A.J. Morton, Acta Met., 1964, 12 (5), p.629.

28. J.C. Fisher, J.H. Hollomon & D. Turnbull, Trans. A.I.M.E., 1949, 185, p.691.

29. M. Cohen, Trans. A.S.M., 1949, 41, p.35.

30. A.J. Goldman, W.D. Robertson & D.A. Koss, Trans. A.I.M.E., Feb. 1964, 230, p.240.

31. H. Esser, W. Eilander, E. Spenlé, Arch. Eisenhutten, 1933, 6, p.389.

32. A.B. Greninger, Trans. A.S.M., 1942, 30, p.1.

33. W.J. Barrett & A.R. Troiano, Metals Technology, August 1948.

34. W. Steven & A.G. Haynes, J.I.S.I. 1956, 183, p.349.

35. W.J. Harris & M. Cohen, Trans. A.I.M.E., 1949, 180, p.447 and references therein.

36. S.G. Glover, J.I.S.I., 1962, 200, p.102.

37. C. Crussard & J. Philibert, 'Phase transformations in metals', Inst. of Met. Monograph 1955, 18, p.309.

38. G.V. Kurdjumov & O.P. Maksimova, Dokl Akad Nauk S.S.S.R. 1948, 61, p.83 (Henry Brutcher Translation No. 2187).

G.V. Kurdjumov & O.P. Maksimova, Dokl Akad Nauk S.S.S.R. 1950, 73, p.95 (Henry Brutcher Translation No. 2565).

39. S.C. Das Gupta & B.S. Lement, Trans. A.I.M.E., 1951, 191, p.727.

40. E.S. Machlin & M. Cohen, ibid, 1952, 194, p.489.

41. S.A. Kulin & C.R. Speich, ibid, 1952, 194, p.258.

42. R.E. Cech & J.H. Holloman, ibid, 1953, 197, p.685.

43. C.H. Shih, B.L. Averbach & M. Cohen, ibid, 1955, 203, p.183.

44. B.L. Fletcher, M. Cohen & S.C. Fletcher, Trans. A.S.M., 1948, 40, p.728.

45. B.L. Averbach & M. Cohen, Trans. A.S.M., 1949, 41, p.1024.

46. A.N. Holden, Acta Met., 1952, 1, p.617.

47. B. Cina, J.I.S.I., 1954, 177, p.406.

48. A.W. McReynolds, J. App. Physics, 1949, 20, p.896.

49. S.A. Kulin, M. Cohen & B.L. Averbach, Trans. A.I.M.E., 1952, 194, p.661.

50. J.R. Patel & M. Cohen, Acta Met., 1953, 1, p.531.

51. L. Kaufman & M. Cohen, Trans. A.I.M.E., 1956, 206, p.1393.

52. See G.V. Kurdjumov, J. of Tech. Phys. U.S.S.R., 1948, 18, p.1004 (also Henry Brutcher Translation No. 2412).

53. F. Forster & E. Scheil, Z. Metallkunde, 1940, 32 (6), p.165.

54. F. Forster & E. Scheil, Z. Metallkunde, 1936, 28, p.245.

55. R.F. Bunshah & R.F. Mehl, Trans. A.I.M.E., 1953, 197, p.1251.

56. C.H. Johansson, Arch. Eisenhutten, 1937, 11, p.241.

57. C. Zener, Trans. A.I.M.E., 1946, 167, p.513.

58. J.C. Fisher, Trans. A.I.M.E., 1953, 197, p.918.

59. L. Kaufman & M. Cohen, "The mechanism of phase transformations in metals, p.187, 1956, London (Inst. Metals).

60. L. Kaufman & M. Cohen, "Progress in Metal Physics", 1958, 7, p.172. see also M. Cohen, Trans. A.I.M.E., 1958, 214, p.171.

61. C.H. Shih, B.L. Averbach & M. Cohen, Trans. A.I.M.E., 1955, 203, p.183.

62. M.H. Richman, M. Cohen & H.G.F. Wilsdorf, Acta Met., 1959, 7, p.819.

63. A.J. Philips, Trans. A.I.M.E., 1930, 89, p.194.

64. A.B. Greninger & V.G. Mooradian, Trans. A.I.M.E., 1938, 128, p.337.

65. I. Isaichev & V. Miretsky, Zhur. Tekhn. Fiziki, 1938, 8, p.1333.

66. W. Jolley & D.Hull, J. Inst. of Metals, 1964, 92, p.129.

67. D. Hull, Bull. Inst. Metals, 1954, 2 (11), p.134.

68. D. Hull & R.D. Garwood, "The Mechanism of phase transformations in metals, p.219, 1956, London (Inst. Metals).

69. A.B. Greninger, Trans. A.I.M.E., 1939, 133, p.204.

70. V. Gawranek, E. Kaminsky & G. Kurdjumov, Metallwirtschaft, 1936, 15, p.380.

71. P.R. Swann & H. Warlimont, Acta Met., 1963, 11, p.511.

72. W. Hume-Rothery & G.V. Raynor, J. Inst. Metals, 1937, 61, p.205.

73. W. Hume-Rothery, G.V. Raynor, P.W. Reynolds & H.K. Packer, ibid, 1940, 66, p.209.

74. C.W. Spencer & D.J. Mack, ibid, 1955, 84, p.461.

75. T.B. Massalski, Acta Met., 1958, 6, p.243.

76. E.T. Peters, "The Eutectoids in the Cu-Si System", M.Sc. thesis, Univ. of Wisconsin, 1958.

77. C.R. Speich & D.J. Mack, Trans. A.I.M.E., 1953, 197, p.549; see also Discussion, L. Muldauer Trans. A.I.M.E., 1954, 200, p.675.

78. A. Sauveur & C.H. Chou, Trans. A.I.M.E., 1929, 84, p.350.

79. C.M. Wayman & C.J. Alstetter, Acta Met., 1962, 10, p.992.

80. Pol Duwez, J. Metals, 1951, 3, p.765.

81. A. Gilbert & W.S. Owen, Acta Met., 1962, 10, p.45;
see also A. Gilbert, Ph.D. Thesis, Univ. of Liverpool, 1960.

82. L.P. Srivastava & J. Gordon Parr, Trans. A.I.M.E., 1962, 224, p.1295.

83. E.A. Owen, E.L. Yates & A.H. Sully, Proc. Phys. Soc., 1937, 49, p.315.

84. E.A. Owen & A.H. Sully, Phil. Mag., 1939, Series 7, 27, p.614.

85. E.A. Owen & Y.H. Liu, J.I.S.I., 1949, 163, p.132.

86. F.W. Jones & W.I. Pumphrey, ibid, 1949, 163, p.121.

87. L. Kaufman & M. Cohen, Trans. A.I.M.E., 1956, 206, p.1393.

88. A.C. Haynes, ibid, 1957, 209, p.1314.

89. L.I. Kogan & R.I. Entin, Doklady Akademi Nauk. S.S.S.R., 1950, 73 (6), p.1173.
see also R.I. Entin, 'Decomposition of austenite by diffusional processes', p.295).

90. G. Krauss & Morris Cohen, Trans. A.I.M.E., 1963, 227, p.278.

91. C.E. Morris, Metal Progress, 1949, 56, p.696.

92. Tomo-Sato, Seikiti Hukai & Yen-Chien Huang, J. Aus. Inst. Metals, 1960, 5 (2), p.149.

93. R.B.G. Yeo, Trans. A.I.M.E., 1962, 224, p.1222;
see also R.B.G. Yeo, Trans. A.S.M., 1964, 57, p.48.

94. G. Krauss, Jr., Acta Met., 1963, 11 (6), p.499.

95. F.W. Jones & W.I. Pumphrey, J.I.S.I., 1949, 163, p.121.

96. W.D. Swanson & J.G. Parr, J.I.S.I., 1964, 202, p.104.

97. M.J. Bibby & J.G. Parr, ibid, 1964, 202, p.100.

98. N.P. Allen & C.C. Earley, J.I.S.I., 1960, 166, p.281.

99. G.V. Kurdjumov, J.I.S.I., 1960, 195, p.26.

100. A.I. Aaronson, 'Decomposition of austenite by diffusional processes', p.387.

101. T. Bell & W.S. Owen, Private communication.

102. P.M. Kelly, 'Metallurgical Developments in high alloy steels', Scarborough, 1964, B.I.S.R.A. Special Report No. 86, p.146.

103. K. Shimizu, J. Phys. Soc. Jap., 1962, 17 (3), p.508.

104. L. Kaufman, Trans. A.I.M.E., 1959, 215, p.218.

105. R.F. West & Sastri, Private communication.

106. W.S. Owen, E.A. Wilson & T. Bell, Second International Conference on High Strength Materials, Univ. of California, Berkeley, 1964. To be published.

107. C.W. Marschall, R.F. Hehemann & A.R. Troiano, Trans. A.S.M., 1962, 55, p.135.

108. D. Turnbull, J. Chem. Phys., 1950, 18, p.769.

Figure 1. Shape change produced by martensite. The scratches are continuous across the interface (after J.S. Bowles Acta Cryst. 1951 4 p.162).

Figure 2. Illustration of shape change produced by martensite plate.

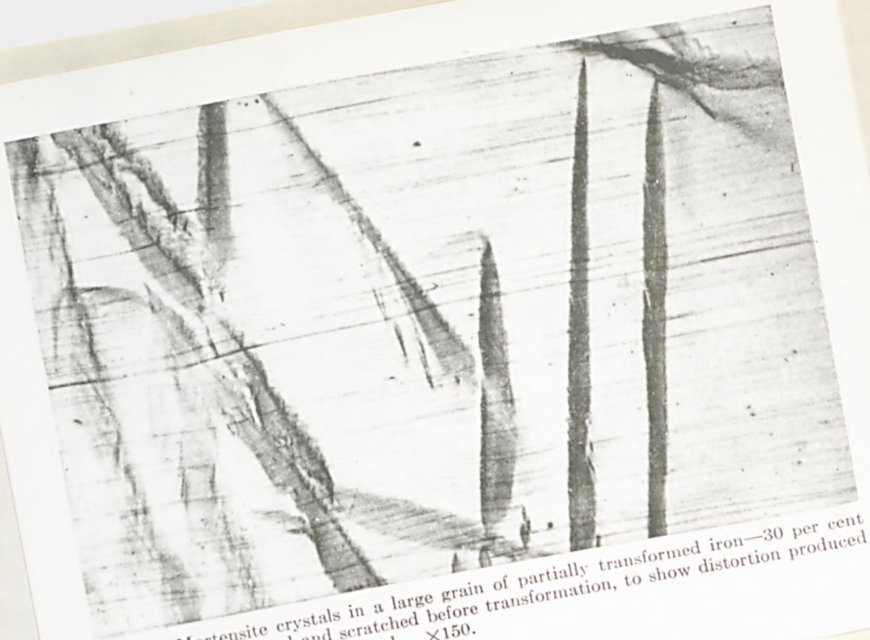

FIG. 19. Martensite crystals in a large grain of partially transformed iron—30 per cent nickel alloy. Polished and scratched before transformation, to show distortion produced by the transformation. Unetched. ×150.

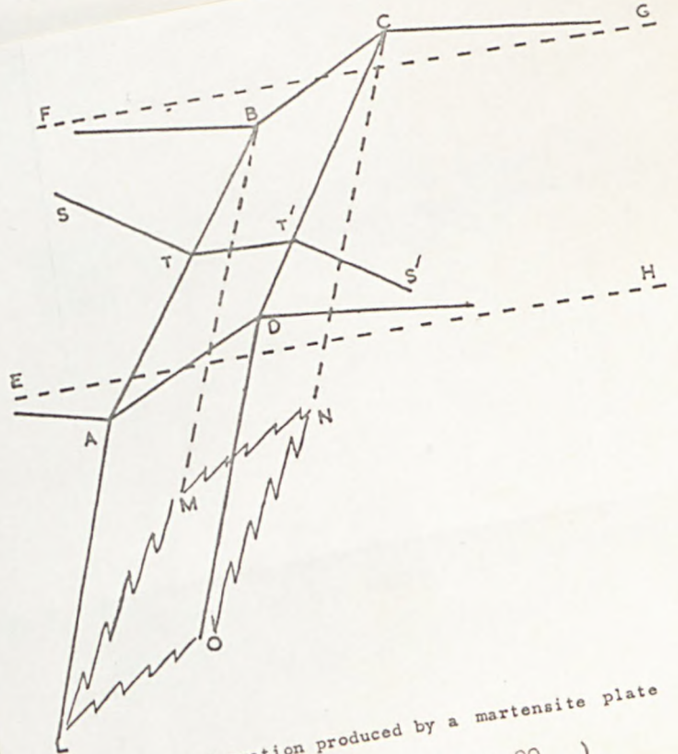

1 The shape deformation produced by a martensite plate (after Dr J.K.Mackenzie J. Aust. Inst. Met. 1960, 5, p.90)

Figure 3. Cu-Zn phase diagram.

Figure 4. Massive α in Cu-38.7% Zn water quenched from 850°C. Etched in ammonical ammonium persulphate x200
(after D. Hull and R.D. Garwood[68])

Figure 5. Massive α in Cu-38.7% Zn quenched into 10% NaOH at 0°C from 850°C. Etched in ammonical ammonium persulphate x150
(after D. Hull and R.D. Garwood[68])

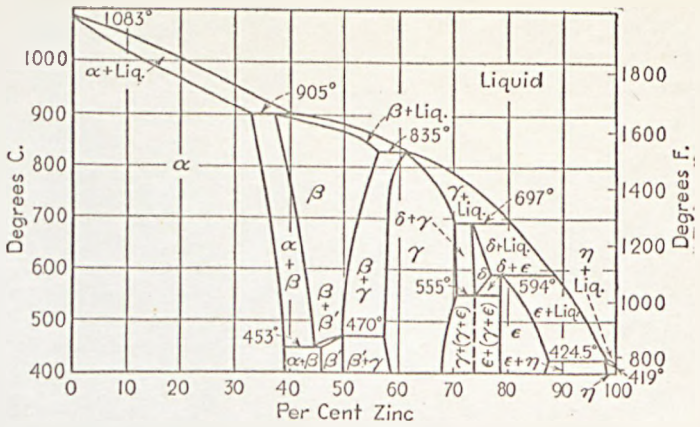

FIG. 1. Constitution diagram for copper-zinc alloys. Compositions in weight per cent. (*National Metals Handbook.*)

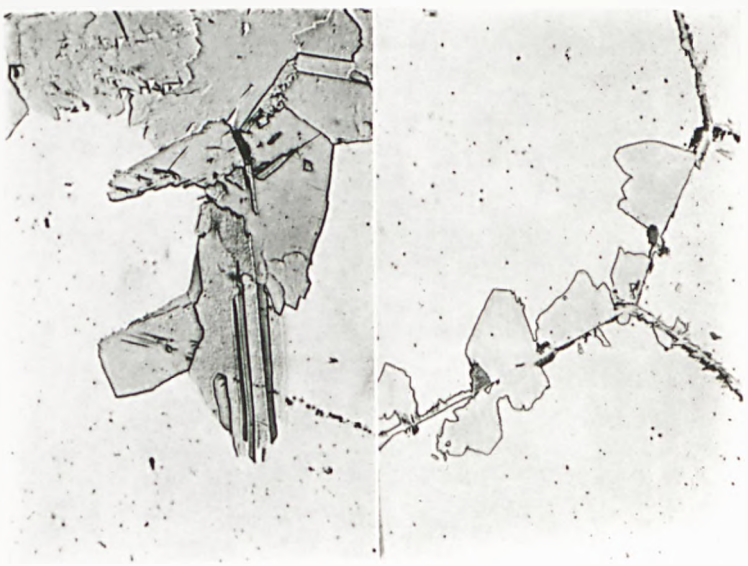

Figure 6. Massive α in Cu-9.3% Al quenched from 1020°C in 10% NaOH. Etched with $NH_4OH + H_2O$ x100 (after Greninger(69))

Figure 7. Cu-Al phase diagram.

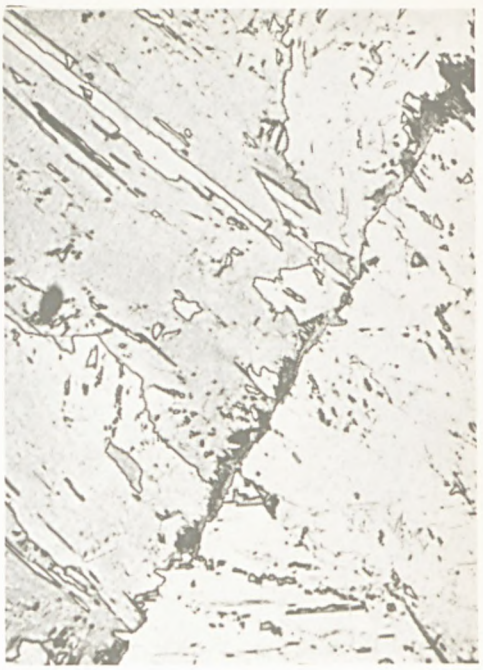

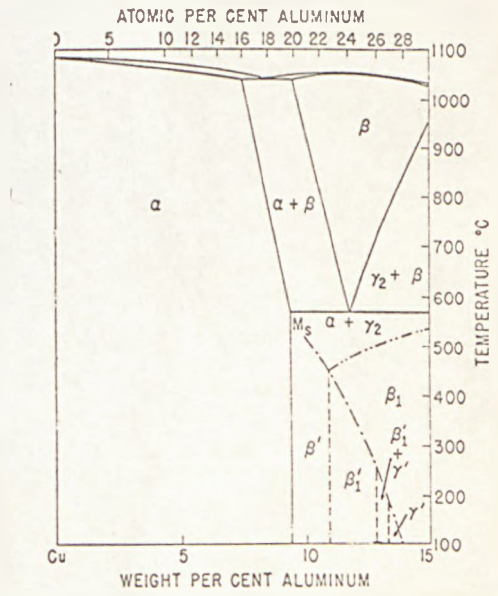

FIG. 1. Copper rich end of the copper aluminum equilibrium diagram (————), also showing M_s temperatures of β', β_1' and γ'(– · – · –), $\beta \rightarrow \beta_1$ ordering temperatures (– · · – · ·)

Figure 9. Cu-Ga phase diagram.

Figure 10. Massive γ_s in Cu-25.4% Ga
(after Spencer and Mack[74])

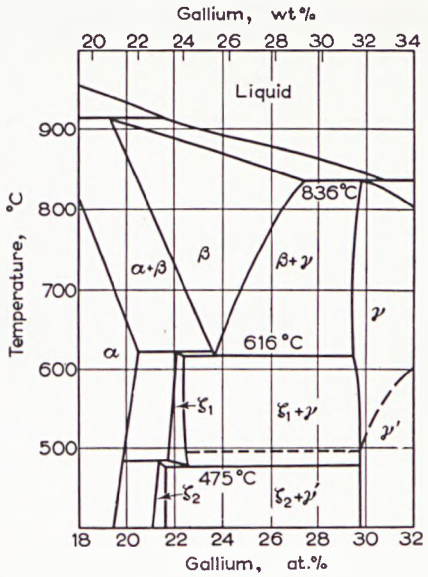

A portion for the copper–gallium equilibrium diagram in the region of the β phase. (After HUME-ROTHERY and RAYNOR *J. Inst. Met.* **61**, 205 (1937); BETTERTON and HUME-ROTHERY *J. Inst. Met.* **80**, 459 (1952).)

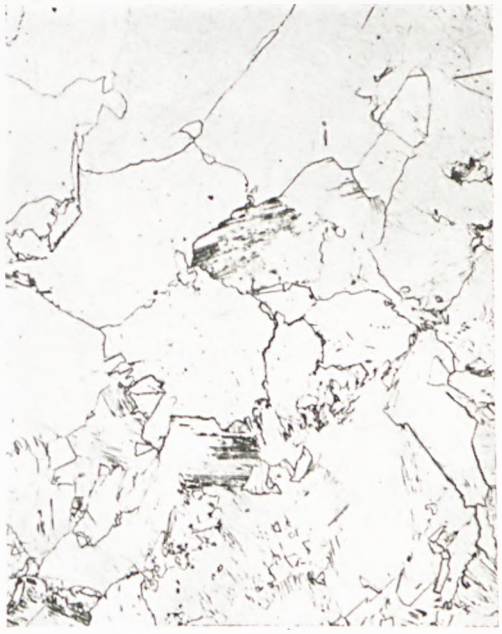

Fig. 18. A Cu-Ga (25.4% Ga) eutectoid alloy in which the entire structure is massive ζ_s. Obtained by quenching from 775°C.[19] 100×.

Figure 11. Massive γ_s crossing β grain boundaries (after Massalski[75])

Figure 12. Massive γ_s in Cu-23.86% Ga (after Massalski[75])

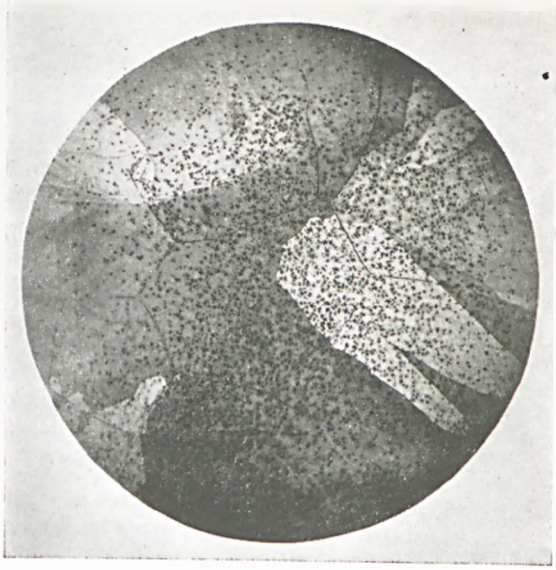

Discussion Fig. 1. Cu–18.40%Ga–~~500~~%Ge, quenched from 750°C. Etched in alcoholic $FeCl_3$. 120×. [Massalski, *J. Inst. Metals*, **88**, 232 (1960).]

Alloy *A*, quenched from 750°C, unetched, polarized light. ×350.

Figure 13. Variation of M_s with carbon content in Fe-C alloys (after Greninger[32])

Figure 14. Fe-Ni phase diagram (from Metals Handbook)

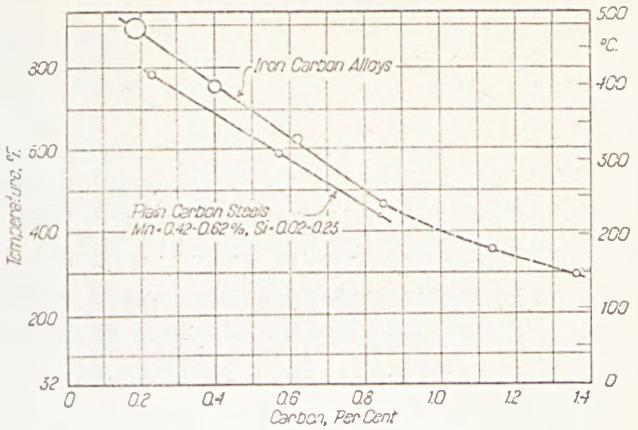

Fig. 4--Influence of Composition upon the Temperature of Ar'', for Specimens Austenized 5 to 10 Minutes at 70 to 90 Degrees Cent. above Ac or Acm. Temperatures for the hypereutectoid compositions were determined microscopically only.

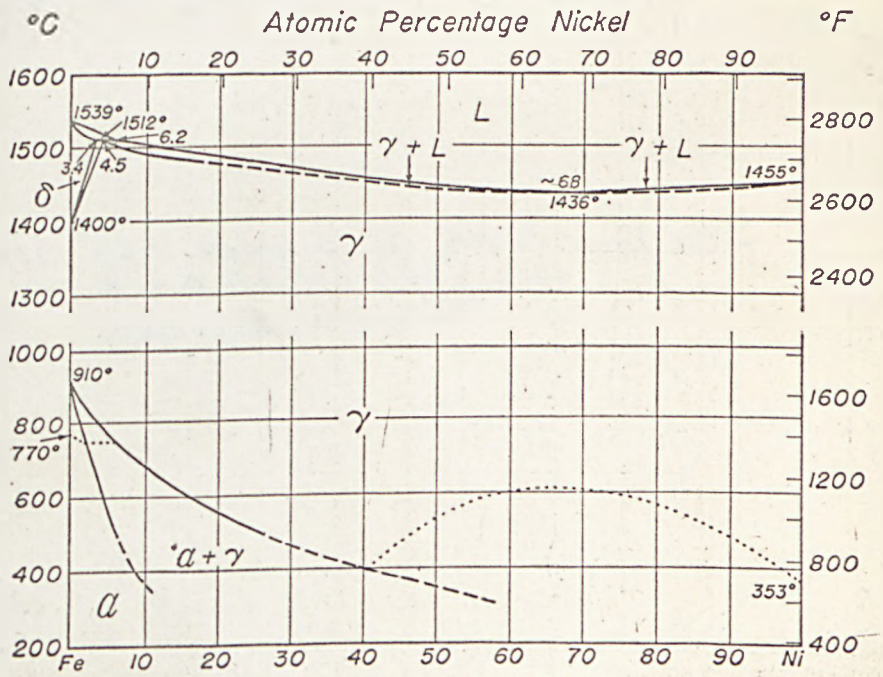

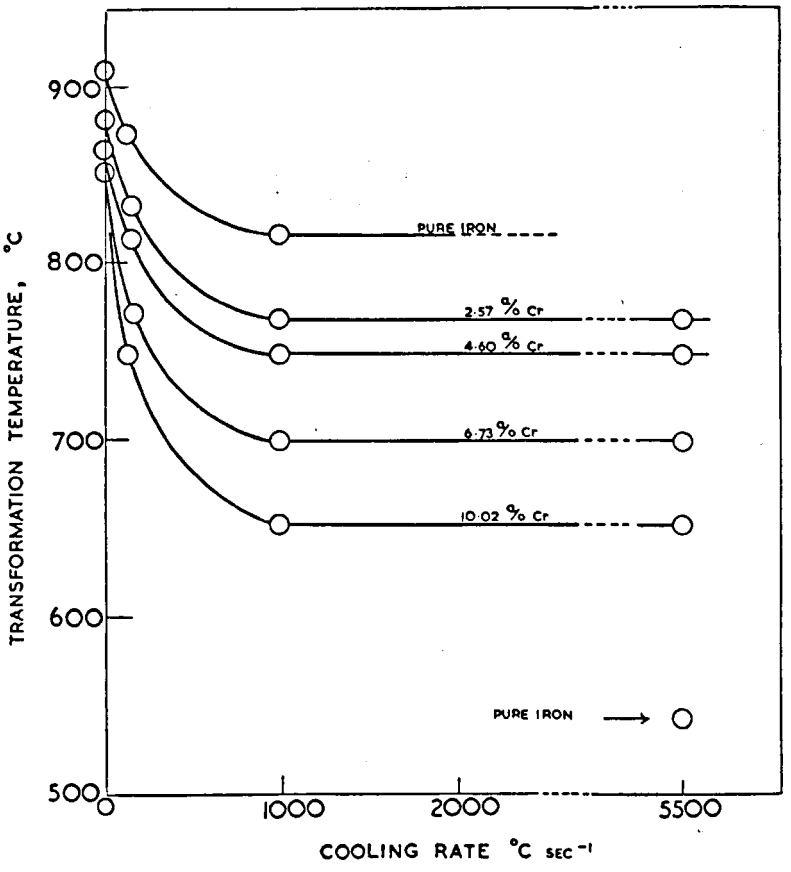

FIG. 2. Variation of transformation temperature with cooling rate in iron–chromium alloys.

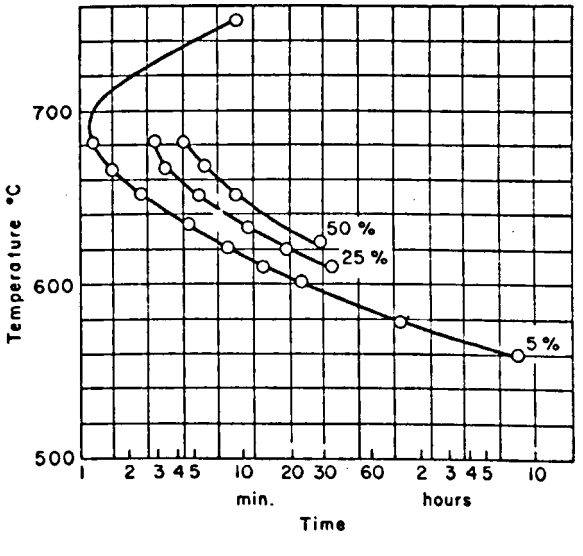

Fig. 1. Diagram of the isothermal $\gamma \rightarrow \alpha$ transformation in Fe-8.5% Cr alloy.

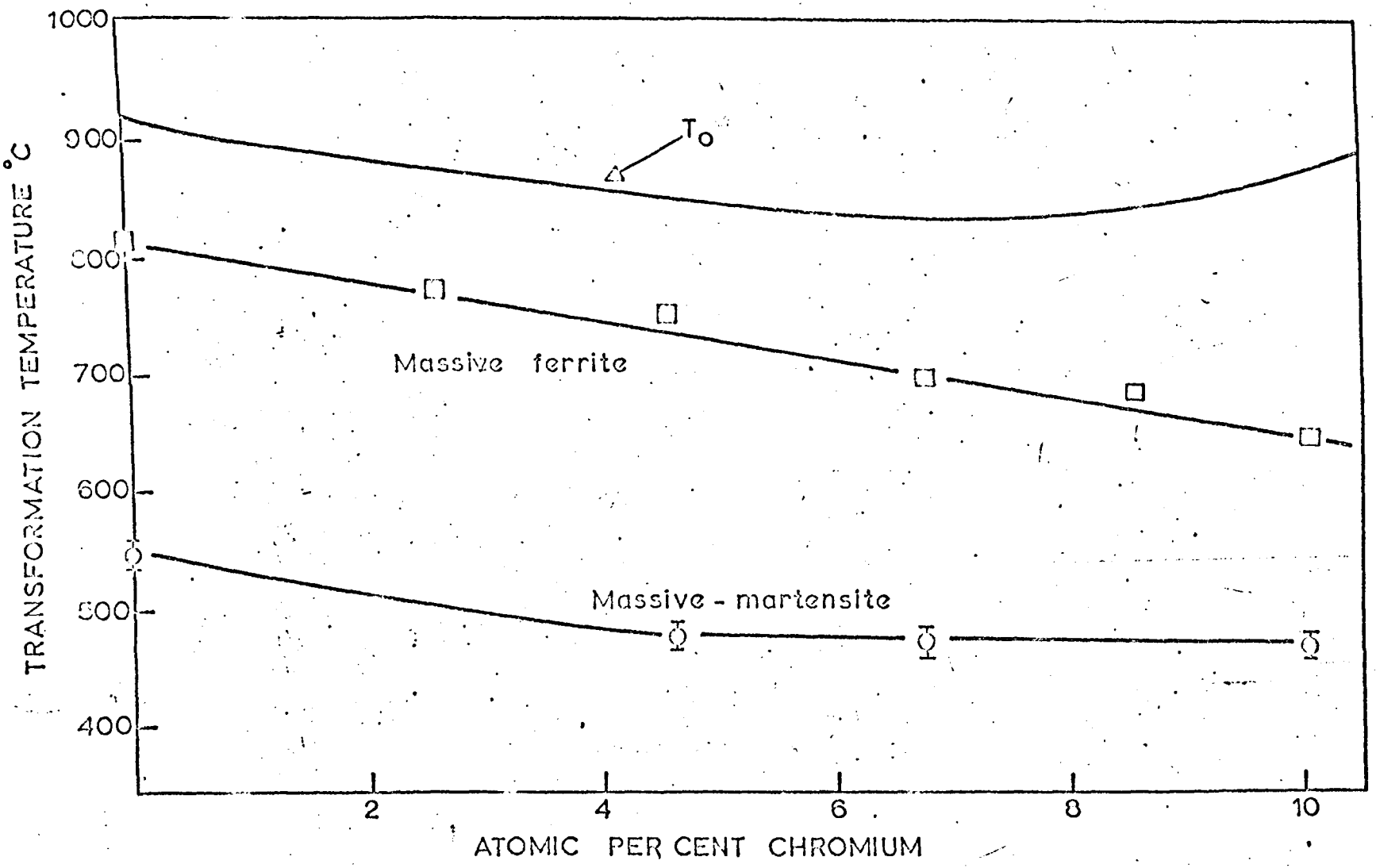

□ A. Gilbert[81], 5,000°C sec^{-1}.

Ⴔ This investigation, 8,000°C sec^{-1}.

□ Nose of Entin's "C" curve[89].

Figure 17. Transformation temperatures obtained on cooling Fe-Cr alloys.

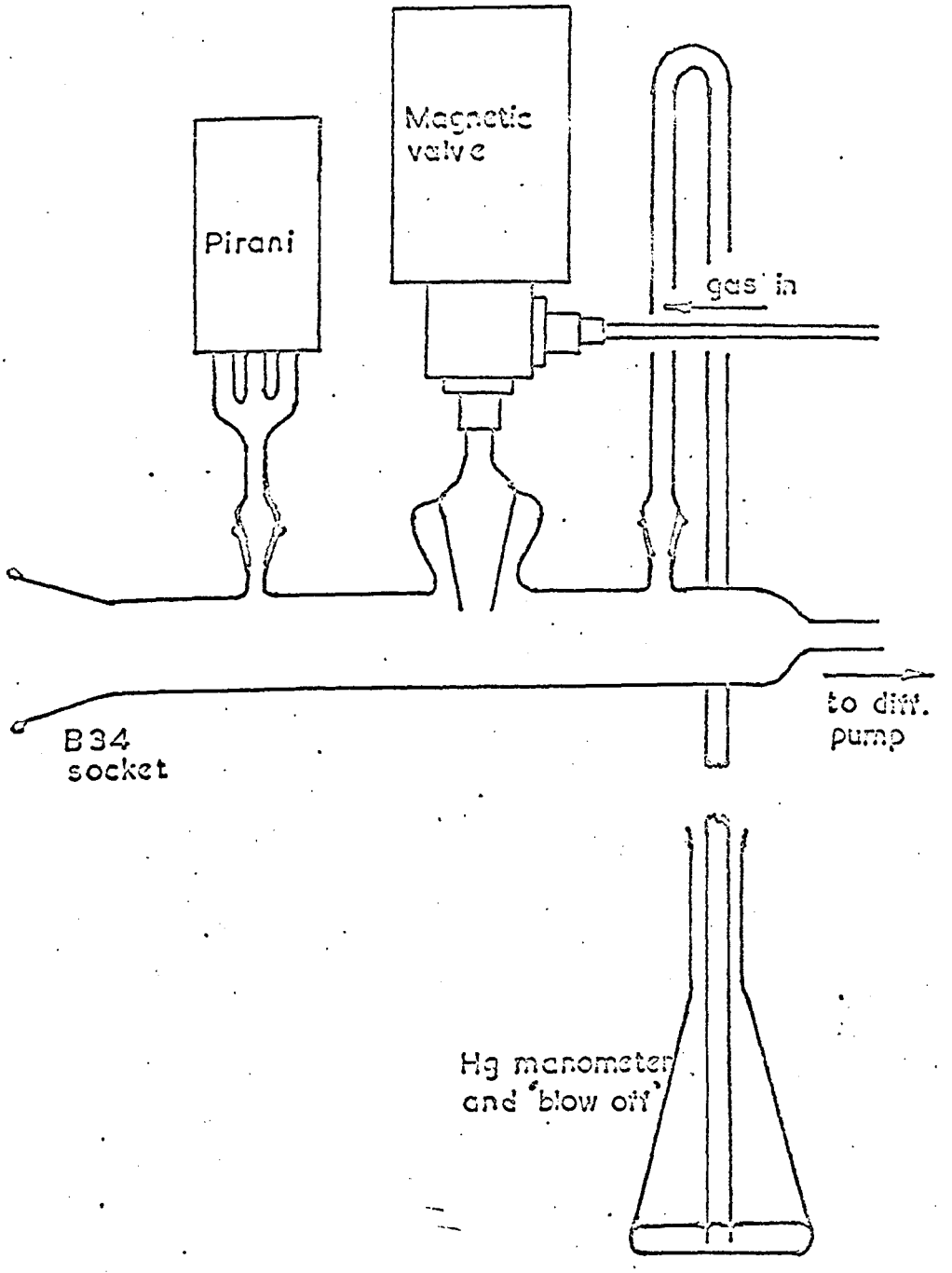

Figure 13. Schematic diagram of apparatus.

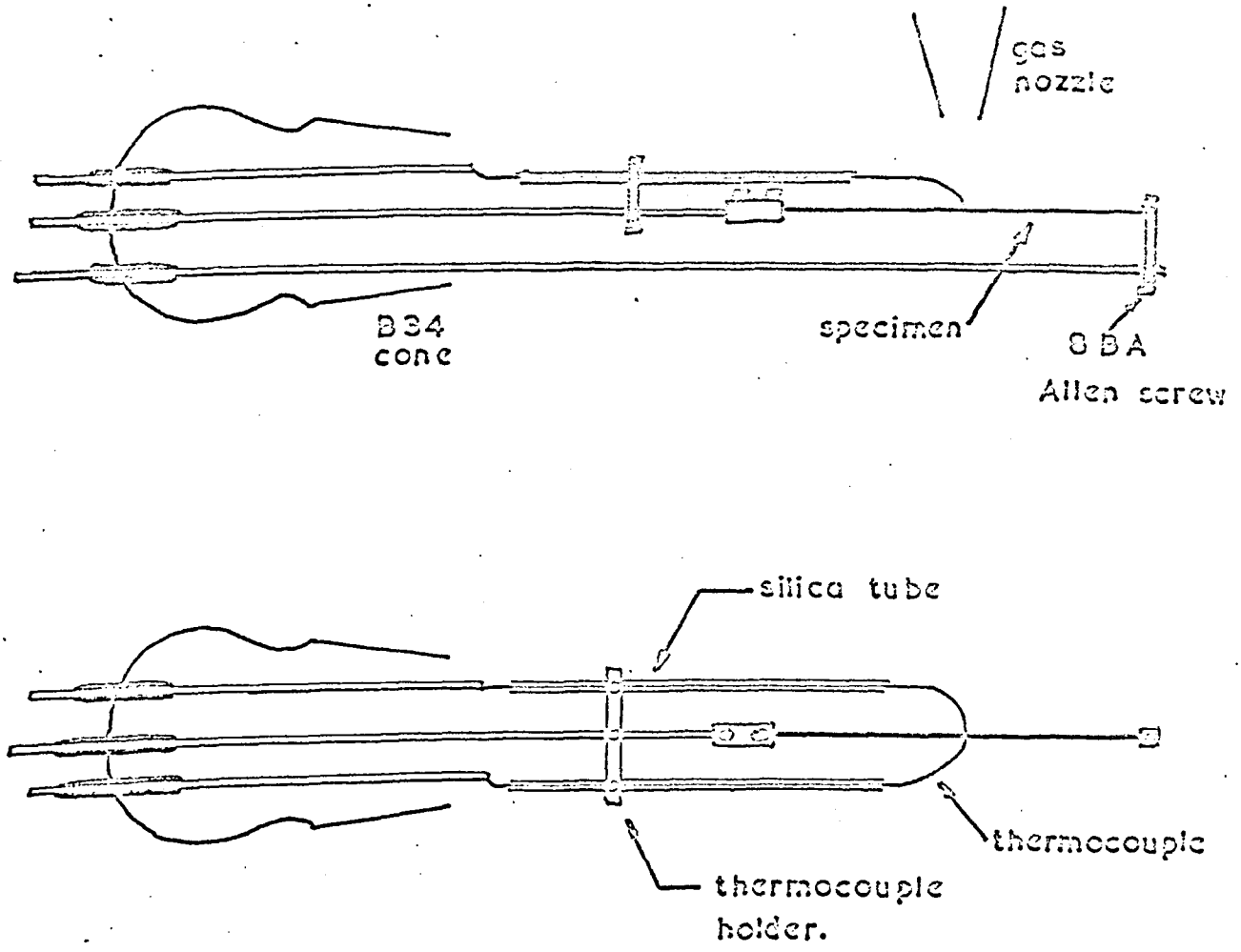

Figure 19. Schematic diagram of specimen holder.

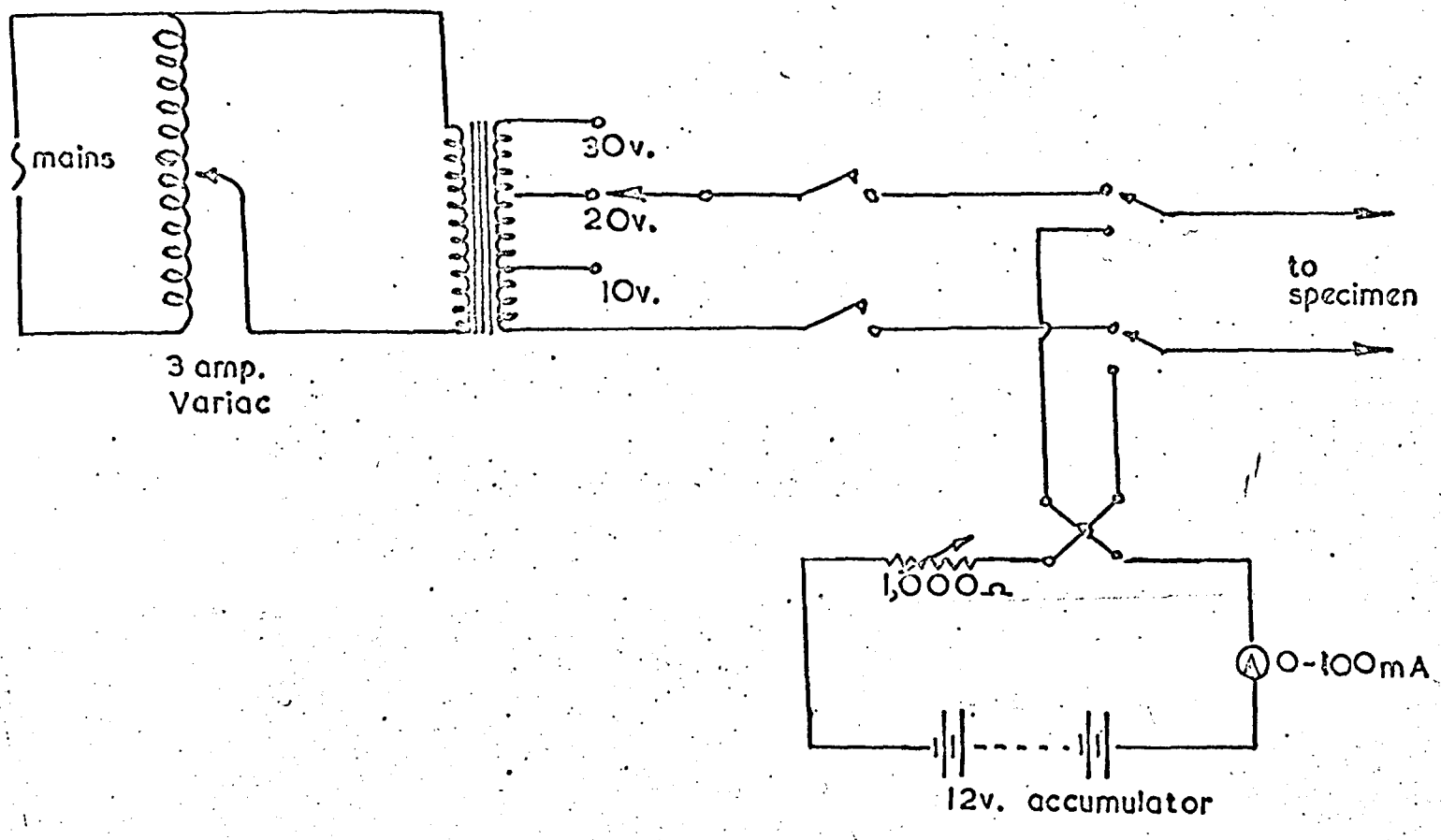

FIGURE 20. Schemetic diagram of A.C.heating circuit and constant D.C.current circuit.

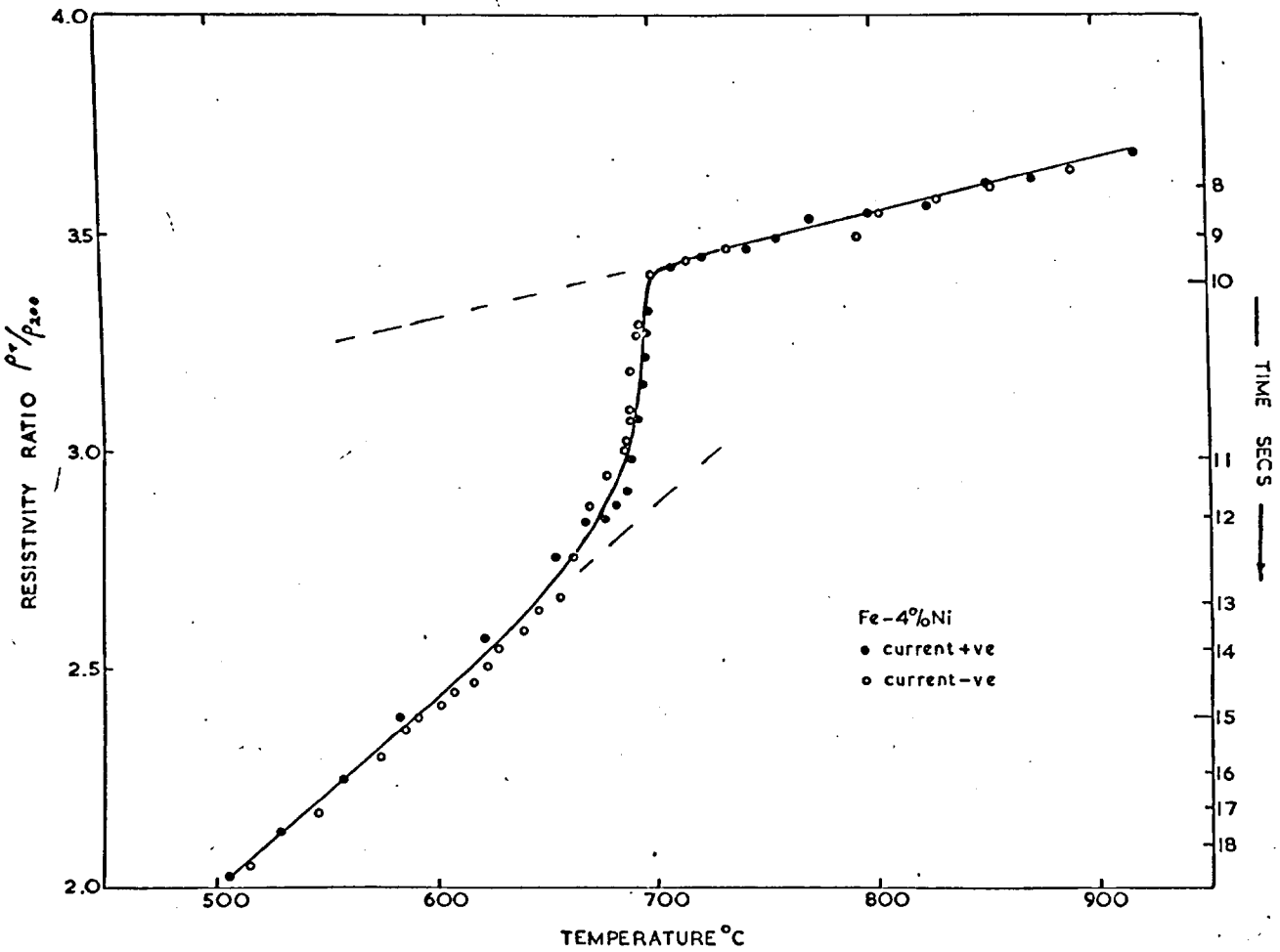

Figure 21. Variation of resistance with temperature on continuous cooling Fe-4% Ni.

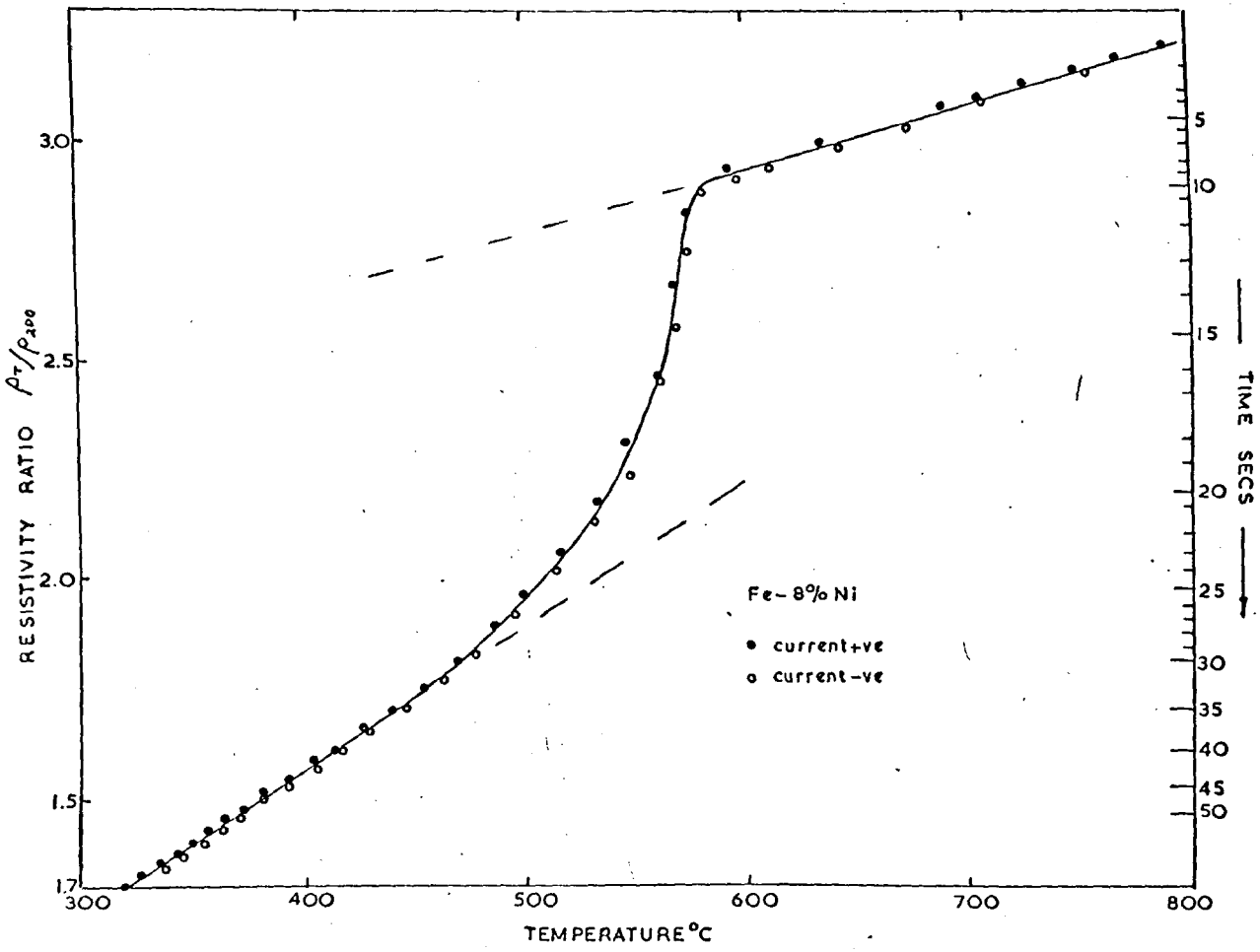

Figure 22. Variation of resistance with temperature on continuous cooling Fe-8% Ni.

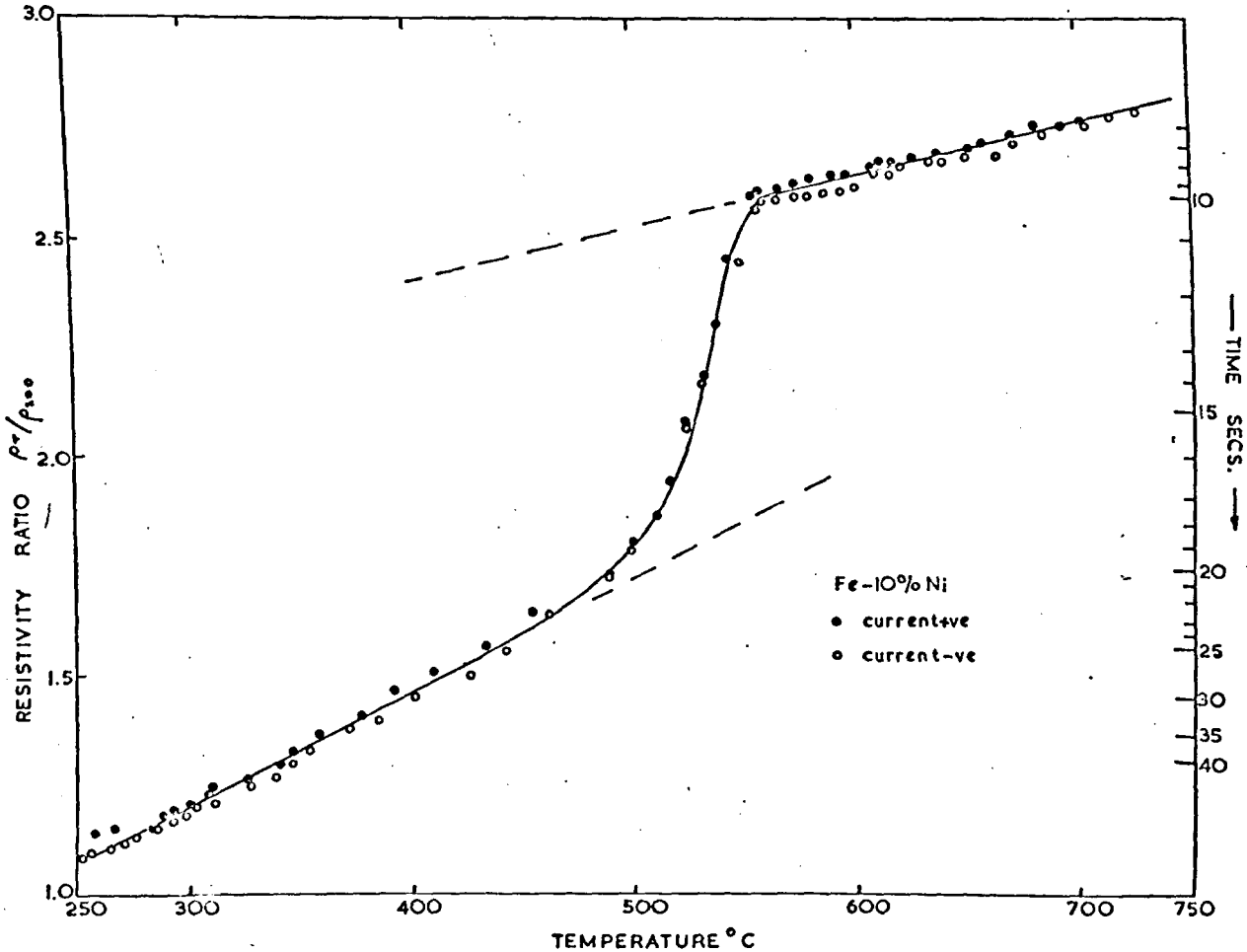

Figure 23. Variation of resistance with temperature on continuous cooling Fe-10% Ni.

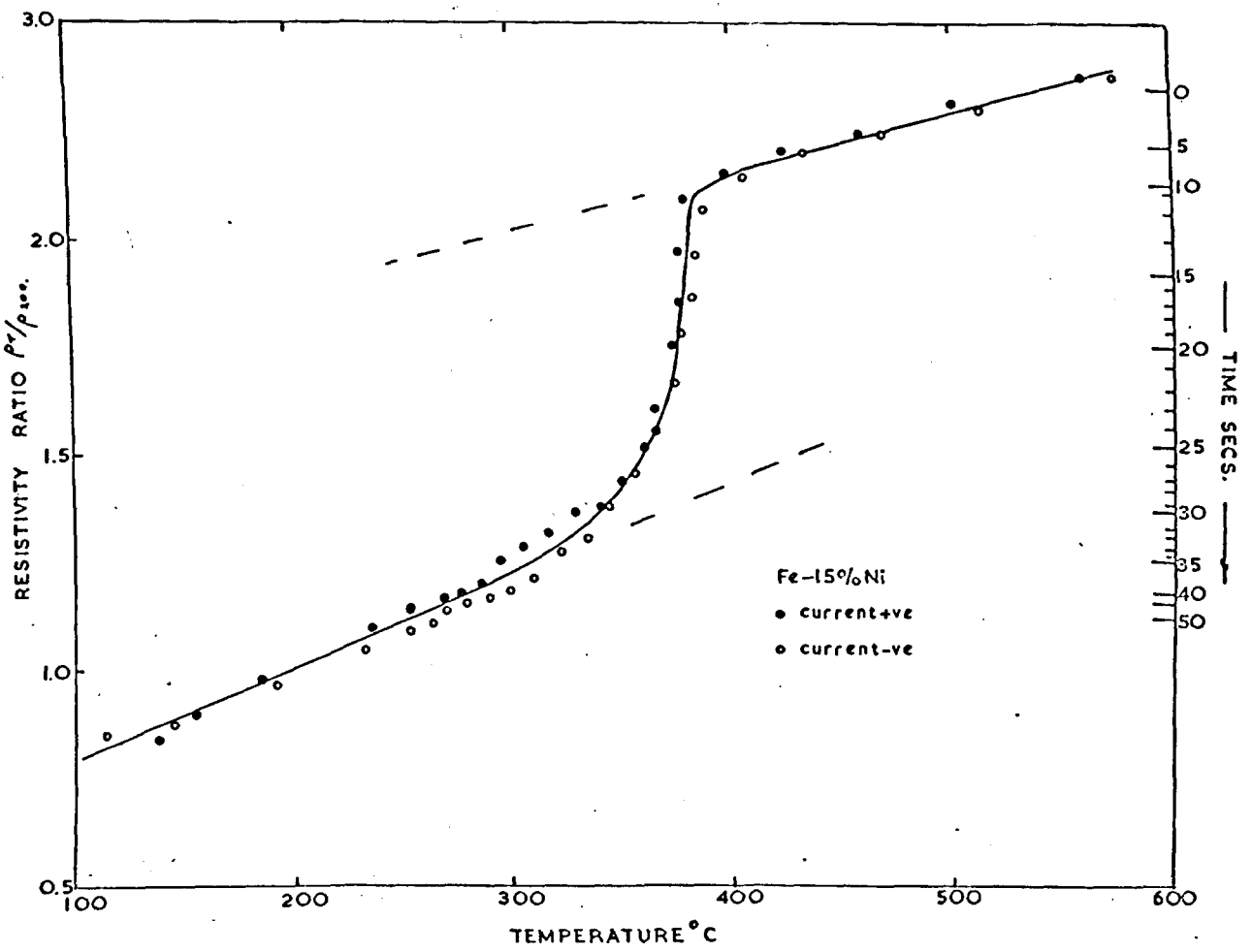

Figure 24. Variation of resistance with temperature on continuous cooling Fe-15% Ni.

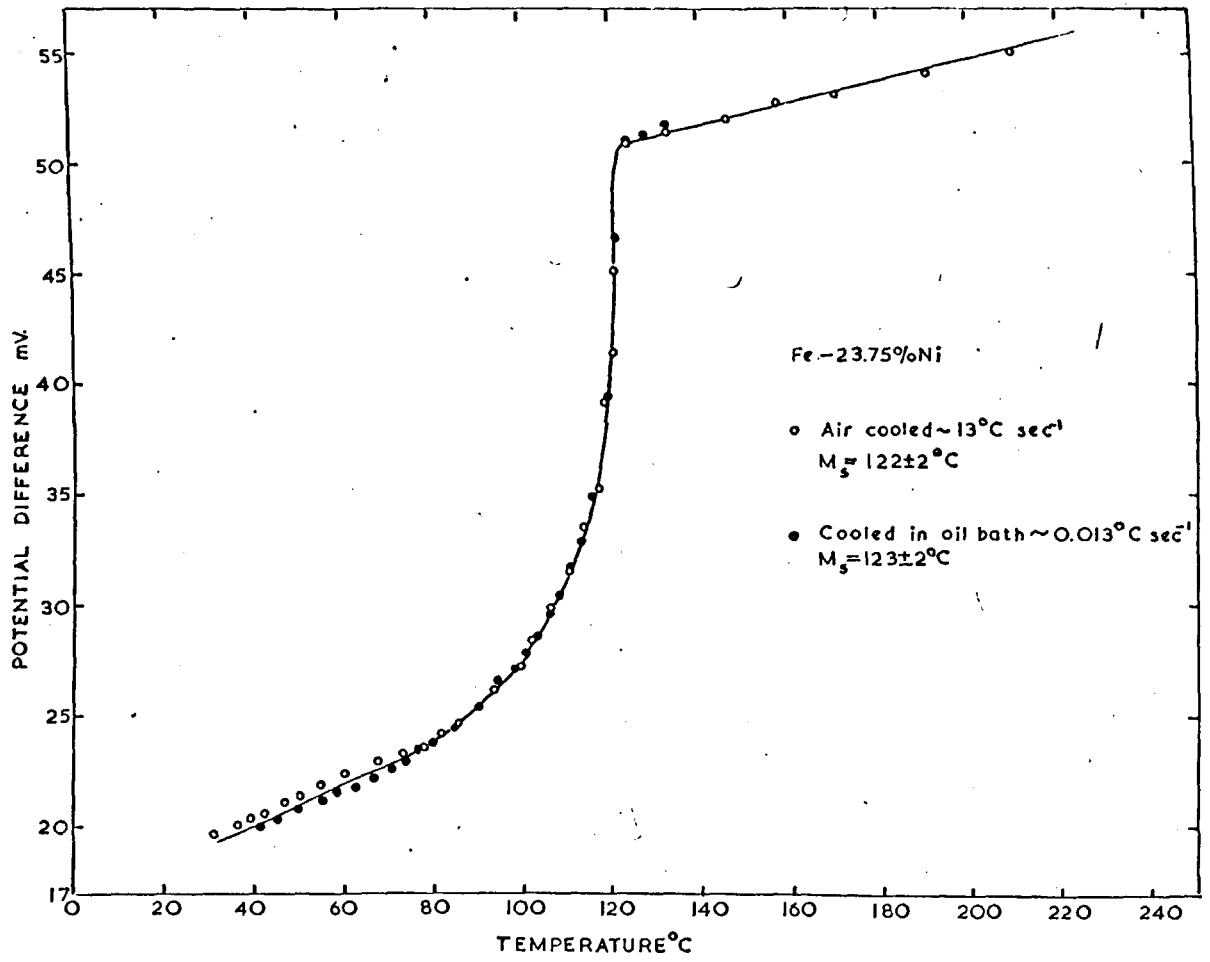

Figure 25. Illustrating the invariance of the resistance/temperature curve with cooling rate in Fe-24% Ni.

Figure 26. Typical microstructure of massive ferrite in Fe-6% Ni; cooling rate ~100°C sec-1; Transformation temperature 628 ± 5°C.

x200

Figure 27. Electronmicrograph of massive ferrite in Fe–6% Ni showing high density of dislocations.

Figure 28. Electronmicrograph of massive ferrite in Fe–6% Ni showing dislocations and high angle boundary.

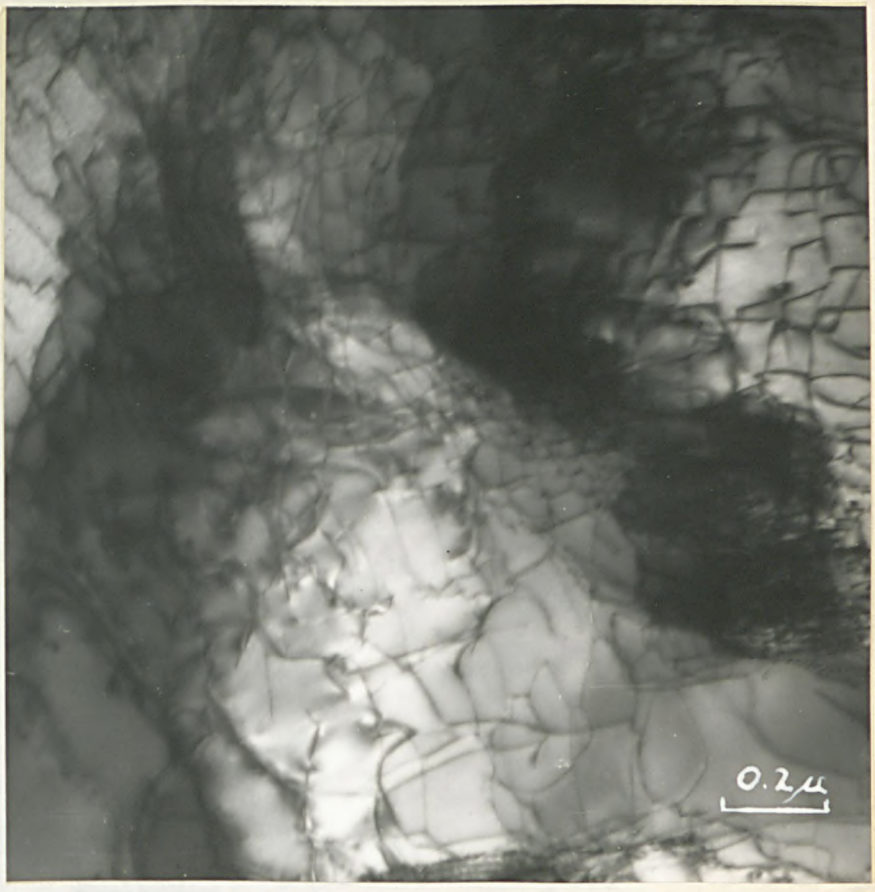
0.2μ

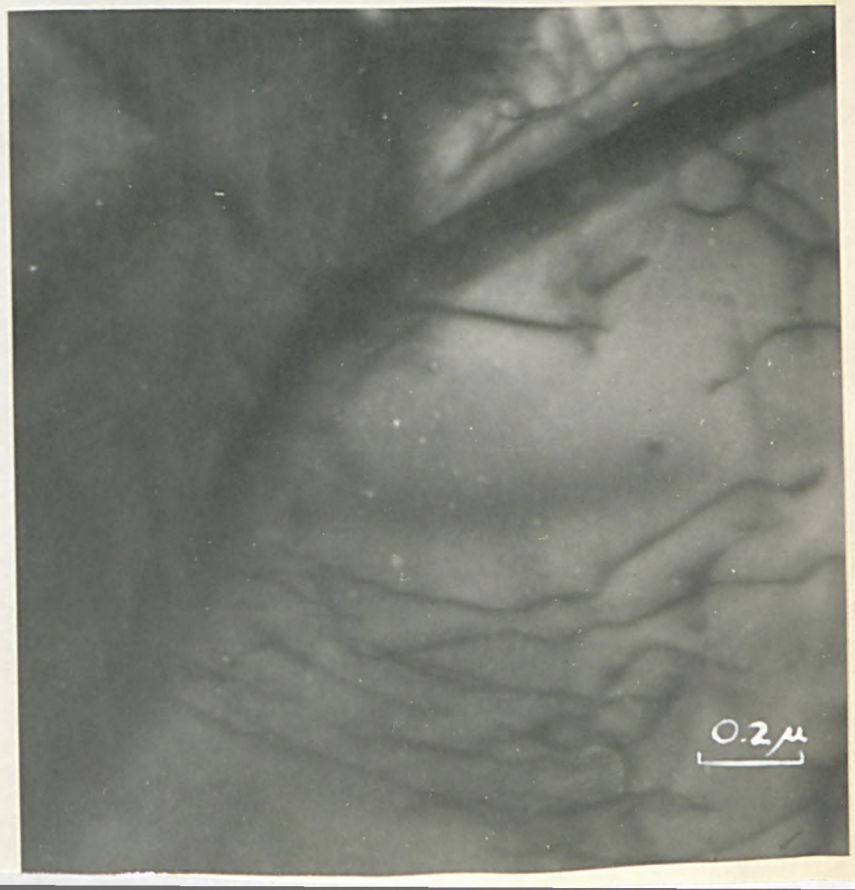
0.2μ

Figures 29 & 30. Massive Ferrite in Fe–4% Ni, showing ferrite grains crossing prior austenite grain boundaries.

x880

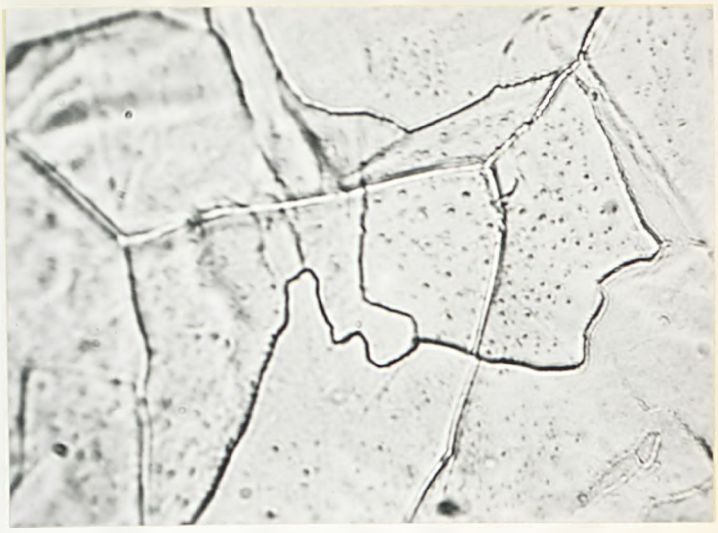

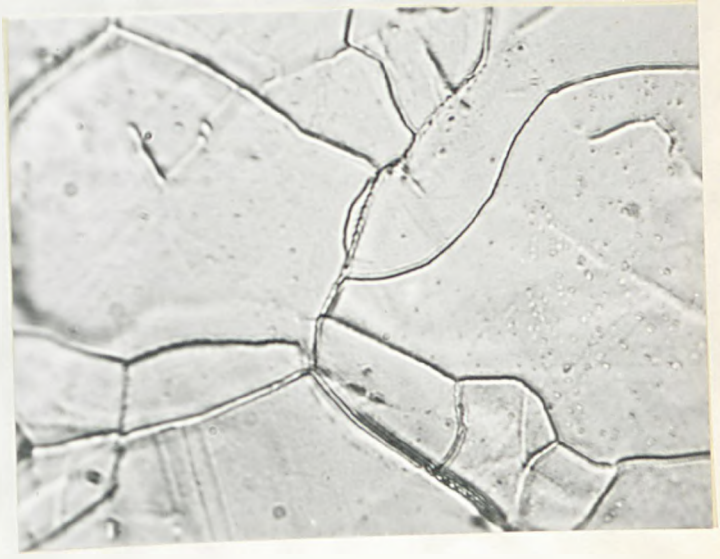

Figures 31 & 32. Massive ferrite in Fe-4% Ni, showing ferrite grains crossing prior austenite grain boundaries.

x880

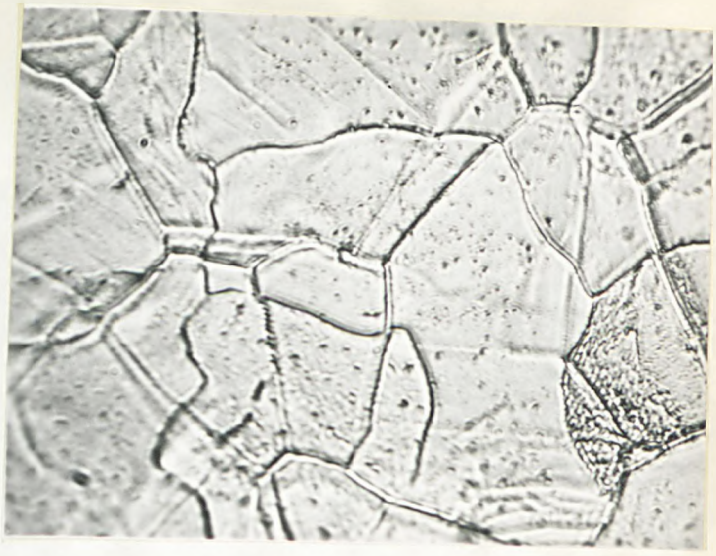

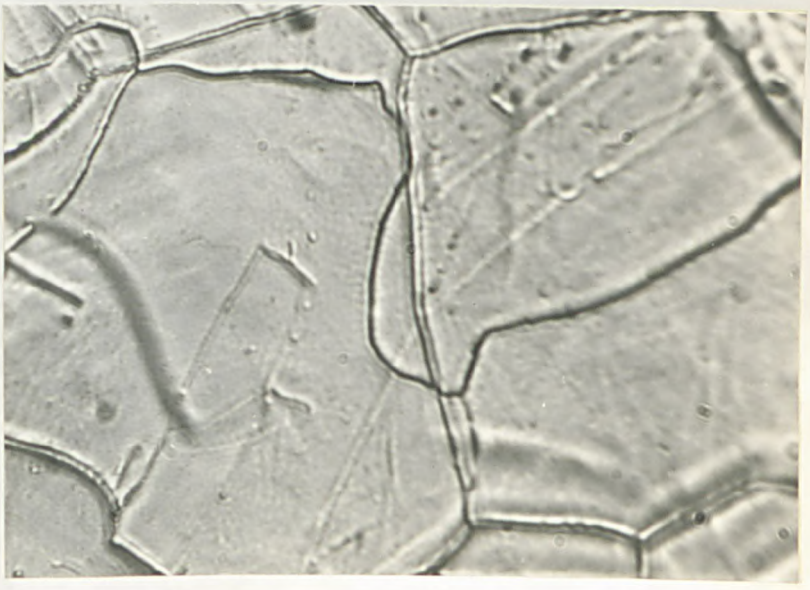

Figure 33. Surface tilts on a pre-polished specimen of Fe-15% Ni; cooling rate $\sim 100^{\circ}C\ sec^{-1}$. Transformation temperature $388 \pm 5^{\circ}C$.

x875

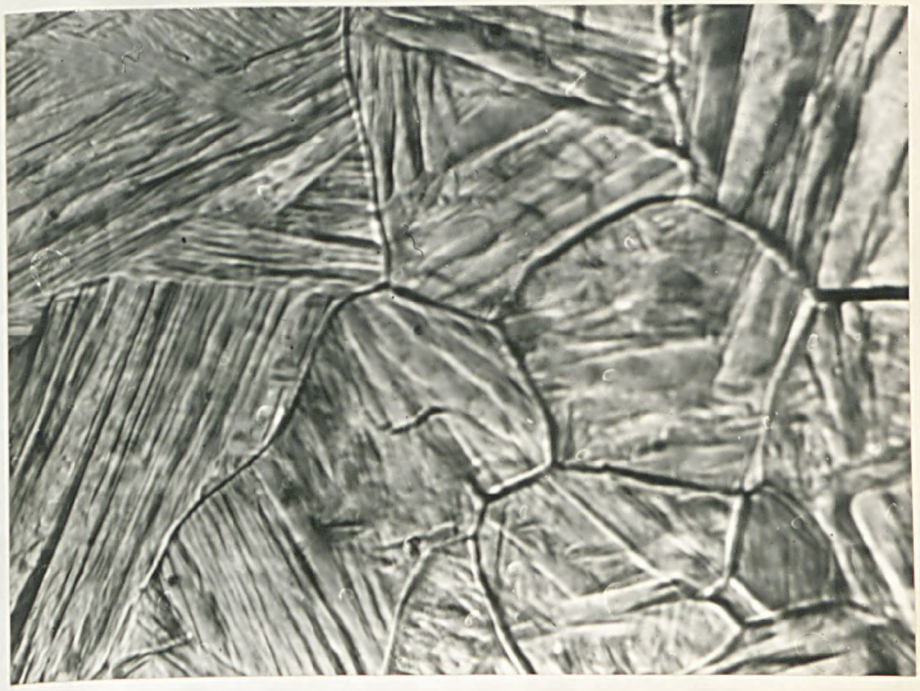

Figures 34 & 35. Electronmicrographs of massive martensite in Fe–15% Ni showing parallel plates containing heavy dislocation density.

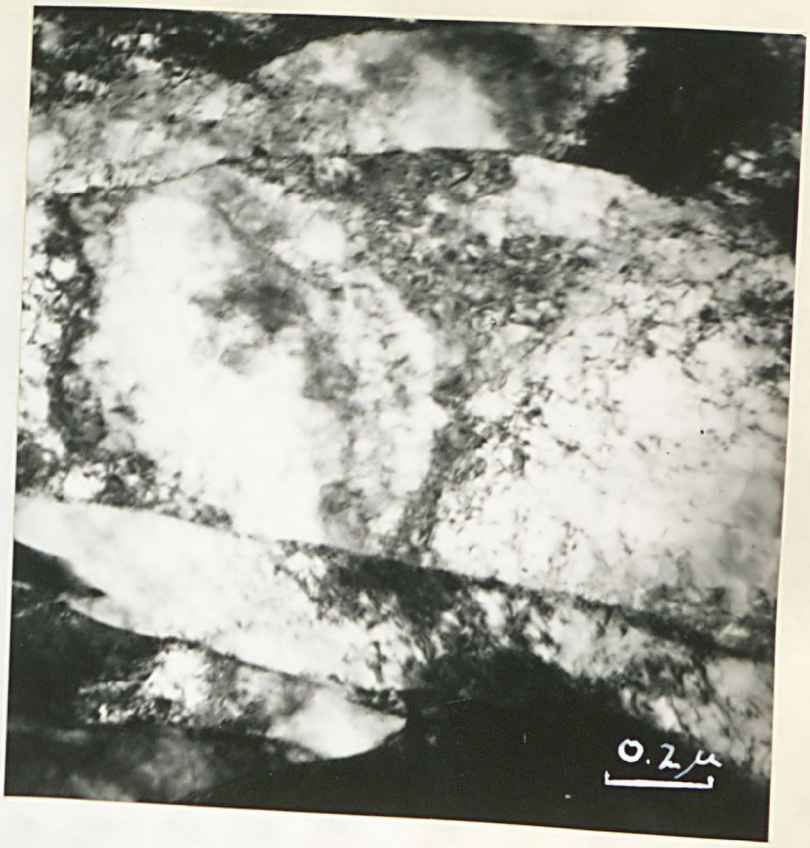
0.2μ


0.2μ

Figure 36. Microstructure of massive martensite in Fe-15% Ni.

x168

Figure 37. Microstructure of massive martensite in Fe-24% Ni.

x350

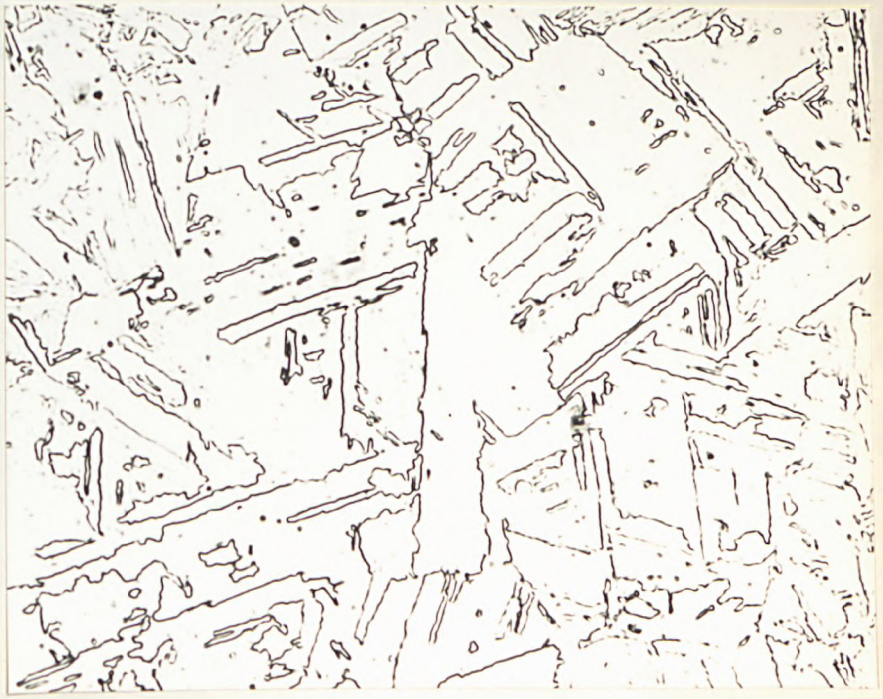

Figure 38. Pre-polished specimen of Fe-15% Ni, partly electropolished and etched.

x420

Figure 39. Mixed structure of massive ferrite and massive martensite in 'pure' iron.

x170

Figure 40. Microstructure of a cicular martensite in Fe-31.75% Ni.

x330

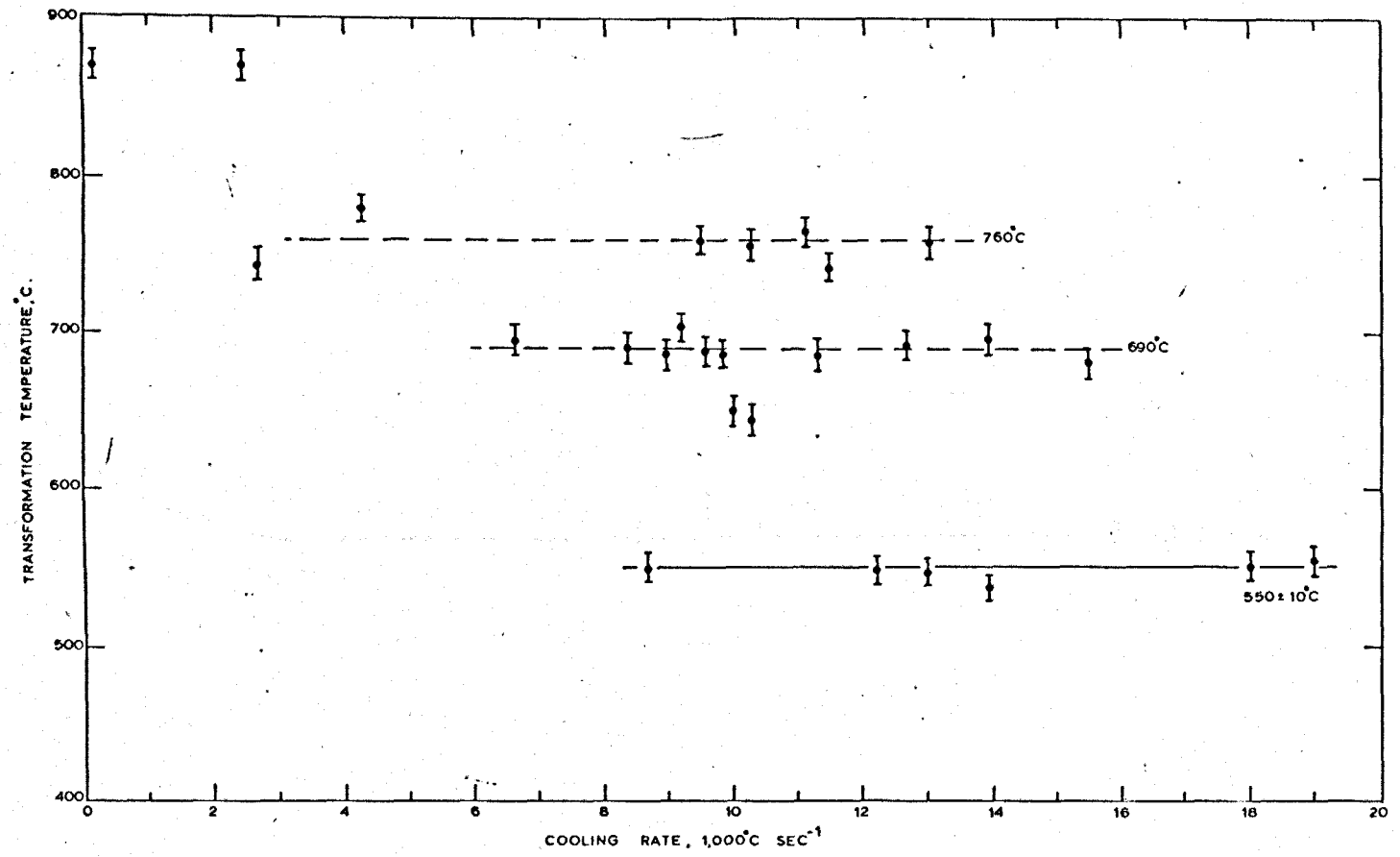

Figure 41. Variation of transformation temperature with cooling rate in 'pure' iron, BISRA ARL8.

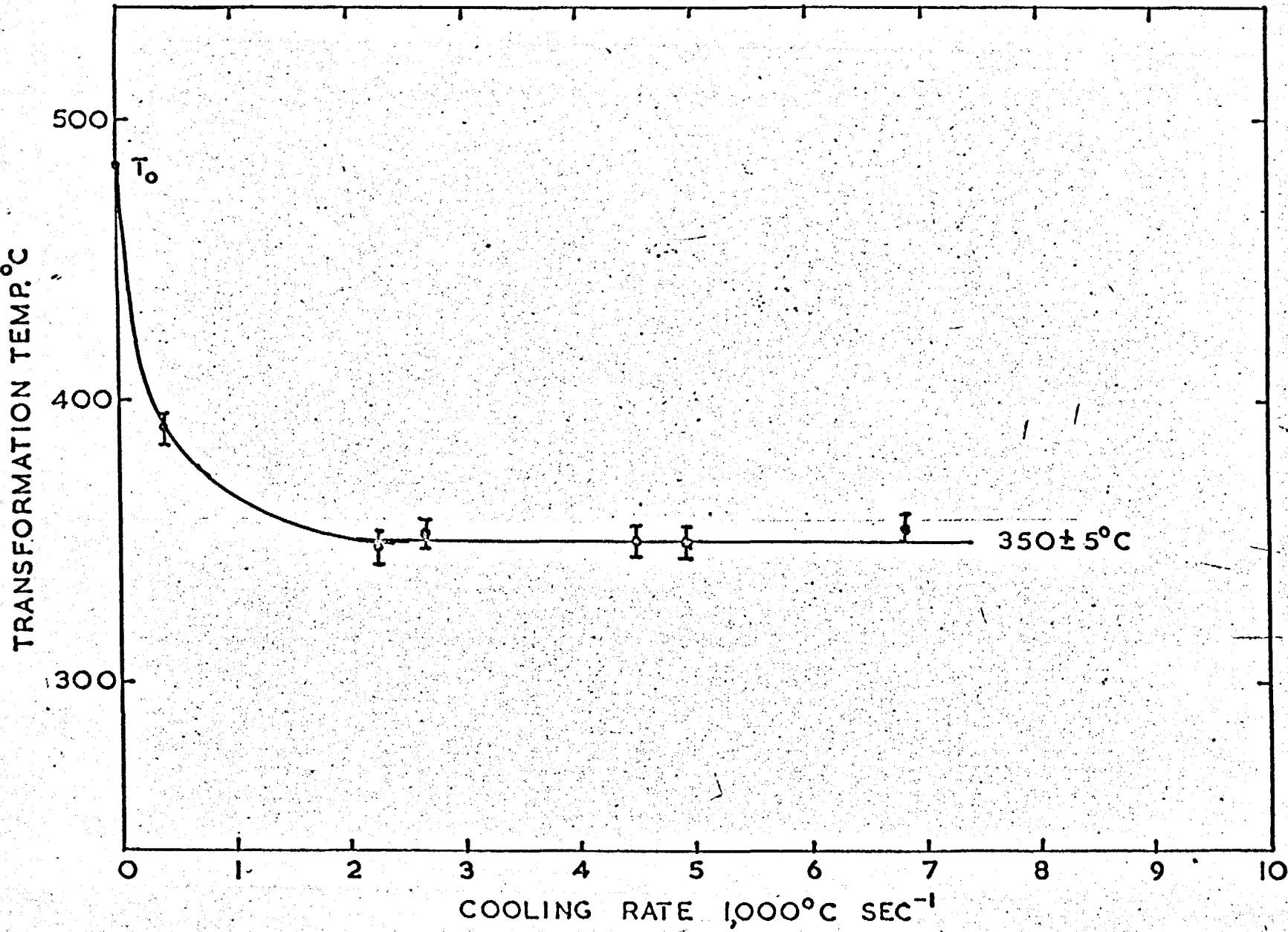

Figure 42. Variation of transformation temperature with cooling rate in Fe - 15% Ni.

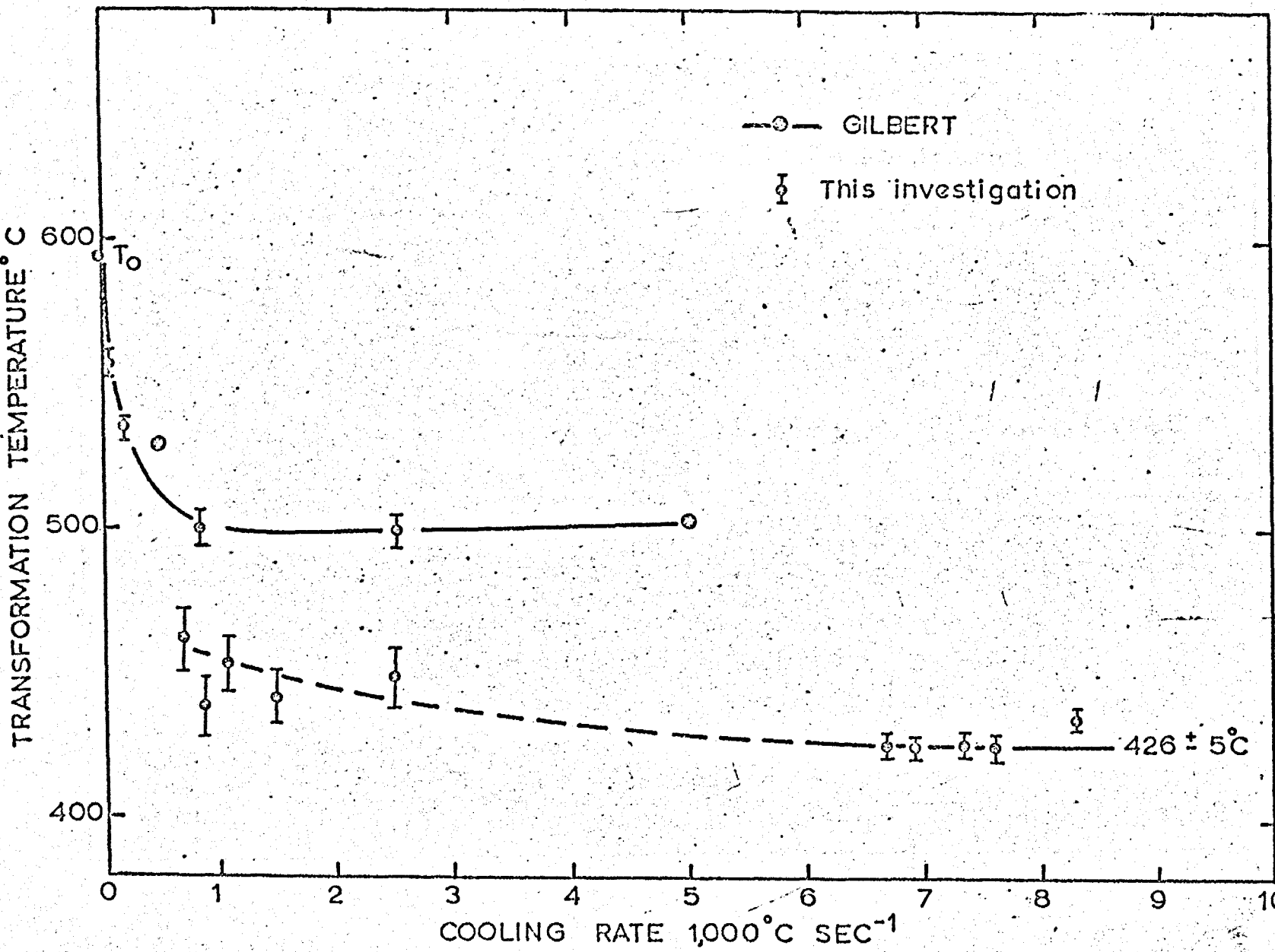

Figure 43. Variation of transformation temperature with cooling rate in Fe-10% Ni.

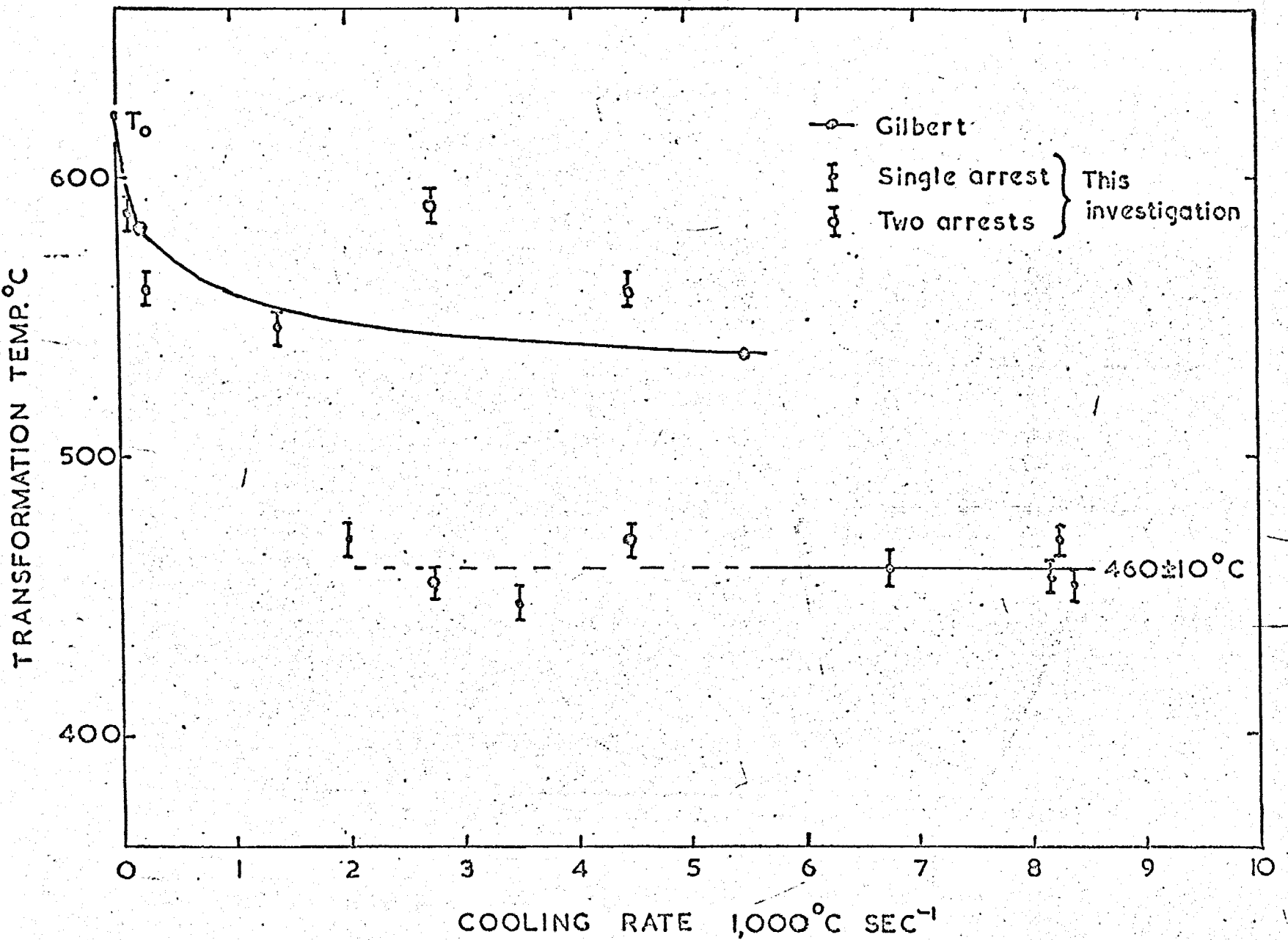

Figure 44 Variation of transformation temperature with cooling rate in Fe-8% Ni.

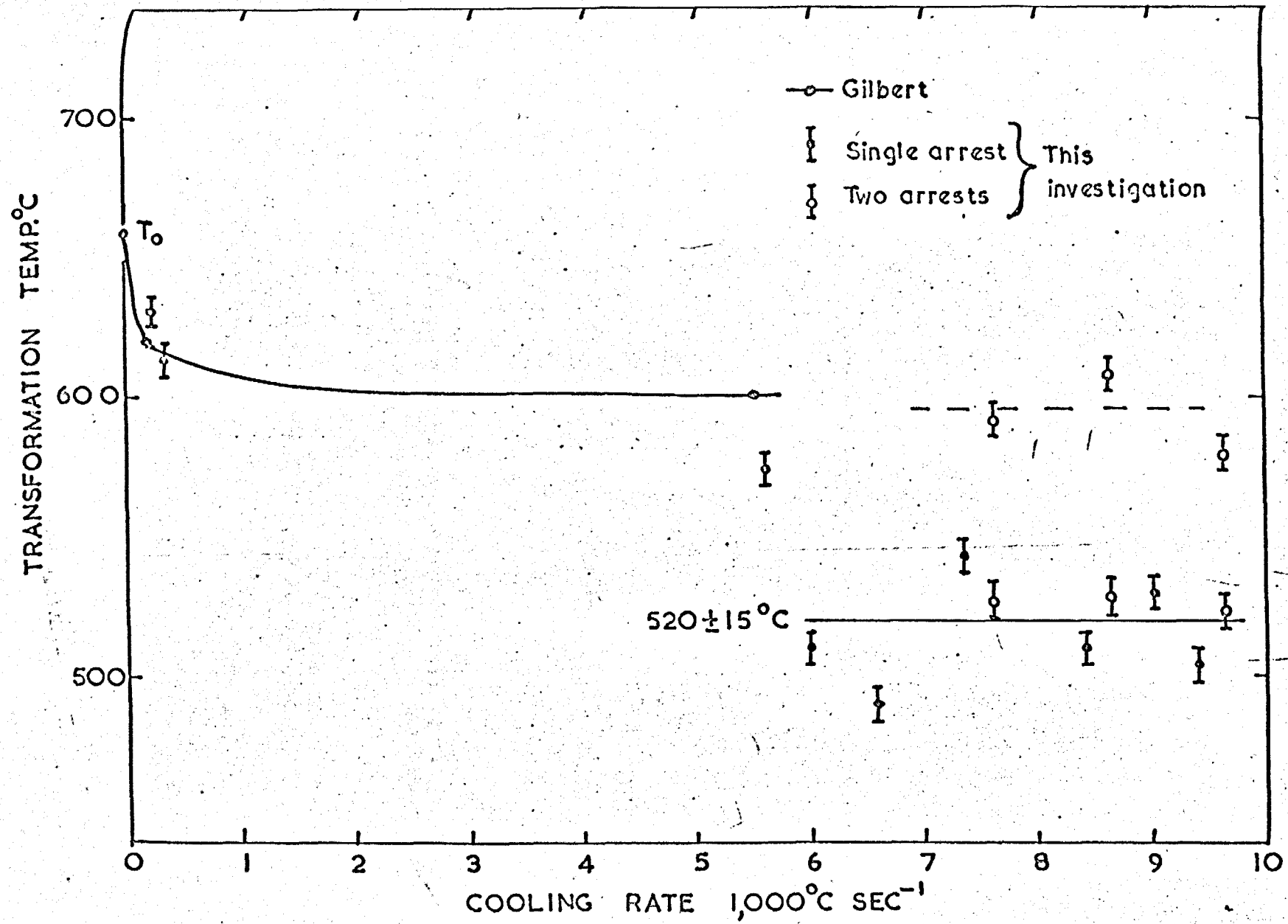

Figure 45. Variation of transformation temperature with cooling rate in Fe-6% Ni.

Figure 46. Massive martensite in Fe-10% Ni. Cooling rate ~ 8,000°C sec^{-1}; Transformation temperature = 426 ± 5°C.

x360

Figure 47. Massive martensite in Fe-6% Ni; cooling rate ~ 8,500°C sec^{-1}; Transformation temperature = 510 ± 10°C.

x930

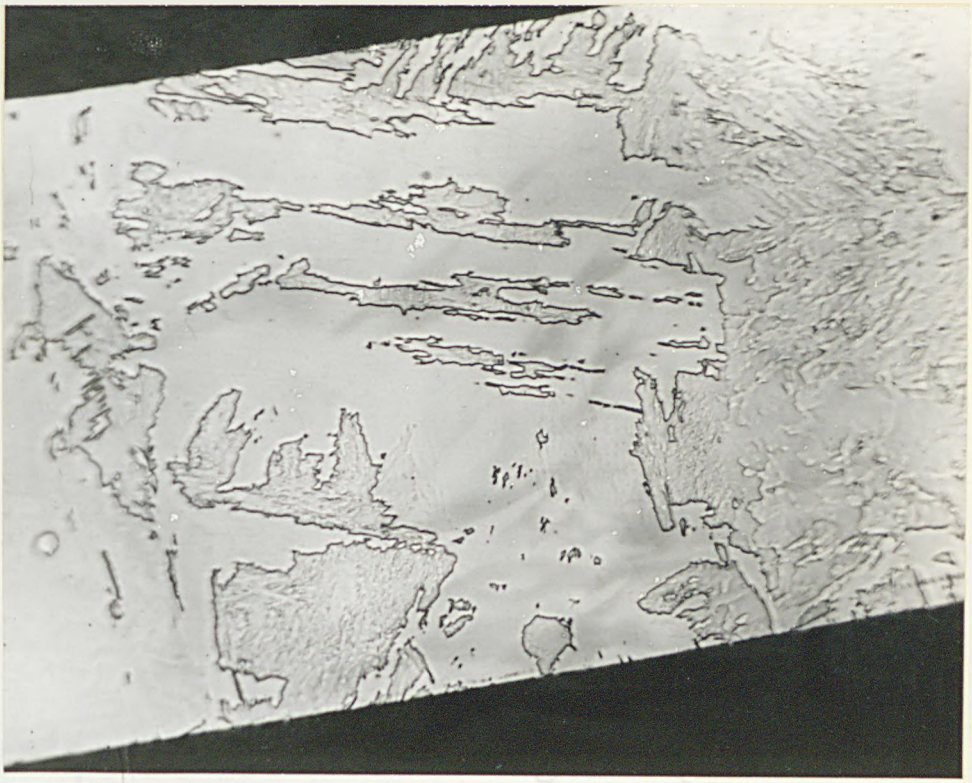

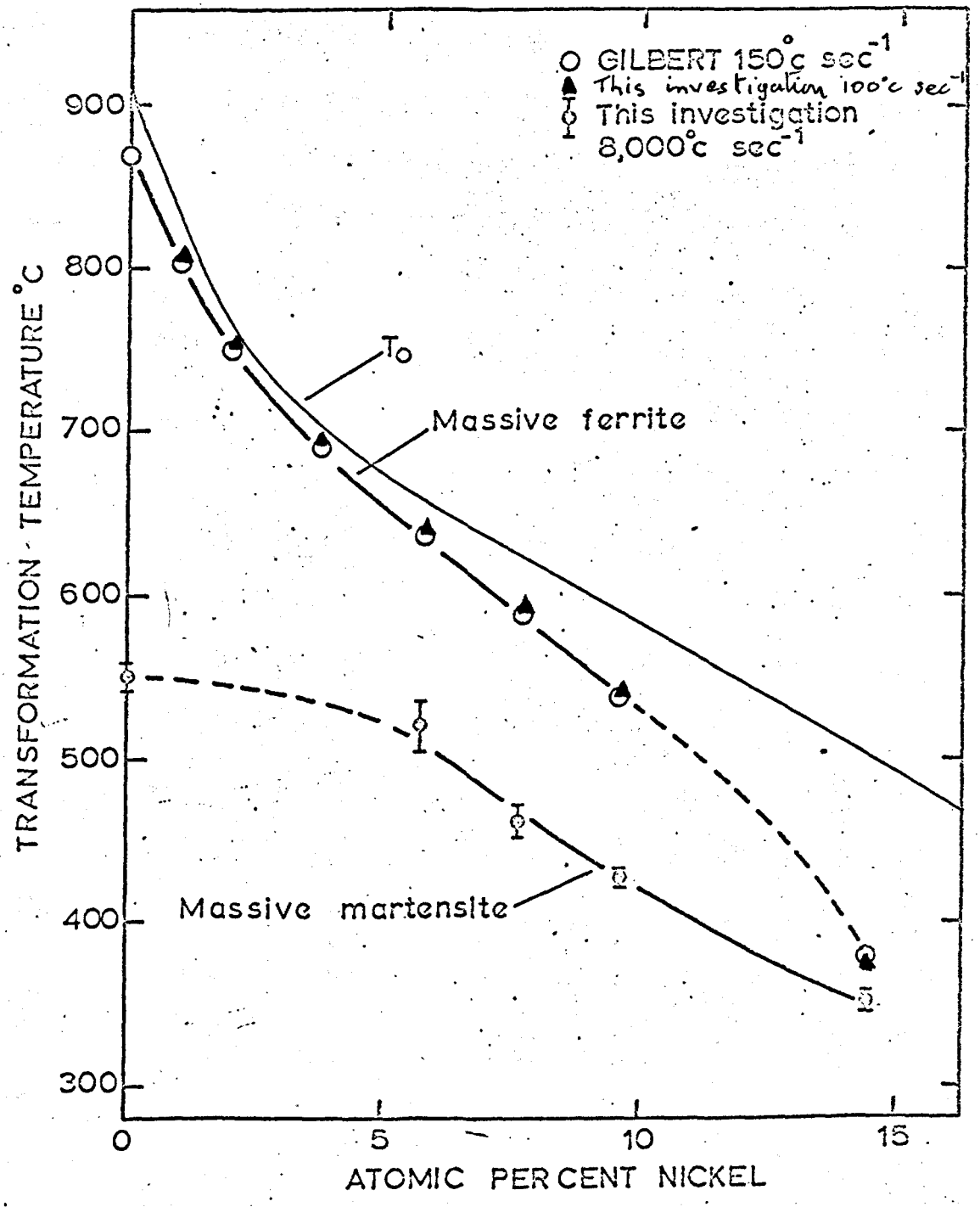

48(a) Transformation temperature obtained on continuous cooling dilute Fe-Ni Alloys.

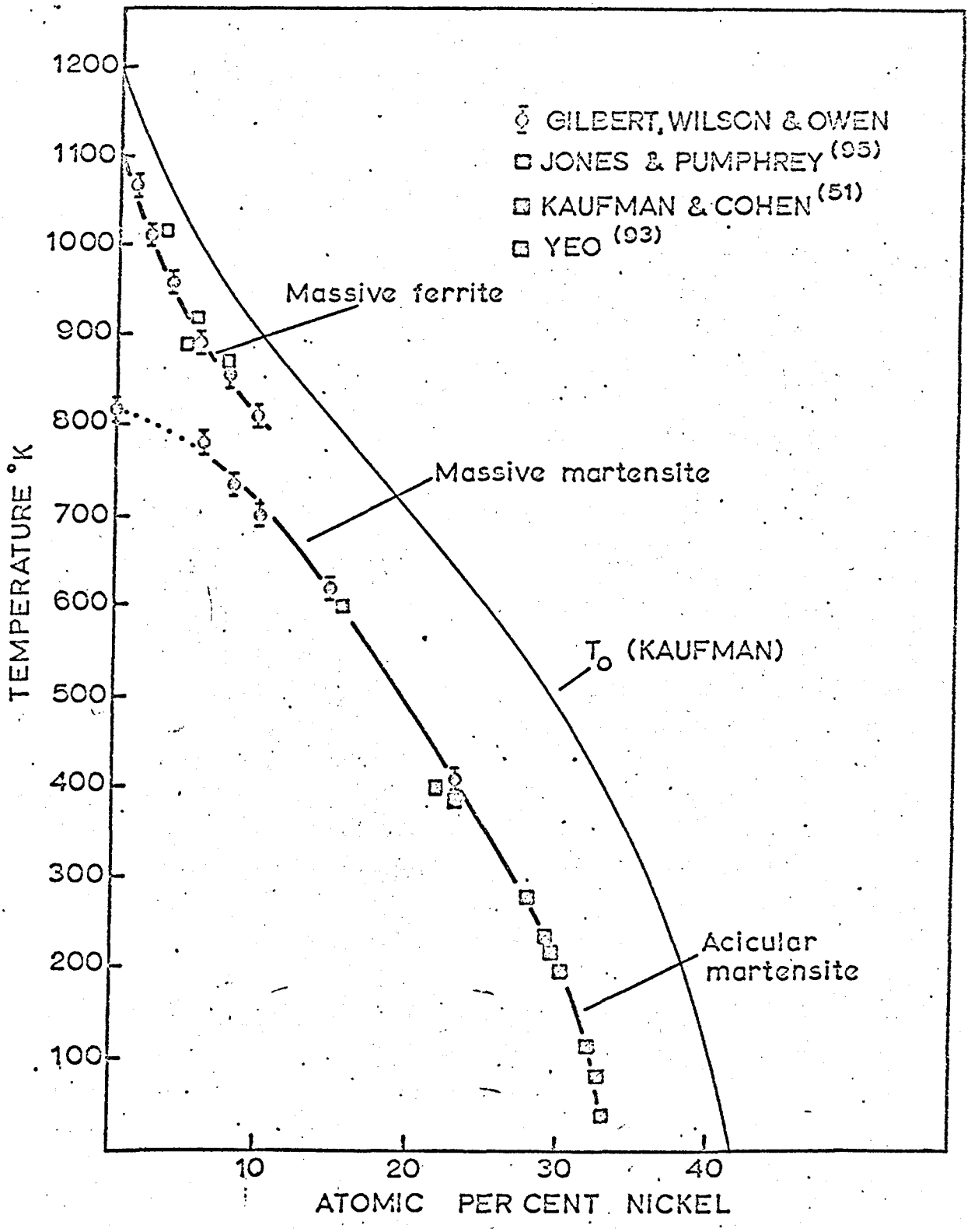

Figure 48(b) Comparison of observed transformation temperature in Fe-Ni alloys with previous work.

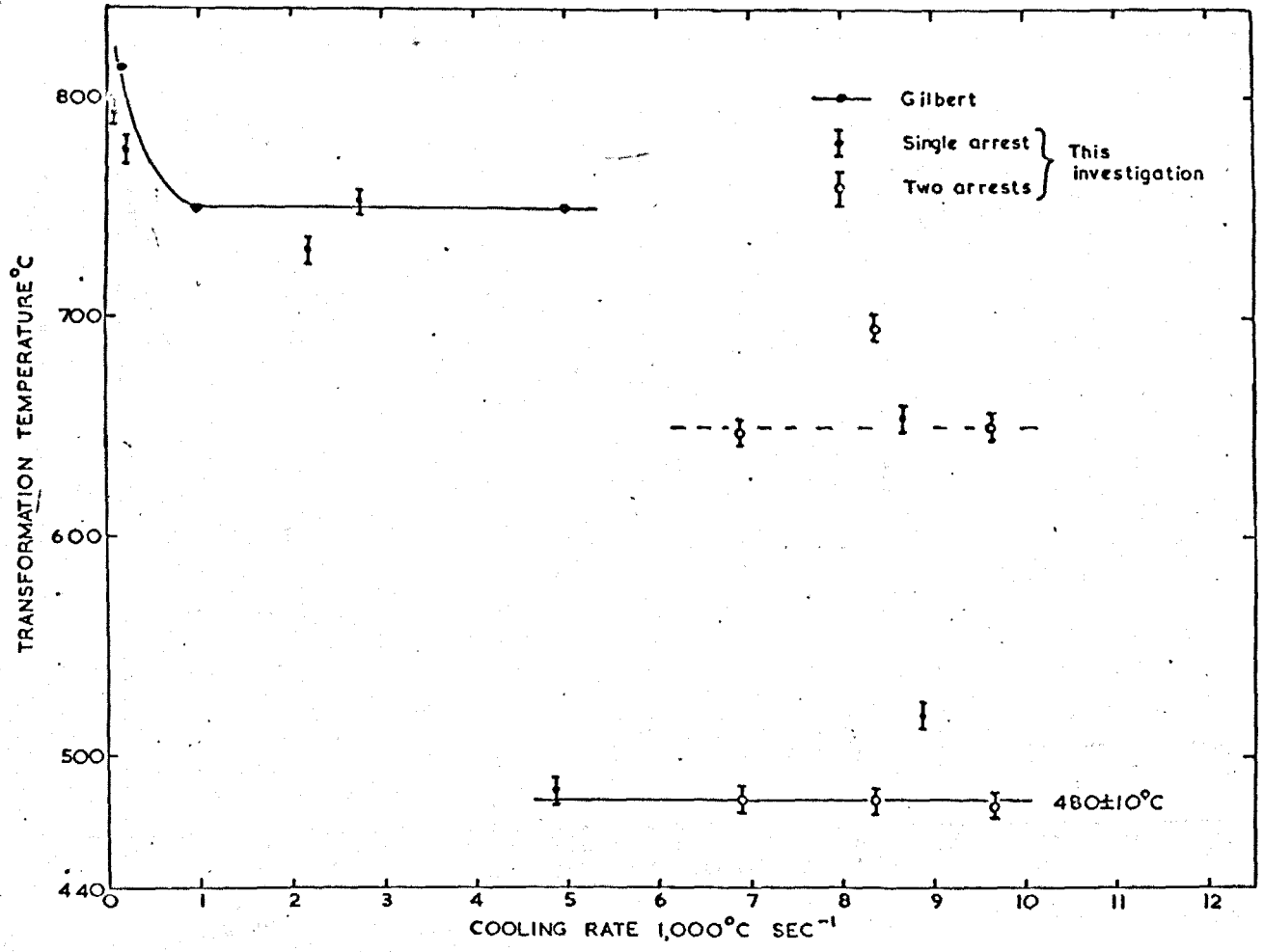

Figure 49. Variation of transformation temperature with cooling rate in Fe-4.3% Cr.

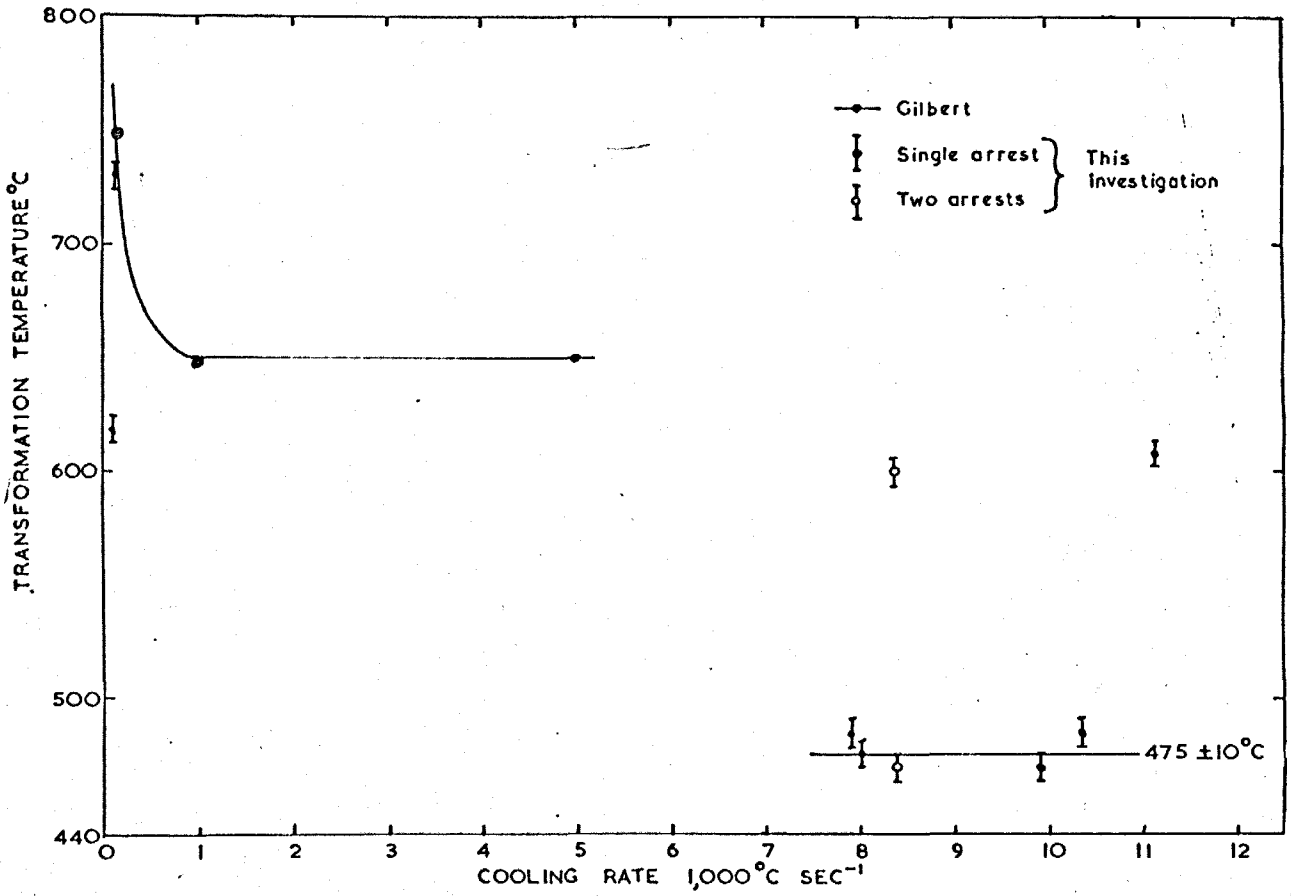

Figure 50. Variation of transformation temperature with cooling rate in Fe-9.4% Cr.

Figure 51. Typical massive martensite structure in Fe-4.3% Cr. Cooling rate ~ 8,200°C sec^{-1}; Transformation temperature = 480 ± 5°C.

x770

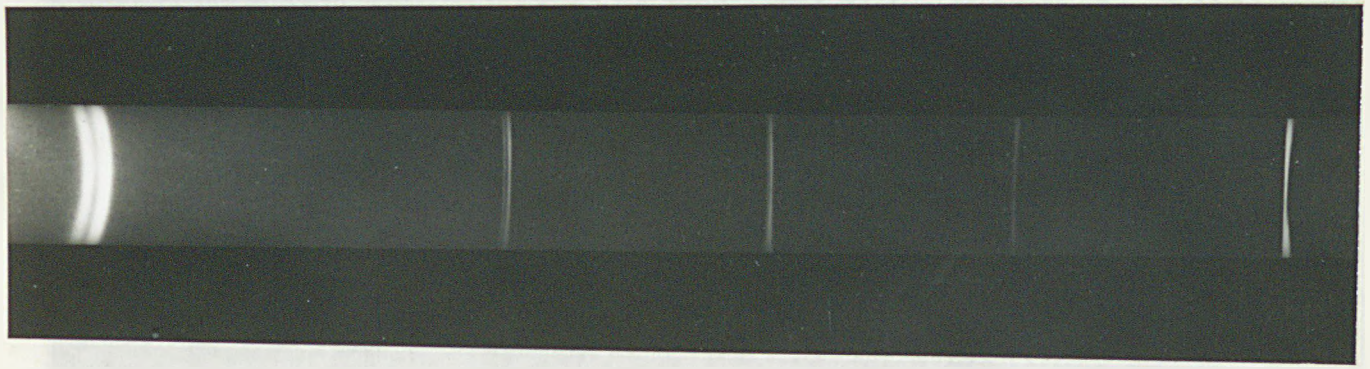

Figure 52. Debye-Scherrer X-ray photograph of massive ferrite in Fe-4% Ni.

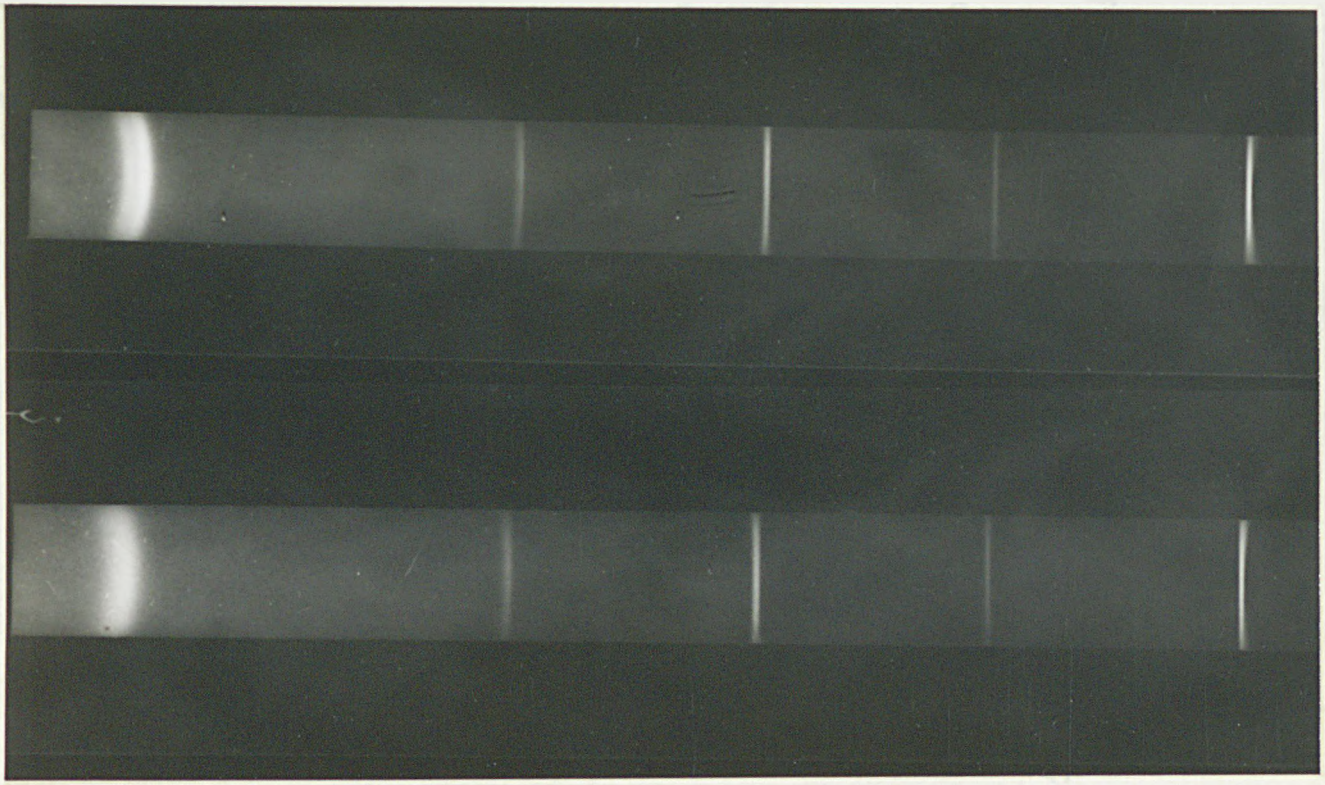

Figure 53. Comparison of X-ray line broadening between massive ferrite and massive martensite in Fe-10% Ni.

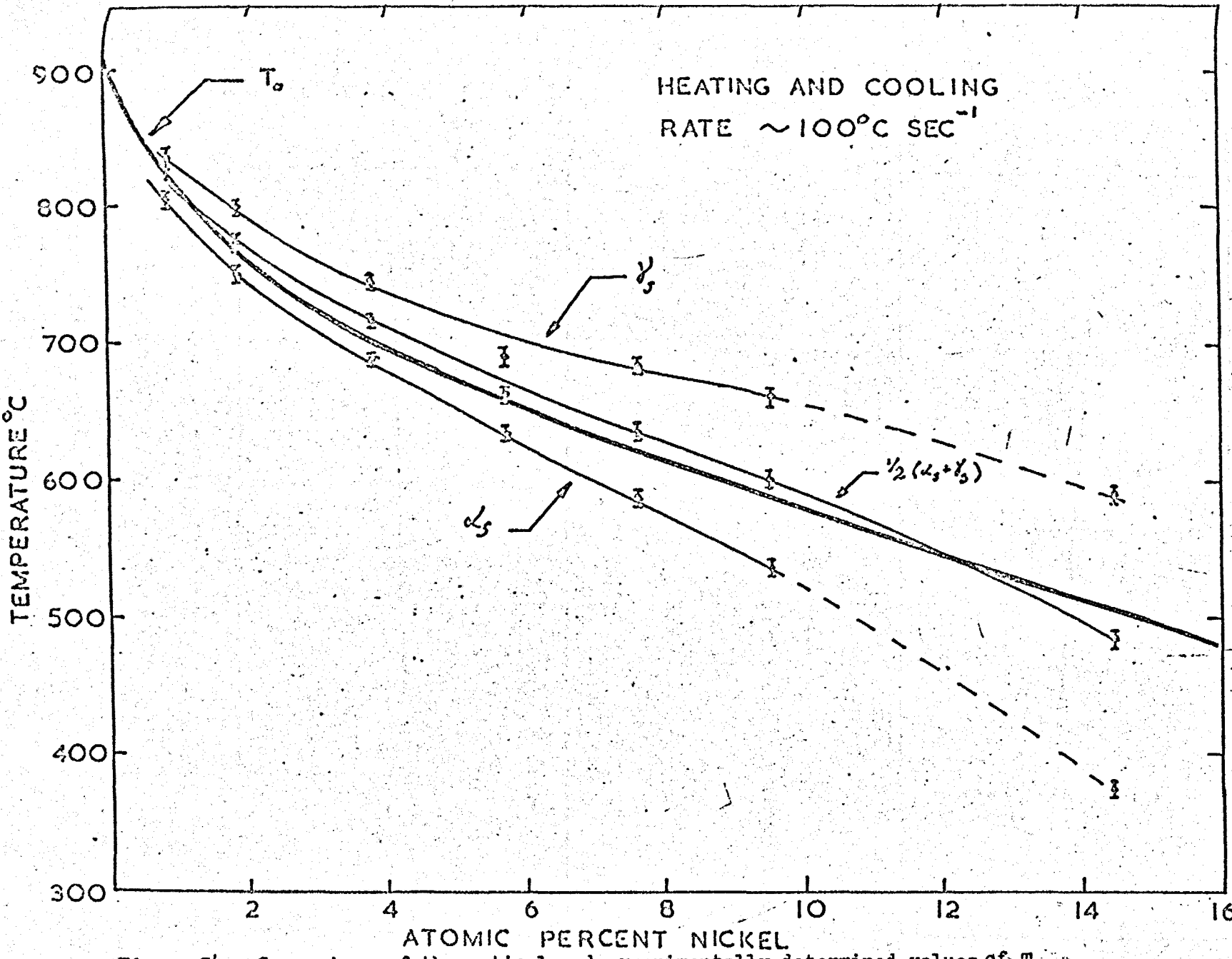

Figure 54. Comparison of theoretical and experimentally determined values of T_o.

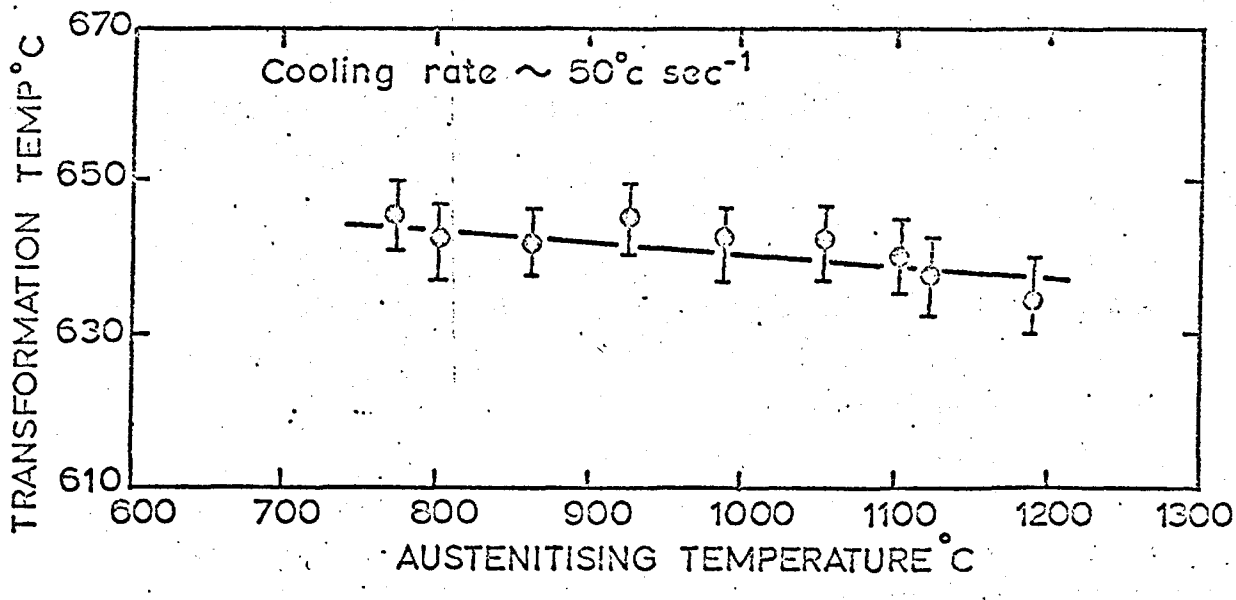

Figure 56. Effect of austentising temperature on transformation temperature for massive ferrite in Fe-6% Ni.

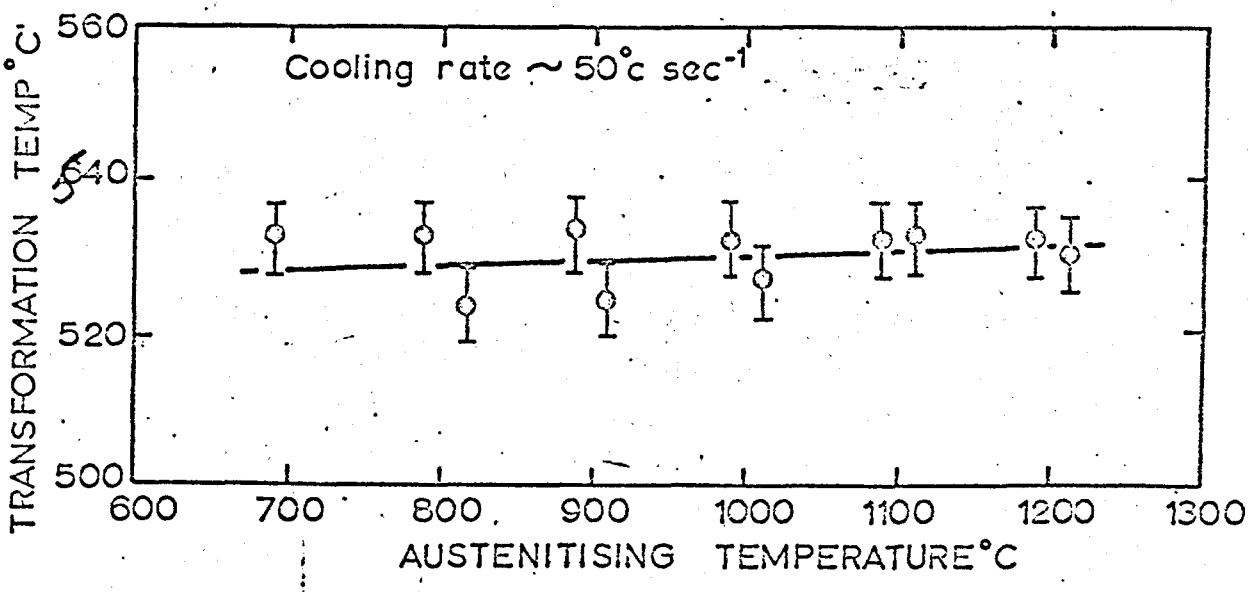

Figure 57. Effect of austenitising temperature on transformation temperature for massive ferrite in Fe-10% Ni.

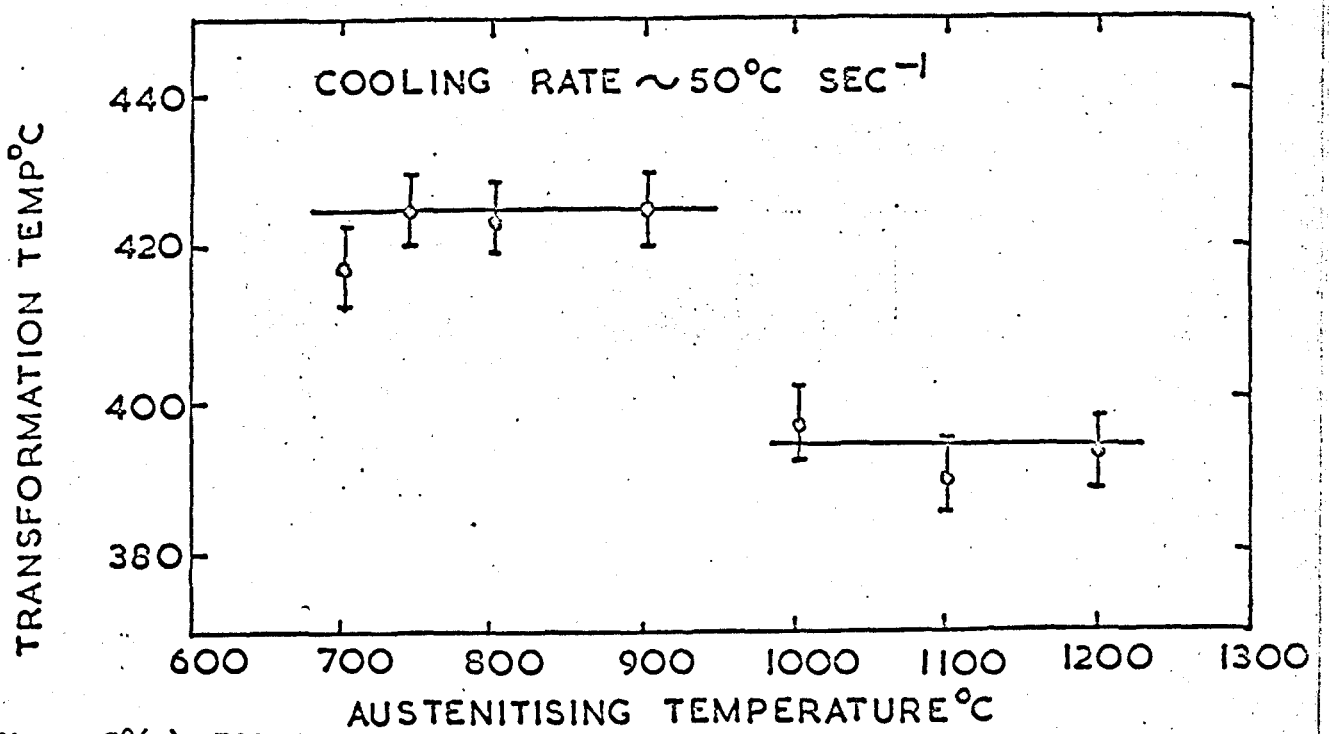

Figure 58(a) Effect of austenitising temperature on transformation temperature in Fe-15% Ni.

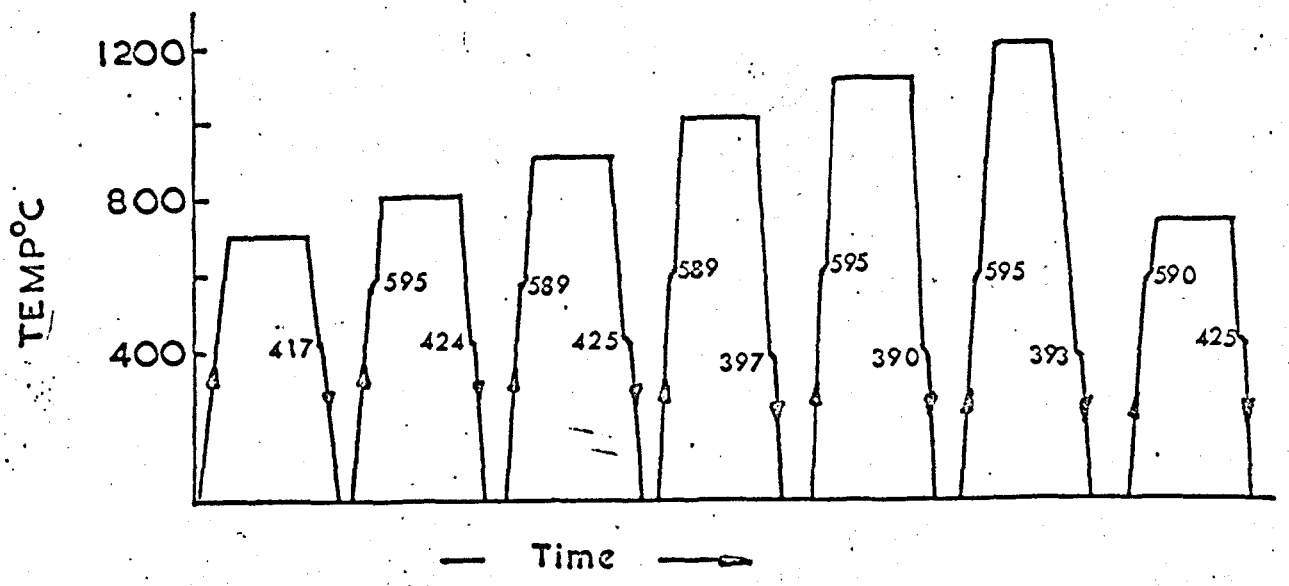

Figure 58(b) Schematic diagram of heating and cooling cycles given to specimen in determining above figure.

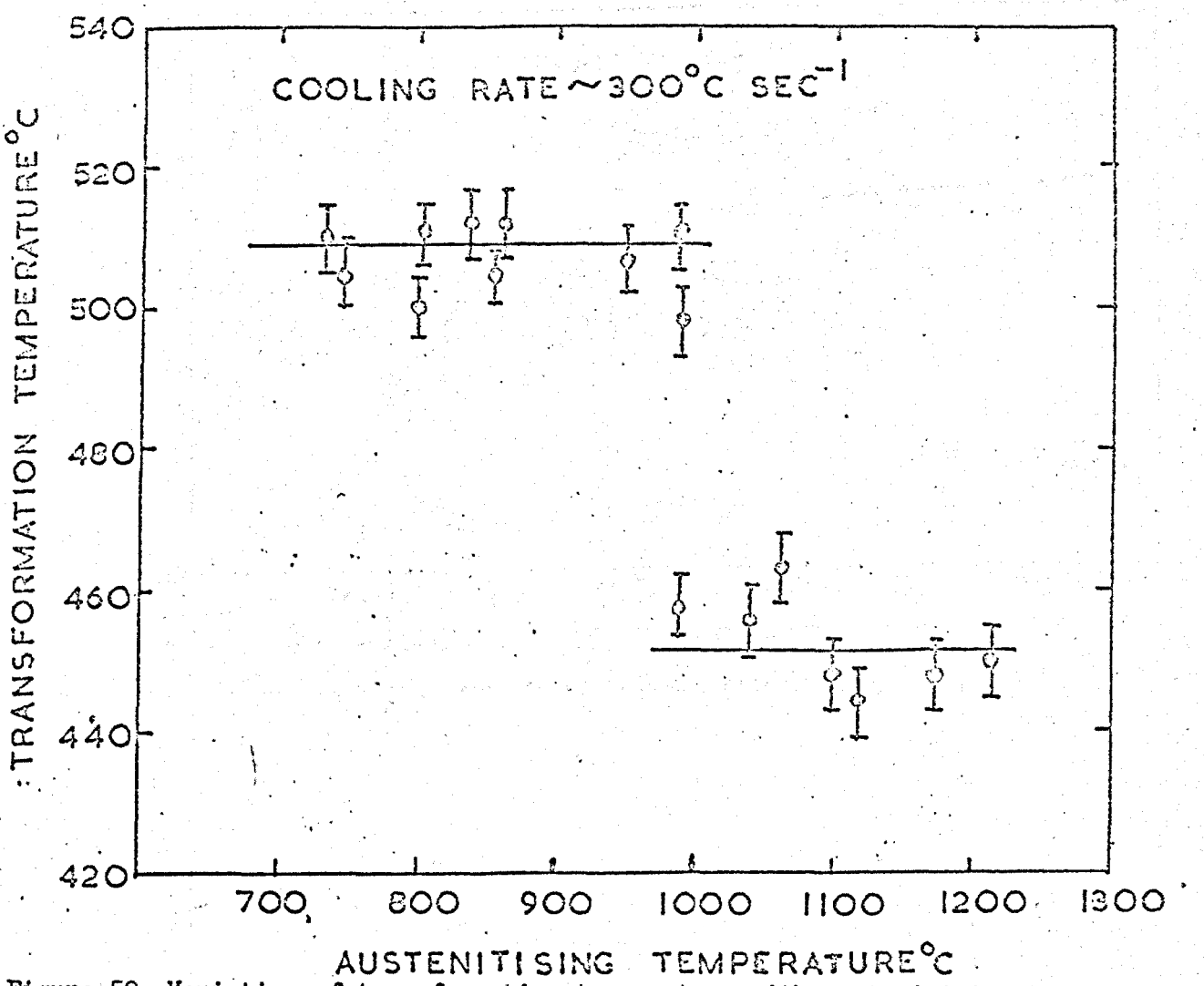

Figure 59. Variation of transformation temperature with austenitising temperature in Fe-10% Ni.

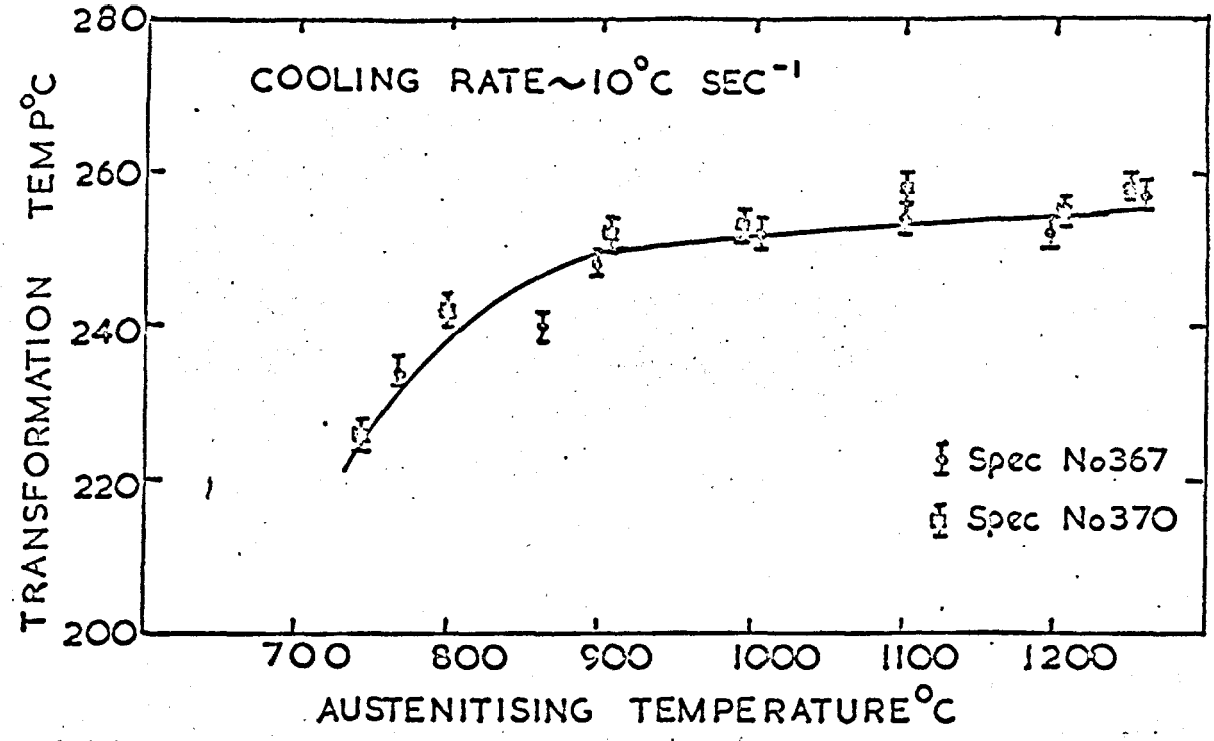

Figure 60(a) Variation of M_s with austenitising temperature in Fe-19% Ni.

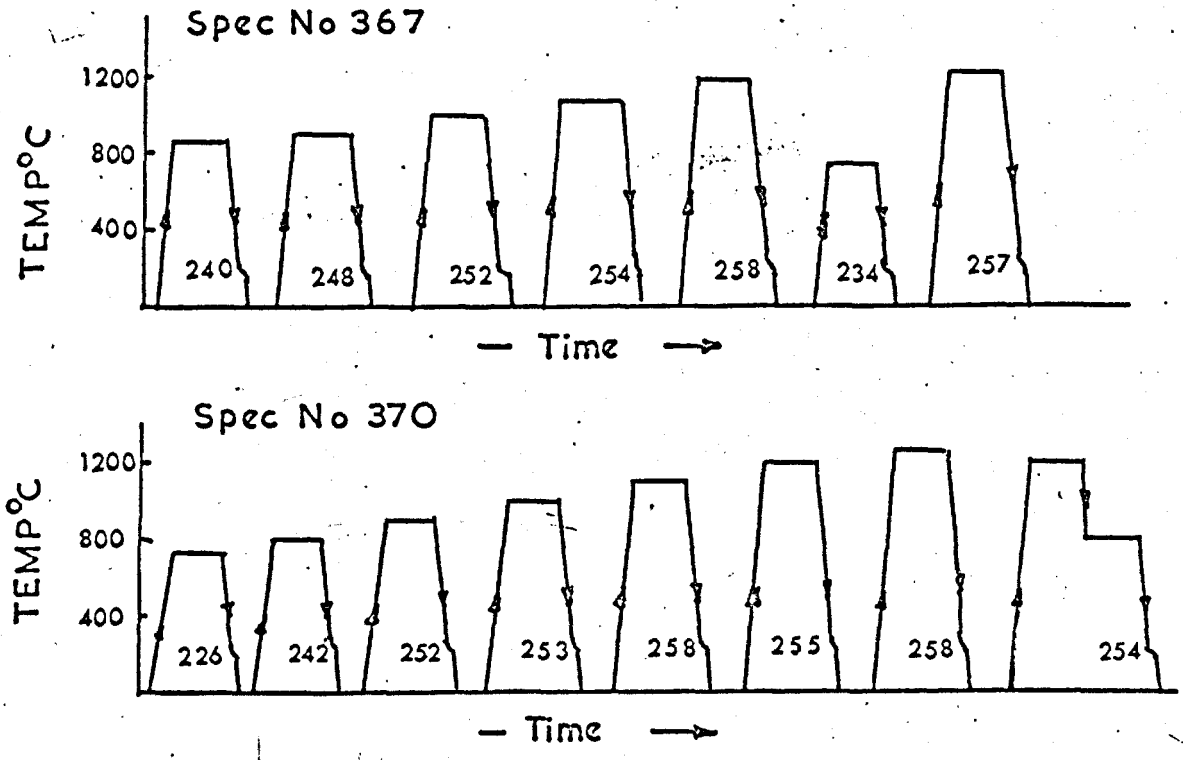

Figure 60(b) Schematic diagram of heating and cooling cycles given to specimens in determining the above curve.

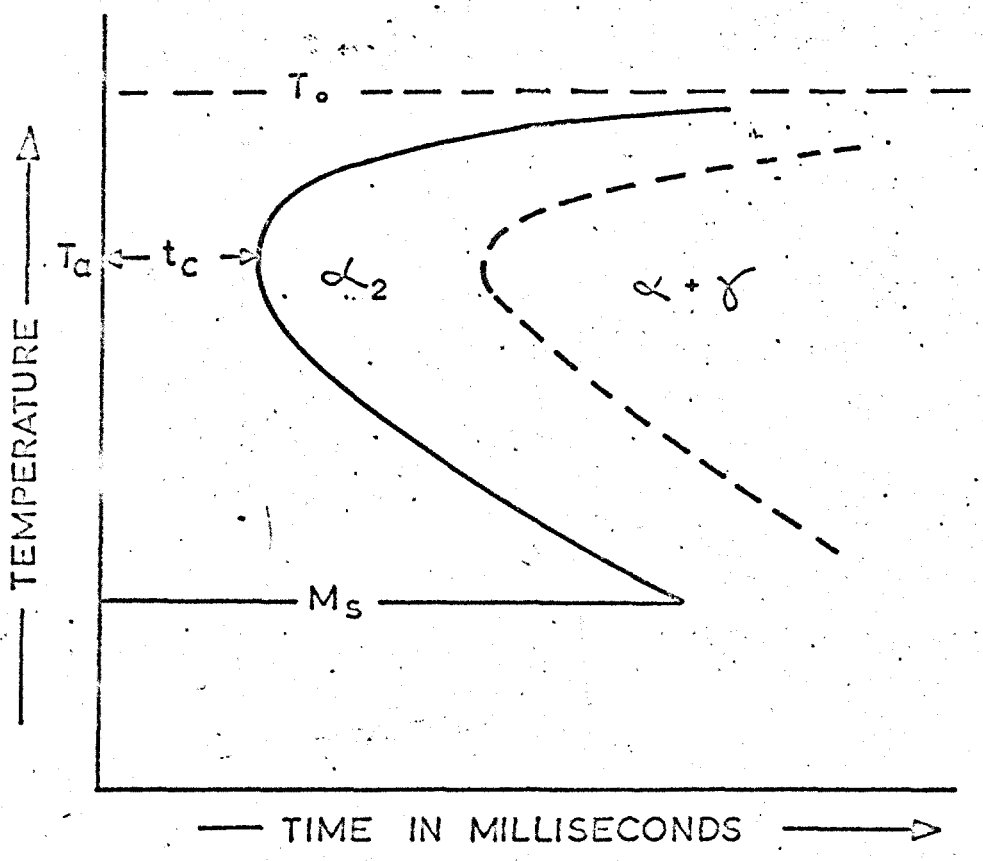

Fig 61. Schematic T.T.T diagram for the Massive ferrite reaction.

In binary substitutional alloys t_c is ~ milliseconds, but increases with certain alloying elements such as Ni and Mn. Interstitials are thought to be the most effective elements in increasing t_c.
The incubation period t_c also increases with austenitising temperature.

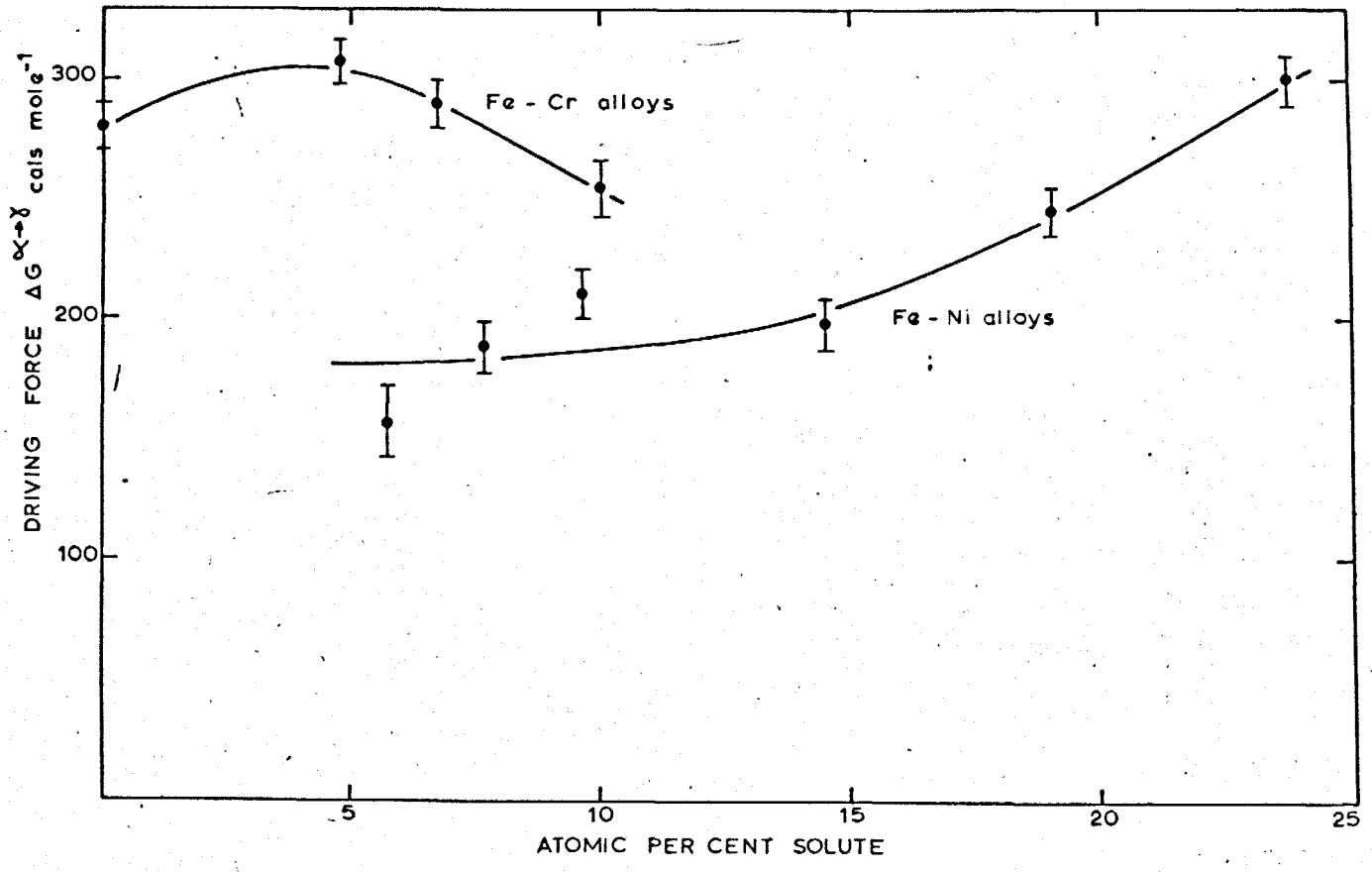

Figure 62. Chemical driving force for the massive martensite reaction in Fe-Cr and Fe-Ni alloys.

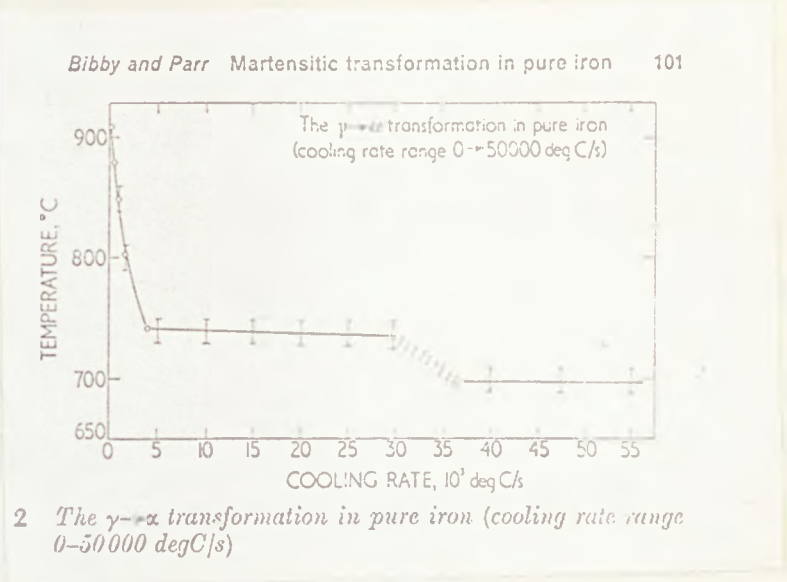

2 *The γ→α transformation in pure iron (cooling rate range 0–50000 degC/s)*

Figure 63. Effect of cooling rate on transformation temperature in Fe-0.025%C after Bibby and Parr[97].

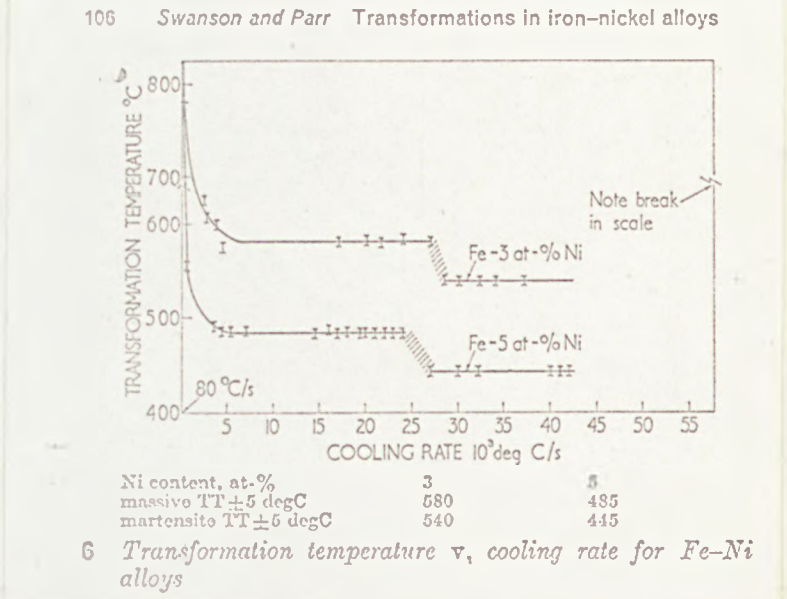

6 *Transformation temperature v, cooling rate for Fe–Ni alloys*

Figure 64. Typical curve of effect of cooling rate on transformation temperature in Fe-Ni alloys after Swanson and Parr[96].

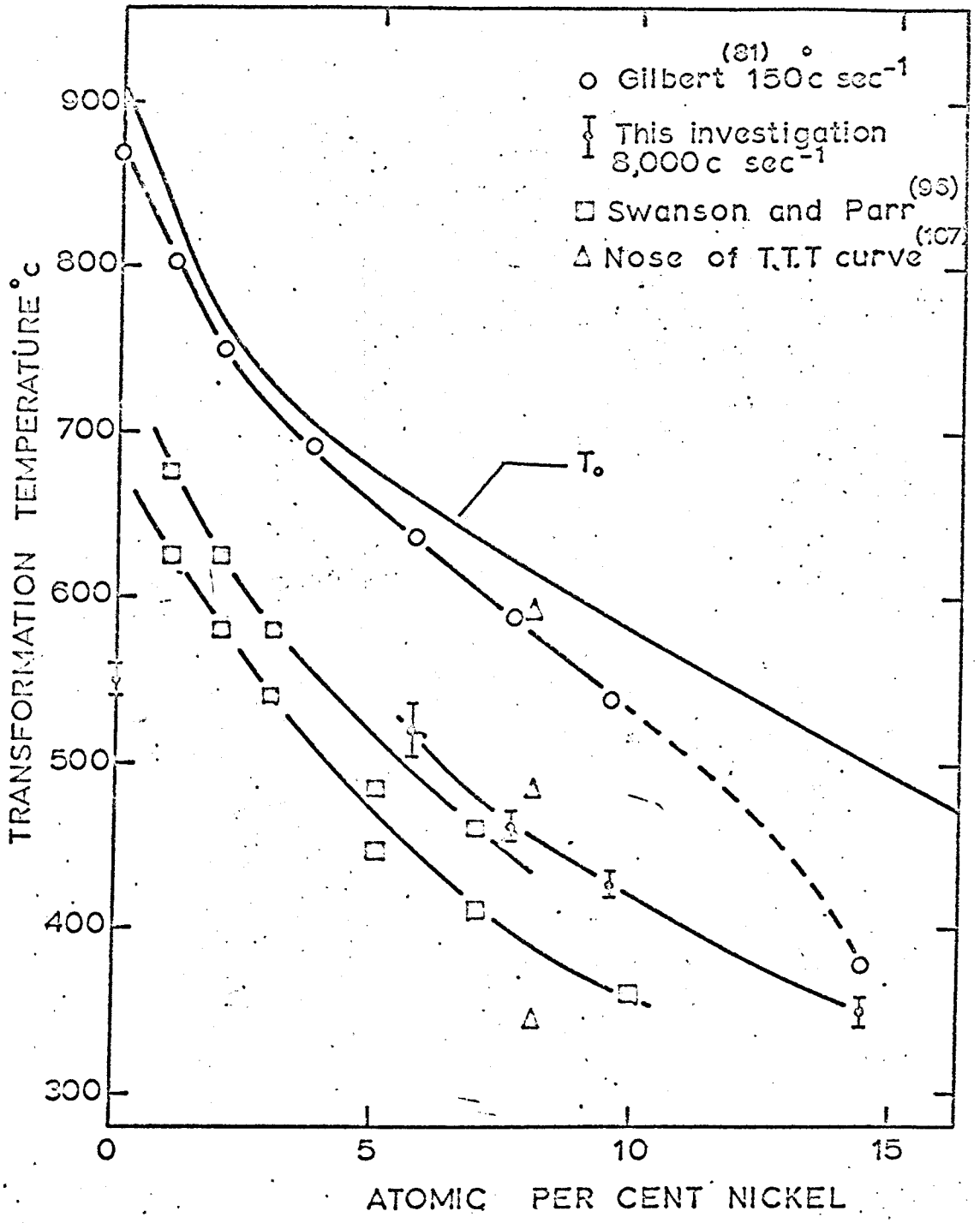

Figure 65. Comparison of observed transformation temperatures obtained on continuously cooling dilute Fe-Ni alloys.

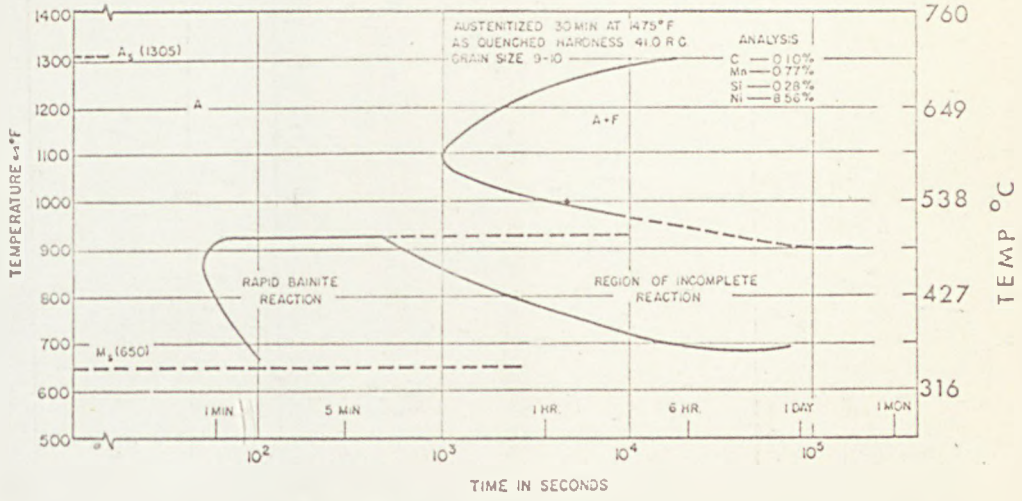

Fig. 2. TTT diagram for 9% Ni steel

Figure 66. T. T. T. diagram for 9% Ni steel after Marschall et al[107]